UNIVERSITY OF CALGARY

Characterization of Solids Removal and Clogging Processes

in Two Types of Permeable Pavement

by

Chris Robert Brown

A THESIS

SUBMITTED TO THE FACULTY OF GRADUATE STUDIES

IN PARTIAL FULFILMENT OF THE REQUIREMENTS FOR THE

DEGREE OF MASTER OF SCIENCE IN CIVIL ENGINEERING

DEPARTMENT OF CIVIL ENGINEERING

CALGARY, ALBERTA

FEBRUARY 2007

UNIVERSITY OF CALGARY

FACULTY OF GRADUATE STUDIES

The undersigned certify that they have read, and recommend to the Faculty of Graduate Studies for acceptance, a thesis entitled "Characterization of Solids Removal and Clogging Processes in Two Types of Permeable Pavement" submitted by Chris Brown in partial fulfilment of the requirements of the degree of Master of Science in Civil Engineering.

_____
*Supervisor, [FULL NAME AND DEPARTMENT]*

_____
*[FULL NAME AND DEPARTMENT]*

_____
*[FULL NAME AND DEPARTMENT]*

_____
*[FULL NAME AND DEPARTMENT]*

_____
*DOCTORAL STUDENTS ONLY External Examiner (or External Reader), [FULL NAME AND INSTITUTION]*

_____
*Date*

**Abstract**

This study investigates the processes and characteristics of solids removal and clogging in two types of permeable pavement: UNI Eco-Stone® and porous asphalt. The objectives of this research were to determine the performance of these two types of permeable pavement with respect to hydraulic performance and water quality, and to try to gain a better understanding of the mechanisms and processes behind solids removal and clogging within permeable pavement structures. Field installations as well as laboratory models were used to measure the pavements' hydraulic and water quality responses to a simulated runoff influent that was loaded with a known quantity and size distribution of sediment.

Results from the study showed that both pavement types are capable of excellent total suspended solids removal, in the range of 90-96% removal of solids from influent. Particle size distribution analysis of accumulated sediment within the structure and in the influent and effluent showed that the particles in the effluent of the pavements is substantially finer than that in the influent, and that, although solids removal occurs throughout the entire structure, the "sieving action" occurs primarily at the geotextile. Further results showed that vacuum sweeping is a viable maintenance technique for the restoration of infiltration capacity in the Eco-Stone®, but not for porous asphalt. And finally, winter sanding activities were shown to have a substantial impact on the long-term surface infiltration capacity of both pavement types.

## Acknowledgements

I would like to express sincere thanks to my supervisor, Dr. Angus Chu, Ph.D, for his knowledge, guidance, and insight throughout the course of this research. Additionally, I am very thankful for the extensive input and advice of my co-supervisor, Bert van Duin, M.Sc, P.Eng.

I would like to extend thanks to Liliana Bozic, M.Sc, P.Eng, Phil Jerome, and all of the other staff at The City of Calgary who were involved with this project. Their assistance in running and coordinating the experiments was invaluable. I also extend thanks to the technical staff from The Department of Civil Engineering at The University of Calgary for putting up with all of my requests for help to move heavy items and locate obscure equipment. I extend special thanks to Canada Lands Company; without them this project never would have happened.

Finally I would like to thank my parents, Rick and Susan, for their love, support, and encouragement.

**Table of Contents**

## List of Tables

**List of Figures and Illustrations**

xi

## Chapter One: Introduction

The use of permeable pavements as a method to improve the management and treatment of stormwater has recently increased dramatically, and has been the focus of numerous studies. The potential to reduce or eliminate the need for traditional stormwater infrastructure by use of Low Impact Development (LID) technologies has become an important area of research and discussion within the stormwater management profession. Designers, city planners, and stormwater management engineers across Europe, North America, and Australia have begun to explore the use of this so-called best management practice (BMP) as a promising, cost-effective way to reduce stormwater peak rates and runoff volumes, and to improve water quality.

Stormwater management in the past has been addressed using systems such as curbs and gutters, sewers, and detention or retention ponds, before discharging the runoff into natural water bodies. This approach leads to the natural hydrologic cycle being completely altered by development practices. Increased urbanization and the resulting increase in impervious surface coverage lead to the requirement for continuous expansion of stormwater infrastructure. Not only does this result in ineffective land use due to the requirement for increasing numbers and sizes of detention ponds, but most detention ponds themselves may have little effect on the actual quantity and quality of runoff entering receiving waters. This ultimately results in an increase in the total volume of surface runoff, an increase in peak runoff flow rates, and reduced runoff quality, all of which have detrimental effects on receiving aquatic ecosystems. Low Impact Development technologies, such as permeable pavement, attempt to resolve these issues

by treating and managing stormwater runoff at its source, thereby reducing the reliance on traditional infrastructure.

A permeable pavement system allows water to flow downward through its pervious surface and into its substructure. The surface itself can consist of any one of a number of different materials, including porous asphalt, porous concrete, and open-jointed paving blocks. The substructure typically consists of one or more courses of aggregate lain on top of a sub-grade, and may include geotextiles to separate the layers from one another. From the substructure, runoff can be stored and either allowed to percolate into the sub-grade or be conveyed through an underdrain to a sewer, a secondary treatment facility, or directly to a water body. Pollutants within the runoff are filtered on-site, typically becoming trapped within the layers of the permeable pavement. As solids accumulate throughout the structure, the surface infiltration capacity (and therefore hydraulic performance) of the pavements decreases until a point where it is considered no longer hydraulically functional. The length of time until this happens, and the degree to which it can be delayed through regular maintenance, is dependent on a wide variety of factors and has been the topic of increased study recently. Unfortunately, much of the data from these studies is likely only applicable to the geographical region in which they took place; there is a need for local regional studies.

Permeable pavement is not a new concept; it has been around in one form or another since at least the early 1970's, but its popularity and widespread use has only begun to emerge in the past decade, in part due to increased research leading to improved design and construction specifications. However, there is still a great deal of research to be done on permeable pavements before they can be successfully implemented in all

situations. Of particular importance in the study of permeable pavements is the establishment of regional data for their performance with regards to long-term surface infiltration capacity and water quality improvement. Although there has been extensive research in these areas, the success of permeable pavements is highly dependent on local geological and climatic conditions, and therefore studies from different geographical locations often have very little applicability to the local installation of permeable pavements. Also, to date there has been very little research into the specific size ranges of particles that can be removed, and precisely where in the pavement structure they are removed. This information is crucial, not only to provide a better understanding of the clogging and filtration processes within permeable pavements, but because local and regional policies often set stormwater treatment targets based on specific size ranges of particles. For example, The City of Calgary states that 85% of particles over 75 μm must be removed by stormwater treatment methods.

The general objectives of this study were to gain a better understanding of the processes involved in clogging and solids removal of porous asphalt and open-jointed paving block permeable pavement systems and to provide local data for the performance of permeable pavements using both laboratory and field investigations. The specific objectives of this study were to:

1) Observe the decline in surface infiltration capacity over the first year after installation of porous asphalt and UNI Eco-Stone® permeable pavements, and to quantitatively compare both pavement types.

2) Determine the degree to which runoff flow rates are attenuated through the permeable pavement structure.

3) Determine the performance of the pavement systems in removing total suspended solids (TSS), and specifically what size ranges of TSS were removed by way of particle size distribution analysis.

4) Investigate possibilities for the maintenance of permeable pavements to restore their surface infiltration capacity.

5) Determine long-term surface infiltration capacities, and thus predicted effective hydraulic life, of both pavement types in the laboratory.

6) Determine the locations where specific size ranges of particles are removed throughout the permeable pavement structure.

7) Observe the effects of the presence of winter sanding material on the surface infiltration capacity of the pavements.

An increased understanding in the clogging and solids removal processes in permeable pavements and, specifically, the location and size ranges of particle accumulation throughout the pavement structure, will enable more efficient design and maintenance guidelines to be established, and potentially maximize the life of future permeable pavement installations. Furthermore, through this study, much needed regional data on water quality and hydraulic performance for porous asphalt and UNI Eco-Stone® permeable pavement installations can be established.

**Chapter Two:    Permeable Pavement – A Review**

A review of permeable pavement is appropriate to provide a better understanding of the background of this area of study, as well as to put into context the research pertaining to this thesis.

## 2.1 Urban Stormwater

When natural landscapes are replaced by impervious areas through urbanization, runoff processes are altered, having a drastic impact on surrounding water bodies. Impervious areas mainly consist of constructed surfaces such as rooftops, sidewalks, roads, and parking lots, which are covered by virtually impenetrable materials such as asphalt, concrete, and stone (Barnes *et al*, 2001). These materials effectively seal the surfaces and prevent any precipitation from infiltrating into the underlying soil. The consequence is that rain events generate higher peak flows and volumes, increased sediment loads to receiving waters, increased contaminant loads from automobile traffic and increased stream bank erosion (James, 2002). The increase in total runoff and the decrease in lag time can also result in less groundwater recharge, which ultimately leads to decreased low flows in stream channels (Field *et al*, 1982).

The underlying cause behind these water quantity problems is loss of the water-retaining function of soil in the urban landscape (Booth and Leavitt, 1999). Water that may have remained in the natural "soil reservoir" for extended periods of time flows rapidly across the land surface and into storm drains, eventually arriving at a water body in short, concentrated bursts of high discharge (Booth, 1991). Additionally, surface

runoff can contain a broad range of pollutants, and has been identified as one of the leading sources of pollution for natural waters (United States Environmental Protection Agency, 2001).

Traditionally, stormwater management has been addressed by replacing the lost functions of the soil with artificial detention ponds, which are essentially designed to mimic the functions of the soil by allowing storage and attenuation of collected water flows. Runoff is conveyed to drains by curbs and gutter systems, and then transported through storm sewers to ponds where the water is temporarily stored and then discharged to a water body. However, detention ponds only control the rate of runoff, still allowing significant increases in water volume, frequency and duration relative to predevelopment conditions (United States Environmental Protection Agency, 2001). Additionally, detention ponds do little to address the concerns of poor water quality in urban runoff (Kresin, 1996).

Source control of stormwater, where both the water and pollution contents of runoff are addressed on-site, is considered by many professionals as a more effective method of achieving the long-term goals of urban stormwater management (Urban Water Resources Centre, 2002b). Several emerging low impact development (LID) technologies utilize this source control concept. Low impact development is a site design strategy with the goal of maintaining, as much as possible, predevelopment hydrologic characteristics through the use of design techniques to create a functionally equivalent landscape (United States Environmental Protection Agency, 2001). Hydrologic functions of storage and infiltration, as well as discharge frequency and volume, are maintained through techniques such as micro-scale stormwater detention areas, reduction of impervious

surfaces, and the lengthening of flow paths and runoff time (Prince George's County, 2000).

One LID technology that can reduce overall impervious surface area is permeable pavement. Permeable pavement allows stormwater to drain freely through its surface, addressing the negative impacts of urbanization and potentially reducing the requirement for typical stormwater infrastructure, while at the same time treating the stormwater through both physical and biological processes.

## 2.2 Overview of Permeable Pavement

Permeable pavements are a Low Impact Development technology that can be used to address the problem of increased stormwater runoff and decreased stream water quality associated with urbanization (Brattebo and Booth, 2003). Because of their ability to allow water to quickly infiltrate through the surface, permeable pavements allow for reductions in runoff volumes and peak runoff rates, as well as improvements in water quality of stormwater runoff (Collins *et al*, 2006). They have been shown to enable a significant decrease in several key stormwater pollutants, as will be discussed further in Section 2.8.1.

Stormwater passes through the pervious surface of the permeable pavement, and percolates through the layers of the sub-structure, where it is temporarily stored. In regions with soils that are highly permeable, the stormwater can be allowed to slowly infiltrate into the native soil (sub-grade) underneath the permeable pavement (Collins *et al*, 2006), whereas in areas with low-permeability soils, effluent water can be conveyed

underneath the pavement through an underdrain to a storm sewer system (James and Langsdorff, 2003).

Throughout this thesis, the term "permeable pavement" will refer to the entire permeable pavement structure (as will be described in Sections 2.4 and 2.5), rather than solely the surfacing material.

## 2.3 Potential Advantages of Permeable Pavement

Some of the potential advantages of using permeable pavement include:

- A reduction in the overall volume of runoff from pavement surfaces and, therefore, a potential decrease in necessary storm drainage infrastructure (Shackel *et al*, 2003)

- Ability to reduce the amount of overland flow reaching receiving waters, thereby potentially decreasing peak flows in rivers and streams (Legret *et al*, 1996)

- Assistance in recharging of aquifers and groundwater (Shackel *et al*, 2003)

- Help in trapping pollutants that might otherwise contaminate groundwater or waterways (Shackel *et al*, 2003)

- A reduction in the nuisance factor to pedestrians and motorists arising from standing puddles (Field *et al*, 1982)

- Reduced land consumption (Kresin *et al*, 1997)

- Can be used to effectively remove water from the driving surface to prevent hydroplaning (James, 2002)

- Reduced traffic noise (Hamzah and Hardiman, 2005)

**2.4 Permeable Pavement Structural Components**

Permeable pavements, like standard non-permeable pavements, can consist of a wide variety of structural components and configurations. While the design process as a whole will not be explored here, it is important to establish consistent terminology for the various potential components of permeable pavement.

The "surface course" directly receives the traffic load and is the initial contact area for stormwater interception. There are several different types and materials of permeable pavement surface courses, and these will be categorized and discussed further in Section 2.5. Typically, below the surface course is a "base course" which increases the overall thickness of a pavement to spread out the traffic load and to facilitate drainage and provide more capacity for temporary water storage (Ferguson, 2005). The base course usually consists of crushed aggregate and/or sands, and may be situated directly above the sub-grade, which is the underlying soil. Certain installations may additionally contain a "sub-base course", which is an additional layer of aggregate located between the base course and sub-grade, and which adds further water storage capacity. Aggregate sizes for the base and sub-base courses are highly dependent upon surfacing type and specific design goals for the permeable pavement installation. There also may be a perforated pipe underdrain system in locations where native soils do not infiltrate well or where it is undesirable to infiltrate (Fancher *et al*, 2003). In this case, the infiltrated water would then be discharged to a conveyance system such as a conventional storm sewer (Kresin, 1996).

Some permeable pavements, especially those utilizing paving blocks (see Section 2.5) contain a bedding course, also called a leveling course, in between the surface and base courses. Typically the bedding course consists of relatively small aggregate on which the pavement is placed and leveled (Ferguson, 2005). Some permeable pavement surfaces contain large aggregate-filled drainage voids as part of their design, which will be discussed in Section 2.5. The aggregate that is used to fill the voids has many terms, such as drainage cell material, fill aggregate or joint fill. Often the material used in these drainage voids is the same as that used in the bedding course (Ferguson, 2005).

There may be a layer of geotextile filter fabric that separates the bedding course from the base course, or the base course from the sub-grade. When installed between the base course and sub-grade (or sub-base and sub-grade), it is used to separate the aggregate from the underlying soil, preventing the migration of fines into the main structure (Cahill Associates Inc., 2005). When installed beneath the bedding course, in addition to keeping the bedding course separated from the base course, it may play a role in filtration of pollutants (Pratt *et al*, 1990; Bond *et al*, 1999).

## 2.5 Permeable Pavement Surface Course

There are several different types of permeable pavement surface courses, each with distinguishing physical characteristics. There is significant discrepancy in terms of the categorization and terminology of the different types of surface courses. One of the most broad-encompassing categorization systems, and the one that will be used for the purposes of this thesis, is that used by Ferguson (2005). This categorization breaks

permeable pavement into nine specific categories, as follows: porous asphalt, porous concrete, open-jointed paving blocks, open-celled paving grids, plastic geo-cells, porous turf, porous aggregate, soft paving materials, and decks.

### 2.5.1 Porous Asphalt

Porous asphalt pavement was first developed in the early 1970's and consists of standard bituminous asphalt in which the fines have been screened and reduced, thus creating small voids and allowing water to pass through (Cahill Associates Inc., 2005). Porous asphalt is usually placed directly on a gravel base course.

### 2.5.2 Porous Concrete

Porous concrete was also developed in the early 1970's (Hun-Dorris, 2005). Similar to porous asphalt, porous concrete is produced by substantially reducing the number of fines in the mix in order to establish voids for drainage. It is cast-in-place to form a rigid pavement slab (Ferguson, 2006), and has a coarser appearance than its conventional counterpart (Cahill Associates Inc., 2005).

### 2.5.3 Open-Jointed Paving Blocks

Open-jointed paving blocks consist of interlocking load-bearing units (often constructed of concrete) that are shaped such that, when laid, they produce open voids between adjacent units. The voids can then be filled with porous aggregate or turf (Cahill Associates Inc., 2005). It is this fill material that gives the pavement its porosity and permeability (Ferguson, 2006). Open-jointed paving blocks are also referred to as

permeable unit pavers, modular interlocking concrete blocks with external drainage cells (MICBEC), or permeable interlocking concrete pavers (PICP).

### 2.5.4 Open-Celled Paving Grids

Open-celled paving grids are units of concrete or brick, which are designed with open cells that can be filled with porous aggregate or grass (Ferguson, 2006). The units are laid side by side and the resulting surface is a gridwork of solid supporting ribs. The solid interlocking units provide structural stability while the vegetation or aggregate in between the grids allows for stormwater infiltration. In situations where grass is used, the pavement can often have an external appearance of a green open space (Ferguson, 2006). Open-celled paving grids are also called turf pavers, modular interlocking concrete blocks with internal drainage cells (MICBIC), or concrete grid pavers (CGP).

### 2.5.5 Plastic Geocells

Plastic geocells are manufactured lattice-like products that hold aggregate or topsoil in their cells, resisting displacement and compaction (Ferguson, 2005). They are similar in functionality to open-celled paving grids, but are more flexible and less structurally stable (Ferguson, 2005). Plastic products can be advantageous due to their light weight and relative ease of installation (Booth and Leavitt, 1999). With adequate base and subgrade preparation, these systems are capable of supporting vehicular traffic loads (Booth and Leavitt, 1999). Fully established plastic geocells are usually completely covered with grass or gravel.

### *2.5.6 Porous Turf, Porous Aggregate, Soft Paving Materials, and Decks*

The remaining categories of permeable pavement are less commonly used for vehicular traffic and require less design and construction considerations from an engineering perspective. As such, they will not be described in this thesis.

## 2.6 Potential Disadvantages/Limitations

In permeable pavement setups where water is allowed to percolate into surrounding soil, a common concern is the potential risk of the stormwater carrying pollutants and impacting nearby groundwater. There has been extensive research showing that the risk of permeable pavement effluent contaminating groundwater or sub-grade soil is very low due to the effective filtration capability of permeable pavements and the low quantity of pollutants in effluent (Dierkes *et al*, 1999; Legret and Colandini, 1999; Legret *et al*, 1999; Dierkes *et al*, 2002; Rankin and Ball, 2004). However, the risk may still be present in some situations, and permeable pavements should not be installed near "stormwater hotspots", including vehicle service and maintenance areas, fuelling stations, or industrial facilities with hazardous waste (McNally *et al*, 2005). The US EPA (1999) recommends a minimum four foot separation between the bottom of a porous pavement system and underlying bedrock or water table. Effluent quality of permeable pavements will be discussed further in Section 2.8.1.

Paving block and paving grid surfaces may be more susceptible to abrasion and damage than conventional pavements because of the voids in the surface structure (Dierkes *et al*, 2002). This is a significant consideration for northern climates such as

Calgary, where snow removal equipment is regularly used on road surfaces. Paving block and grid systems in general should be limited to low-speed traffic areas (< 60 km/h). The concern is that drainage aggregate from paving blocks can be kicked up and the surface can be compromised with higher traffic speeds (Fancher *et al*, 2003).

There are some potential structural problems associated with porous asphalt pavements. Due to the high void volume, there can be rutting and deformation under heavy loads, and they are susceptible to structural distress when the bitumen-aggregate bond is weakened due to contact with water (St. John and Horner, 1997). Additionally, spillage of gasoline and other hydrocarbons from automobiles may break down the asphalt binder to greater depths than on conventional pavements since the pores permit liquid penetration (Field *et al*, 1982; Rodriguez *et al*, 2005).

By far the most significant potential limitation to all permeable pavements is their sensitivity to clogging with sediments, and the subsequent decline in infiltration capacity. Many studies have focused on this area, and the subject will be reviewed further in Section 2.8. As a result of the clogging potential, special cleaning and maintenance methods must be implemented to ensure sufficient infiltration capacity in permeable pavement, which introduces added labor and costs when compared to conventional pavement.

## 2.7 Attenuation and Runoff Reduction

There have been extensive studies that have shown that all types of permeable pavements are capable of significantly reducing surface runoff, attenuating discharge

peaks and producing a lagged response to rainfall inputs (Pratt *et al*, 1995; Andersen *et al*, 1999; Booth and Leavitt, 1999; Pagotto *et al*, 2000; Hunt *et al*, 2002; Schluter *et al*, 2002; Brattebo and Booth, 2003; Shackel *et al*, 2003; Rankin and Ball, 2004; Briggs *et al*, 2005). The quantitative degree to which these hydrologic improvements occur is dependent on many factors and is unique for every permeable pavement installation (Kuang and Sansalone, 2006). As such, data from these studies are only valuable for the specific site and conditions in which they apply, and specific numerical results will therefore not be presented in this literature review.

With regards to runoff reduction for permeable pavements, it is important to explain and define an "I/P ratio". An I/P ratio is the ratio of impervious to permeable pavement area for the permeable pavement surface (Urban Water Resources Centre, 2002). In practice, permeable pavements may receive both the directly incident rainfall and runoff from adjacent areas. As such, one must consider the drainage area upstream of the permeable pavement area, as well as the area of the pavement itself. Permeable pavements installed in locations with higher I/P ratios will naturally receive more runoff than those installed in locations with lower I/P ratios. This factor is often overlooked in the literature when evaluating the performance of permeable pavements in reducing surface runoff.

## 2.8 Surface Infiltration Capacities, Sealing/Clogging, and Maintenance

Surface infiltration capacity is a measure of the pavement's ability to drain water from its surface into its base and/or sub-base. According to James (2004), "The

infiltration capacity is the result of the combined forces acting on the water molecules, including gravity, negative pore water pressure, drag forces on the aggregate acting against the flow, and the forces associated with passage of air upwards escaping the base aggregate". It is one of the most fundamentally important measures of a permeable pavement's adequacy as a stormwater management system. Factors leading to surface infiltration capacity degradation, as well as potential methods of restoration, have been the topic of increasingly more research in recent years.

Previous studies on permeable pavements have shown widely varying results for both initial and long-term infiltration capacities. Even studies on installations of similar ages and in the same geographic region often report very different results. A compilation of reported literature values for infiltration capacities of permeable pavements from a variety of studies, along with descriptions of the studies themselves, is presented in Table 2-1. As much relevant information as possible has been provided about the studies, but in some instances complete information was not available. The reason there is such a wide discrepancy in results is that there are such a large number of factors that affect the infiltration capacity of permeable pavement.

**Table 2-1: Summary of Research on Infiltration Capacities of Permeable Pavement**

| Author | Description of Installation/Study | Surface Infiltration Capacity Findings | Notes/Comments |
|---|---|---|---|
| (Hossain *et al*, 1992) | 1067 m long porous asphalt test section on lanes of an Arizona highway near Phoenix. Received heavy traffic. No maintenance program reported. | Initial: 2540 mm/hr<br><br>After 5 years: 711 mm/hr | |
| (Borgwardt, 1994) | Field evaluation of two train station parking lots in Germany, consisting of UNI Eco-Stone® (open-jointed paving blocks) aged two and five years. No maintenance program reported. | <u>2 year old lot</u><br>72 mm/hr (saturated conditions)<br><br><u>5 year old lot</u><br>145 mm/hr (saturated conditions) | Newer installation showed lower infiltration capacities due to presence of fine sand in drainage openings and poorly washed aggregate base material. |
| (Balades *et al*, 1995) | Field evaluation in France where various street cleaning techniques were applied to permeable pavement surfaces in an attempt to restore infiltration capacity. Unfortunately the types of pavement surfaces were not reported in the study itself, but Ferguson (2005), when citing this study, states that the pavements were porous asphalt. | <u>Sweeping followed by suction</u><br>- When infiltration capacity was less than 3600 mm/hr, no improvement.<br>- When infiltration capacity was between 28800 and 36000 mm/hr, original rates (54000-58000 mm/hr) obtained after 2 passes.<br><br><u>Suction only</u><br>1st site, initial: 1800 mm/hr<br>After 2 passes: 7200 mm/hr<br>2nd site, initial: 54000 mm/hr<br>After 2 passes: 72000 mm/hr.<br><br><u>High pressure wash with suction</u><br>Shopping mall, initial: 2520-7200 | Moistening followed by suction actually had a negative effect on infiltration capacities.<br><br>In addition to maintenance observations, it was found that, in general, in the first year of operation of various permeable pavement types, there was little change in infiltration capacity, but thereafter decline was rapid, reaching 50% of the original rate after 2 or 3 years. |

| Author | Description of Installation/Study | Surface Infiltration Capacity Findings | Notes/Comments |
|---|---|---|---|
| | | mm/hr<br>After 2 passes: 21600 mm/hr<br><br>Industrial park, initial: 10800 mm/hr<br>After 2 passes: 21600 mm/hr | |
| (Pratt *et al*, 1995) | Two sites on public car parking lots with 9 year old open-celled paving grids in the UK. Received no maintenance. | After 9 years of operation: 990 mm/hr | |
| (Kresin *et al*, 1997) | Point measurements of infiltration capacity taken at a number of plots at 2 UNI Eco-Stone® (open-jointed paving block) installations of different ages in Guelph, Ontario. Top 5 mm of fill aggregate removed and tests repeated to investigate regeneration of infiltration capacity. | <u>Site 1 (3 years old) Averages:</u><br>Initial: 5.8 mm/hr<br>After removing 5 mm fill: 7.7 mm/hr<br><br><u>Site 2 (1 year old) Averages:</u><br>Initial: 14.9 mm/hr<br>After removing 5 mm fill: 40.0 mm/hr | <u>% fill material < 75 microns</u><br>Site 1: 6.6%<br>Site 2: 1.9% |
| (St. John and Horner, 1997) | 2-year old porous asphalt shoulder test sections on highway in Redmond, Washington. The soil underlying the porous asphalt test sections was gravel-sand fill material. The test sections consisted of mix AR-4000 binder. 2 years worth of winter sanding material were applied with simulated rainfall. | After 11 months: 44500 mm/hr<br><br>After 20 months: 1450 mm/hr<br><br>After 48 months, following manual winter sanding application: 36 mm/hr | Difficult to distinguish between effects of winter sand application and accumulation of natural sediment of the test sections between 20 and 48 months of pavement's life. |
| (Fwa *et al*, 1999) | Laboratory test in Singapore to assess clogging potential of various mixes of porous asphalt. 100 mm thick asphalt layer, | <u>Mix W6</u><br>Initial: 27969 mm/hr<br>Terminal: 1818 mm/hr | W6, PA and PB each contain about 90% aggregate coarser than 2 mm, while almost 100% |

| Author | Description of Installation/Study | Surface Infiltration Capacity Findings | Notes/Comments |
|---|---|---|---|
| | 500 mm X 500 mm, no sub-surface layers. Known quantities of local residual soils applied, followed by known volumes of water, repeatedly until infiltration capacity remained constant. | Mix PA<br>Initial: 63962 mm/hr<br>Terminal: 4752 mm/hr<br><br>Mix PB<br>Initial: 77160 mm/hr<br>Terminal: 5640 mm/hr<br><br>Mix PE<br>Initial: 210312 mm/hr<br>Terminal: 117232 mm/hr | was above 2 mm for PE. PE also had significantly higher air void % than the other mixes.<br><br>W6 had 4% binder Penetration Grade 60/70 Asphalt, while all other mixes had 5% binder Polymer Modified Asphalt. |
| (Dierkes *et al*, 2002) | 15 year old open-jointed paving block installation in Stadtlohn, Germany, 1-3 mm fill aggregate, bedding course depth of 5-8 cm (2-5 mm aggregate), 20-25 cm thick sub-base of crushed stones (8-45 mm aggregate), no filter layer. Very high daily traffic frequency. | Central region of parking box: 440 L/s/ha (158 mm/hr)<br><br>Edges of parking box: 2000 L/s/ha (720 mm/hr) | |
| (Dierkes *et al*, 2002) | Experimented with a relatively new type of cleaning device that works as a high pressure cleaner with direct vacuum suction. The device was used to clean a 4-year old open-jointed paving block installation in Germany. Infiltration capacities were measured before and after at 3 randomly selected points. | Before cleaning: less than 1 L/s/ha (0.36 mm/hr) in all locations.<br><br>After cleaning: 1545 – 5276 L/s/ha (556 – 1899 mm/hr) | |
| (Urban Water Resources Centre, | Laboratory investigation: Determined "effective life" of 3 types of permeable pavement by observing changes in infiltration capacity resulting from artificial | Laboratory<br>Formpave, Initial: 151000 mm/hr<br>35 sim. Years: 72000 mm/hr | For lab tests, average reduction of hydraulic conductivity was 59%, 68% and 75%, respectively, for Formpave, |

| Author | Description of Installation/Study | Surface Infiltration Capacity Findings | Notes/Comments |
|---|---|---|---|
| 2002b) | sediment loading. Types 1 and 2: Formpave and Ecoloc (both open-jointed paving block), 50 mm bedding layer, 300 mm base course, separated by geotextile. Type 3: Grasspave (plastic geocell), geotextile below surface, no bedding layer, 300 mm base course.<br><br>Field investigation: Four separate field sites near Adelaide, Australia monitored over a one year period. Site 1: Formpave, 1 year old. Site 2: Formpave, 6 months old. Site 3: Ecoloc, 1 year old. Site 4: Grasspave, 3 years old. | Ecoloc, Initial: 130000 mm/hr 35 sim. Years: 58000 mm/hr<br><br>Grasspave, Initial: 14400 mm/hr 35 sim. Years: 3600 mm/hr<br><br>Field<br>Site 1, Initial: 900 mm/hr<br>After 12 months: 211 mm/hr<br><br>Site 3, Initial: 2571 mm/hr<br>After 12 months: 592 mm/hr<br><br>Site 4, Initial: 614 mm/hr<br>After 12 months: 202 mm/hr | Ecoloc and Grasspave, over 35 simulated years of sediment application.<br><br>For field tests, Site 2 had data processing problems.<br><br>Extreme discrepancy between laboratory and field infiltration capacity measurements. |
| (James and Gerrits, 2003) | Two different 8 year old UNI Eco-Stone[®] (open-jointed paving block) installations at Guelph, Ontario. Difference between two types was the thickness of the bedding layer (75 mm and 100 mm). Base course was 400 mm layer of granular A aggregate. No maintenance procedures other than snow removal and spring sweeping had been performed. Infiltration capacity was measured before and after various depths of drainage cell material was manually excavated. Multiple "traffic zones" were investigated. | 75 mm bedding layer<br>Low traffic, initial: 150 mm/hr<br>After excavating 20 mm: 200 mm/hr<br>Med. Traffic, initial: 15 mm/hr<br>After excavating 20 mm: 200 mm/hr<br><br>100 mm bedding layer<br>Low traffic, initial: 9 mm/hr<br>After excavating 20 mm: 24 mm/hr<br>Med. Traffic, initial: 3 mm/hr<br>After excavating 20 mm: no change | Highly trafficked areas showed little to no improvement in infiltration capacity for both installations.<br><br>Thicker bedding layer had less initial infiltration capacities as well as less improvement after excavation. |
| (Clausen, 2004) | UNI Eco-Stone[®] (open-jointed paving blocks) at a residential community in | Initial: 196 mm/hr<br>After 1 year of operation: 153 | |

| Author | Description of Installation/Study | Surface Infiltration Capacity Findings mm/hr | Notes/Comments |
|--------|-----------------------------------|----------------------------------------------|----------------|
| | Connecticut. | | |
| (James, 2004) | Collected street sediment was applied in conjunction with intense artificial rains to a full-scaled UNI Eco-Stone® (open-jointed paving block) outdoor model rig in Guelph, Ontario. Different types/combinations of fill, bedding, and base course aggregate were studied. | Experiment #1<br>Initial: 252 mm/hr<br>After 4.8 kg/m² TSS: 17 mm/hr<br><br>Experiment #2<br>Initial: 152 mm/hr<br>After 3.4 kg/m² TSS: 67 mm/hr<br><br>Experiment #3<br>Initial: 263 mm/hr<br>After 6.4 kg/m² TSS: 171 mm/hr | Experiment 1 – 250 mm "Aerofoil" base, no bedding layer, 40 mm "aerofoil" fill<br>Experiment 2 – 250 mm "Aerofoil" base, no bedding layer, 40 mm 1:1 sand fill<br>Experiment 3 – 200 mm "Milton Granular A" base, 5 mm "Aerofoil" bedding layer, 40 mm 1:3 sand fill |
| (Briggs et al, 2005) | 100 mm open-graded friction course porous asphalt in Durham, New Hampshire, monitored during winter at 3 locations monthly over first 6 months of installation's life. Pavement was subjected to heavy winter sanding and salt. | Nov '04: 2500 mm/hr (3 location avg)<br><br>Jan '05: 4100 mm/hr (3 location avg)<br><br>Feb '05: 3600 mm/hr (3 location avg)<br><br>Mar '05: 3600 mm/hr (3 location avg)<br><br>Apr '05: 4200 mm/hr (3 location avg) | No consistent change seen over study period, despite heavy winter sanding. |
| (Bean, 2005) | 15 open-celled paving grids, 14 open-jointed paving blocks, and 11 porous concrete field sites were tested in North Carolina, Maryland, Virginia, and Delaware to determine surface infiltration capacities. | Open-Celled Paving Grids<br>Median pre-maintenance: 49 mm/hr<br>Median post-maintenance: 86 mm/hr<br><br>Open-Jointed Paving Blocks | Open-celled paving grids were filled with soil and grassy vegetation, while paving blocks were filled with coarser aggregate. |

| Author | Description of Installation/Study | Surface Infiltration Capacity Findings | Notes/Comments |
|---|---|---|---|
| | Effects of maintenance and proximity to fines were investigated. Maintenance consisted of removing the top layer of residual material (13-19 mm). | Median, sites w/out fines: 20000 mm/hr<br>Median, sites w/ fines: 80 mm/hr<br><br>Porous concrete<br>Median, sites w/out fines: 40000 mm/hr<br>Median, sites w/ fines: 130 mm/hr | On average, maintaining the paving grid lots increased the permeability by 76%. Similarly, close proximity to fines decreased infiltration capacity by about 99%. |
| (Dierkes *et al*, 2005) | 6 month old open-jointed paving block field installation in Germany. Different joint fills were used to identity the effects of the material. Fills used were: limestone split 2/5 mm, recycled concrete, limestone split 1/3 mm, volcanic material, and recycled "blend" material. | Split 2/5: 3800 mm/hr<br>Split 1/3: 5000 mm/hr<br>Volcanic: approx. 13000 mm/hr<br>Blend: approx. 6100 mm/hr<br>Recycled Concrete: Approx. 14600 mm/hr | The steeper gradation (1-3 mm) surprisingly had a higher infiltration capacity. |

*2.8.1 Factors Affecting Infiltration Capacity*

It is important to identify the factors that can affect surface infiltration capacity of permeable pavement because it may help in devising methods to extend the hydraulic life of the pavement, and will assist in the design of permeable pavement installations on a regional basis.

General factors affecting infiltration capacity include overall site usage (e.g. parking lot vs. major roadway), frequency of use, adjacent land use, site maintenance practices (e.g. winter sanding and salting, street sweeping), and age of the pavement installation (Kresin, 1996). James and Gerrits (2003) found the infiltration capacity to be much lower in areas of high traffic intensity, and found that small amounts of vegetation in the drainage voids of paving block installations actually improved infiltration capacity. Davies (2002) found that the level of compaction of permeable pavement surfacing has a significant effect on its infiltration capacity, with highly compacted surfaces showing much lower values than less compacted surfaces.

Specifically for paving block and paving grid installations, the material and gradation of the bedding layer and joint fill material, as well as the area and depth of the drainage voids themselves, have a significant impact on infiltration capacity (James and Gerrits, 2003). For porous asphalt and porous concrete installations, pore structure characteristics such as pore size distribution, void space, tortuosity and specific surface area can affect hydraulic functioning (Kuang and Sansalone, 2006), as well as binder content, binder type, and the percentage of  coarse aggregate (over 2 mm) in the mix (Fwa *et al*, 1999).

The combined effects of the above factors on infiltration capacity and how each particular pavement will respond are highly unpredictable (Kresin, 1996). Additionally, surface infiltration capacities for permeable pavements have been found to be extremely spatially variable (Kresin *et al*, 1997; Briggs *et al*, 2005; Dierkes *et al*, 2005). Spatial variations which can affect infiltration rate in a non-uniform manner include compaction from traffic in specific locations (i.e., wheel ruts), vegetative growth, and heavier sediment deposition in low lying areas of the pavement surface (Kresin *et al*, 1997). This variability and unpredictability in infiltration capacities is the underlying reason why there is such a large discrepancy between reported literature values for hydraulic performance. This highlights the need to study permeable pavements for specific scenarios and locations, and exemplifies why one cannot simply take performance data from one source and assume it applies adequately to another scenario.

### 2.8.2 Clogging/Surface Sealing

In general, the factors mentioned in Section 2.8.1 can combine over time in any number of ways to create an accumulation of fine, compacted matter on the upper surface of the pavements, often referred to as a "crust". When the crust forms, the infiltration capacity is substantially reduced, eventually to the point of completely negating the hydraulic performance of the permeable pavement. When that occurs, the pavement is considered "clogged".

Clogging, or surface sealing, in permeable pavements has been the topic of numerous studies over the past two decades. Balades *et al* (1995) describe the clogging process for permeable pavement structures as beginning with coarser (i.e. coarse sand)

particles getting caught in the surface of the permeable surfacing material, followed by pores located between the grains of sand becoming obstructed by progressively finer particles which can no longer migrate within the pavement structure. The capacity for particles to pass through the upper layers of the pavement decreases slowly and progressively as finer and finer particles are trapped, until a relatively impermeable matrix (or "crust") is formed (Balades *et al*, 1995).

Studies of density of pavement layers using gamma rays, by Balades *et al* (1995), have shown that the clogged area is usually limited to the upper few centimeters of the surface structure. Several other studies have confirmed this qualitatively (Balades *et al*, 1995; Pratt *et al*, 1995; James and Gerrits, 2003; James, 2004). Clogging in permeable pavements is therefore characterized by an increase in the quantity of material retained in the upper surface, and not necessarily by migration of sediment particles to the sub-surface layers of the structure (Balades *et al*, 1995). Although the ultimate cause of clogging is the accumulation of fine sediment in the upper pavement pores (James, 2004), this must be preceded by the accumulation of coarser material in order to trap the fine particles.

In terms of the specific characteristics of accumulated surface material that are responsible for reduced infiltration capacities and eventual clogging, the presence of fine sediment matter appears to be the most significant. Permeable pavement sites free of fines have been reported to have significantly higher infiltration capacities than sites with sandy fines present (Bean *et al*, 2004). Colandini *et al* (1995) found clogging materials to mostly be composed of sand, with a variable silt proportion and a very low content of clay.

The primary mechanisms that lead to the deposition of fine matter on permeable pavement surfaces are increased mechanical wear, the deposition of rubber, brake dust, and petroleum products from automobile traffic (Kresin *et al*, 1997), as well as local residual soils deposited from stormwater runoff or dirty wheels (Cahill, 1994; Fwa *et al*, 1999). Also of importance is the grinding, crushing, and compaction action of vehicular traffic (Kresin *et al*, 1997) on surface sediments. Atmospheric deposition, in which nearby fines become airborne and are deposited on the surface by wind or precipitation, also plays a role.

The amount of time until a crust forms and clogging occurs for a specific permeable pavement is entirely different for individual cases. Given the wide range of influencing factors in the infiltration capacity and clogging potential of permeable pavements, it is difficult to predict the ultimate time to failure for permeable pavements in general (Pratt *et al*, 1995).

### 2.8.3 Possible Maintenance Activities

Although there is certainly a progressive loss of surface infiltration capacity over the lifespan of the permeable pavement due to accumulation of sediment, there is significant evidence showing that proper maintenance can restore most or all of the infiltration capacity and extend the functional life of the pavements. Maintenance operations focus on trying to remove the material responsible for clogging in the upper section of the surface course. The type, frequency, and success of maintenance operations vary between different pavement surface types, as well as local geological and climate conditions.

James and Gerrits (2003) studied an eight year old UNI Eco-Stone® (open-jointed paving block) installation, in which no maintenance procedures other than snow removal and spring sweeping had been performed since the pavement was first installed. Infiltration capacity was measured at 110 test plots, and in order to test the regeneration of infiltration capacity, various depths of drainage cell material were manually removed (2.5, 5, 10, 25, and 50 mm), and infiltration capacities measured again. They found that regeneration of infiltration capacity could be accomplished by removing small amounts of drainage cell material from the paving blocks. The detailed results for this study appear in the infiltration research summary in Table 2-1.

Balades *et al* (1995) applied various street cleaning techniques to several different permeable pavements, including parking lots and heavily trafficked roads. Infiltration rates were measured before and after cleaning, and the rates are summarized in Table 2-1. The study found that moistening followed by sweeping actually had a negative effect on infiltration capacities. Sweeping with suction produced positive effects, and high pressure water jet with simultaneous suction were the most successful at restoring infiltration rates. Unfortunately the study did not specify the types of permeable pavements that were analyzed, although Ferguson (2005), when citing this study, states that the pavements were porous asphalt.

Dierkes *et al* (2002) experimented with a relatively new type of cleaning device that works as a high pressure cleaner with direct vacuum suction. The device was used to clean a 4-year old open-jointed paving block installation. Results are shown in Table 2-1. The device improved infiltration capacities significantly.

In addition to the above maintenance techniques, it is also an option in the case of paving grids or blocks, to temporarily remove the blocks and replace the bedding material. Pratt *et al* (1995) states that this is the best long-term (i.e. 10-15 years) maintenance, since the paving blocks/grids can be easily and cheaply removed and reconstructed. Porous asphalt and porous concrete are at a disadvantage in that the surface course must be replaced in its entirety once it is irreversibly sealed (Kresin *et al*, 1997).

Further research is needed to determine appropriate maintenance activities for specific types and locations of permeable pavement.


## 2.9 Water Quality

Major pollutants, and their sources, that can be found in urban stormwater runoff can be categorized as shown in Table 2-2.

**Table 2-2: Types and Sources of Pollutants in Urban Runoff (from (Rankin and Ball, 2004))**

| Pollutant | Potential Sources |
| --- | --- |
| Sediment | Pavement wear, vehicular tire tracking, maintenance activities, runoff from adjacent land |
| Nitrogen | Roadside fertilizer applications |
| Phosphorus | Roadside fertilizer applications |
| Lead | Auto exhaust, tire wear, lubricating oil and grease, bearing wear |
| Zinc | Tire wear, motor oil, grease |
| Iron | Auto rust, steel highway structures (guard rails), moving engine parts |
| Copper | Metal plating, bearing and brush wear, moving engine parts, brake lining wear, fungicides, insecticides, pesticides |
| Cadmium | Tire wear, insecticide application |
| Chromium | Metal plating, moving parts, brake lining wear |
| Nickel | Diesel fuel and gasoline exhaust, lubricating oil, metal plating, brush wear, brake lining wear, asphalt paving |
| Manganese | Moving engine parts, auto exhaust |
| Cyanide | Deicing compounds |
| Sodium/Calcium Chloride | Deicing salts |
| Sulfate | Roadway surfaces, fuels, deicing salts |
| Petroleum Hydrocarbons | Spills, leaks, motor lubricants, anti-freeze and hydraulic fluids, asphalt surface leachate |
| PCB | PCB catalyst in synthetic tires |
| PAH | Asphalt surface leachate |

Permeable pavement has been shown to be capable of removing some of these pollutants from stormwater runoff through the mechanisms of filtration, adsorption, and biological activity.

### 2.9.1 Total Suspended Solids (TSS) Removal

Total Suspended Solids (TSS) is a highly important pollutant to remove from stormwater runoff because it is harmful to aquatic ecosystems. It increases water turbidity, inhibits plant growth and diversity, affects river biota, and reduces the overall

number of aquatic species. The specific size of solids present is also an important factor, as it may have different impacts on the above mentioned harmful effects. In addition, several pollutants, including certain heavy metals, lead, phosphorus, and PAHs tend to be associated with particulate matter, especially finer particles (Balades *et al*, 1995; Colandini *et al*, 1995; Legret and Colandini, 1999; Environment Australia, 2002; Walker and Hurl, 2002; Teng and Sansalone, 2004). There is currently debate as to what particular size fraction of TSS is the most important to remove from stormwater runoff, but current City of Calgary and Alberta Environment regulations state that 85% of TSS greater than or equal to 75 microns must be removed. Very little research to date has been done into the analysis of the removal of specific size fractions of TSS by permeable pavements, and this will be a major focus of this thesis.

The primary mechanism behind TSS removal is mechanical filtration through the pavement structure (Stotz and Krauth, 1994; Urban Water Resources Centre, 2002a). As described in Section 2.8.2, most solids accumulation (and thus removal) has been found to occur in the top several centimeters of the pavement structure. The geotextile layer above the base course may also play a role in limiting the transport of pollutants into the sub-structure, and can affect overall filtration efficiency (Pratt *et al*, 1990; Bond *et al*, 1999). Effluent from permeable pavements generally has a finer gradation than the influent due to the filtration processes (Legret *et al*, 1996).

### 2.9.2 Heavy Metal Removal

There has been extensive research done on heavy metal removal efficiency for permeable pavements. In general all types of permeable pavements have been shown to be

effective at trapping dissolved heavy metals in runoff to some degree (Dierkes *et al*, 1999;

Legret and Colandini, 1999; Dierkes *et al*, 2002; Brattebo and Booth, 2003; Fach and

Geiger, 2005). Specific removal efficiencies are dependent upon the characteristics of the

individual pavement installations and the characteristics of the influent.

Heavy metals in permeable pavements are primarily removed by filtration, as

indicated by findings that most metals are precipitated in the upper 2 cm of the surfacing

layer of permeable pavement, with very little migration into the structure itself (Legret *et

al*, 1996; Dierkes *et al*, 1999; Legret and Colandini, 1999; Dierkes *et al*, 2002). This is not

surprising since the same trend has been found with total suspended solids (as discussed in

Section 2.8.2) and metals have been found to be associated with solids, especially sizes of

less than 100 μm (Colandini *et al*, 1995; Andral, 1999). Again this illustrates the

importance of determining the sizes of particles that are removed from stormwater by

permeable pavements.


### *2.9.3 Oil biodegradation*

Substantial quantities of hydrocarbons can be deposited on pavement surfaces by

vehicular traffic, and this poses a concern with regards to effluent quality of permeable

pavements. There has been some research conducted into the ability of permeable

pavement structures to retain and treat petroleum-based pollutants through microbial bio-

degradation (Pratt *et al*, 1999; Newman *et al*, 2002a; Newman *et al*, 2002b; Coupe *et al*,

2003; Bayon *et al*, 2005; Puehmeier *et al*, 2005; Spicer *et al*, 2005)

Pratt *et al* (1999) subjected a full-scale model permeable pavement to

hydrocarbon contamination representative of typical urban loadings and monitored water

quality and bio-degradation indicators. The study found that petroleum contamination in the effluent was reduced to 2.4% of the oil applied to the structure, and that the structure could be used as an effective in-situ aerobic bioreactor.

Bacteria are not the only inhabitants of oil-degrading bio-films in permeable pavements. Newman *et al* (2002b) studied the development of protozoan colonies after a fixed period of time. Six months after setting up the model structures, a complex community had been produced, and bacteria, fungi, all the major protozoan groups and metazoa were observed to inhabit the permeable pavement system. These microorganisms may also play an important role in oil degradation within permeable pavement.

### 2.9.4 Summary of Water Quality Findings

Table 2-3 contains a summary of reported literature data for the efficiency of permeable pavements in removing various pollutants from stormwater runoff. Similar to the data for infiltration capacities, there is clearly a large discrepancy between the water quality performances of permeable pavements, depending on the pavement type, usage, and location.

**Table 2-3: Research Summary for Water Quality Improvement Through The Use of Permeable Pavements**

| Author | Type of Permeable Pavement Surface | Reported Removal Efficiency (%) [Average Effluent Concentration, if reported] | | | |
|---|---|---|---|---|---|
| | | **TSS** | **Heavy Metals** | **Nutrients** | **Hydrocarbons** |
| (Dierkes *et al*, 1999) | Open-jointed paving blocks, 2/5 mm bedding layer, 9/32 mm gravel base course. Joints are filled with 0/2 mm sand. | | Cd – 98% [0.7 µg/L] Cu – 96% [18 µg/L] Pb – 98% [<4 µg/L] Zn – 97% [19 µg/L] | | |
| (Pratt *et al*, 1999) | Open-jointed paving blocks w/ gravel bedding layer and 20-50 mm granite base course, geotextile between bedding layer and base course. | | | | 97.6% [22 mg/L] |
| (Rushton, 2001) | Open-jointed paving blocks with swale | 92% [4 mg/L] | Cu – 88% [3.35 µg/L] Pb – 89% [1.25 µg/L] Zn – 82% [18.6 µg/L] | TN – 57% [0.496 mg/L] TP – 40% [0.131 mg/L] | |
| (Urban Water Resources Centre, 2002a) | Open-jointed paving blocks, 50 mm bedding layer (6 mm screenings), 300 mm base course (20 mm gravel), with geotextile between bedding layer and base course. | 40% [52 mg/L] | Cd – <MDL[1] Cu –11% [na] Ni – 22% [2.2 µg/L] Pb – 44% [16.8 µg/L] Zn – 43% [75 µg/L] | TKN - 49% [0.64 mg/L] TP - 43% [0.0768 mg/L] | |
| (Fach and Geiger, 2005) | Open-jointed paving blocks and porous concrete with 30 mm bedding layer (2/5 mm) and 400 mm thick base course (0/45 mm gravel). | | Cu – 96-99% for all surface types Pb – 96-99% for all surface types Zn – 96-99% for all surface types | | |

| Author | Type of Permeable Pavement Surface | Reported Removal Efficiency (%) [Average Effluent Concentration, if reported] | | | |
|---|---|---|---|---|---|
| | | TSS | Heavy Metals | Nutrients | Hydrocarbons |
| (Dierkes *et al*, 2005) | Open-jointed paving blocks, laboratory setting, 0/45 mm base course, various joint fill materials used. Negligible difference between results for different joint fill. | | Cd – 99%<br>Cu – 98%<br>Pb – 99%<br>Zn – 94-96% | | |
| (Bean, 2005) | Open-jointed paving blocks, 80 mm No. 72 stone bedding layer, 200 mm No. 57 stone base course. | 72% [12.4 mg/L] | Cu – 63% [6 μg/L]<br>Zn – 88% [8 μg/L] | TP – 65% [0.07 mg/L]<br>TN – 35% [0.98 mg/L] | |
| (Hogland *et al*, 1987) | Porous asphalt w/ base course of unreported composition and thickness. Pollution is a result of snowmelt. | 95% [38 mg/L] | Cd – 33% [0.04 μg/L]<br>Cu – 42% [0.22 μg/L]<br>Pb – 50% [0.02 μg/L]<br>Zn – 62% [0.22 μg/L] | TP – 71% [0.04 mg/L]<br>TKN – Increase [0.5 mg/L] | |
| (Balades *et al*, 1995) | Porous asphalt | 80-90% | Pb – 80-90% | | |
| (Legret *et al*, 1996) | 0/14 mm porous asphalt (60 mm thick), 0/20 mm stabilized aggregate bedding layer (200 mm thick), 10/80 mm crushed stones base course (350 mm thick). | 64% [12 mg/L] | Cd – 67% [0.49 μg/L]<br>Cu – Increase [15 μg/L]<br>Pb – 79% [5.4 μg/L]<br>Zn – 72% [46 μg/L] | | <MDL[1] |
| (Legret and Colandini, 1999) | 60 mm layer of 0/14 mm porous asphalt, 200 mm layer of aggregate bedding layer, 350 mm layer of 10/80 mm | 77% [7 mg/L] | Cd – 81% [0.25 μg/L]<br>Cu –26% [8.26 μg/L]<br>Pb – 91% [2.43 μg/L]<br>Zn – 72% [45.6 μg/L] | | |

| Author | Type of Permeable Pavement Surface | Reported Removal Efficiency (%) [Average Effluent Concentration, if reported] | | | |
|---|---|---|---|---|---|
| | | TSS | Heavy Metals | Nutrients | Hydrocarbons |
| | crushed material for base course. | | | | |
| (Pagotto *et al*, 2000) | Porous asphalt (30 mm thick), field installation, installed on top of pervious surface, high traffic loading. | 87% [8.7 mg/L] | Cd – 69% [0.28 µg/L] Cu – 35% [20 µg/L] Pb – 78% [8.7 µg/L] Zn – 66% [77 µg/L] | TKN – 43% [1.2 mg/L] | 92% [0.09 mg/L] |
| (Kuang and Sansalone, 2006) | Porous concrete, 25% total porosity | Total – 80% Over 75 µm – 100% Less than 25 µm – 50% | | | |
| (Urban Water Resources Centre, 2002b) | Formpave and Ecoloc (both open-jointed paving block), 50 mm bedding layer, 300 mm base course, separated by geotextile. Grasspave (plastic geocell), geotextile below surface, no bedding layer, 300 mm base course. | Ecoloc – 89% [22.8 mg/L] Formpave – 94% [13 mg/L] Grasspave – 97% [6.2 mg/L] | | | |
| (Brattebo and Booth, 2003) | Open-celled paving grid (Turfstone) | | Cu – 83% [1.33 µg/L] Zn – 64% [7 µg/L] | | <MDL[1] |
| | Plastic geocell (Gravelpave ) | | Cu – 89% [0.89 µg/L] Zn – 62% [8.23 µg/L] | | <MDL[1] |
| | Plastic geocell (Grasspave) | | Cu – <MDL[1] Zn – 39% [13.2 µg/L] | | <MDL[1] |

| Author | Type of Permeable Pavement Surface | Reported Removal Efficiency (%) [Average Effluent Concentration, if reported] | | | |
|---|---|---|---|---|---|
| | | TSS | Heavy Metals | Nutrients | Hydrocarbons |
| | Open-jointed paving block (Eco-Stone®) | | Cu – 89% [0.86 µg/L]<br>Zn – 69% [6.8 µg/L] | | <MDL[1] |
| (Sansalone and Buchberger, 1995) | Not specified | 90-100% | 60-100% (overall) | | |

---

[1] MDL – Minimum Detectable Limit

**2.10 Cold Weather Performance**

Cold weather poses numerous problems for urban stormwater management. Frost heave and winter maintenance activities cause structural problems, and snow conditions can often pose a much greater water quality threat than rain conditions. Total concentrations of metals and solids are higher in snowmelt runoff compared to rainfall runoff. This is because snowmelt runoff volume is smaller than that of a rainfall runoff event, and furthermore a snow bank may exist for several months, during which time it can trap metals and solids before melting into runoff (Westerlund *et al*, 2003). Winter maintenance activities such as sanding and salting can also add to the pollutant load on roadways.

In addition to water quality and structural issues, the infiltration capacity of the permeable pavement surface itself becomes an issue during cold weather. There has been some research, however, showing positive results with regards to cold weather hydraulic performance of permeable pavements. Stenmark (1995), in his experiments, showed that the infiltration capacity of porous asphalt in cold temperatures indicated sufficient capacity during snowmelt periods, provided the street surface was not completely covered with ice and the asphalt not severely clogged with particles.

Backstrom and Bergstrom (2000) found that when porous asphalt was exposed to alternating melting and freezing over two days, which are conditions similar to the snowmelt period, the infiltration capacity was reduced by approximately 90%. They estimated that for snowmelt conditions, the infiltration capacity was $1 - 5$ mm/min. The results show that porous asphalt retains some of its infiltrating function during winter

conditions. The infiltration capacity at freezing point was approximately 40% of the infiltration capacity at 20°C.

Backstrom (2000) compared ground temperatures on a full-scale porous asphalt installation with a conventional pavement installation in Lulea, Sweden during periods with prolonged freezing conditions, and during snowmelt. The study found that the porous asphalt was more resistant to freezing than the conventional impermeable pavement due to higher water content in the underlying soil, which increased the latent heat in the ground. Similarly, the thawing process was found to be more rapid than in a comparable impermeable pavement. Furthermore, the study found that frost penetration depth is shallower, and the frost period is shorter for porous asphalt compared to its impervious counterpart, indicating that there is a lower risk for frost heave damage.

In a study of two porous asphalt parking lots in Rochester, New York, Field *et al* (1982) found that there was no observable structural degradation after 100 freeze/thaw cycles, and water drained through the pavement without problems during the winter.

In terms of winter sanding material, St. John and Horner (1997) found that the manual addition of 2 years worth of winter sanding material to a porous asphalt road shoulder in Redmond, Washington decreased the infiltration rate from 1450 mm/hr to 36 mm/hr. This is a very important topic, but little research has been done in this area.

## 2.11 Summary

Throughout this review, the most evident recurring observation of previous research is that the performance of permeable pavements in all aspects varies

dramatically between different scenarios. From this it is apparent that, for this low impact development implementation to be successful, studies need to be done on a regional basis to establish adequate design parameters for the conditions and requirements of individual locales, as well as for each type of permeable pavement.

**Chapter Three: Methods and Materials**

The research for this thesis included both field and laboratory experiments. The experimental locations will be described in detail in the following sections.

## 3.1 DESCRIPTION OF FIELD INSTALLATION

Two pilot scale permeable pavement installations, with surface courses of porous asphalt and UNI Eco-Stone® open-jointed paving blocks, were installed in November 2005 on Hochwald Avenue SW in Calgary, Alberta, Canada (see Figure 3-1). The street is a collector road located at Currie Barracks, a former military base, and is used both by local traffic and as a shortcut by residents on either side of Currie Barracks. The site is located directly in front of a stop sign, and receives moderate traffic from both light-duty, as well as occasional heavier-duty (i.e. Mack truck) vehicles. While typical permeable pavement installations are recommended in literature to be located in low traffic applications such as parking lots, the site was selected based on the desire by Canada Lands Company to evaluate the extreme limits of permeable pavement in regards to hydraulic and structural robustness.

Both the porous asphalt and UNI Eco-Stone® pavement sections measure approximately 8 meters long by 6 meters wide, and are on a 3% longitudinal slope. The porous asphalt surface consists of a 65 mm thick layer of open grade friction course with a maximum aggregate size of 11 – 16 mm and no particles finer than 600 μm. The asphalt has an in-place void space of 18-22% and polymer modified binders and fibers. The UNI

Eco-Stone® blocks measure 115 mm by 215 mm, and are 80 mm high, with an overall surface void ratio of 12.18%. Both installations contain a 30-50 mm bedding course layer beneath the surface course (gradation shown in Figure 3-3), and a 400-500 mm base course layer (gradation shown in Figure 3-4), below which is the existing sub-grade. Figure 3-2 details the original design specifications for the Eco-Stone installation. The aggregate was supposed to have been pre-washed to remove fines, but unfortunately this was not done due to miscommunication. In an attempt to compensate, the pavements were soaked with several ~10,000 L applications of clean water after installation in an attempt to flush out the fines. There is a Carthage Mills 15% monofilament woven geotextile separating the bedding course and base course layers, and a non-woven geotextile separating the base course from the sub-grade. A perforated pipe under-drain is situated at the bottom of the base course of both pavements, draining to a nearby monitoring manhole. Gate valves at the inlet for the manhole can be used to alternate and control the flow from one or both of the pavement reservoirs. There were also several lysimeters installed beneath the bedding course for both pavements, with the original intention to monitor sub-surface flow patterns. Unfortunately, the lysimeters were disturbed during the installation process of the surface courses of the pavements, and they were not used due to compromised functionality.

At the downstream end of each pavement surface is a concrete pad, running the width of the road, which was used during experiments to seal a wooden beam to the surface in order to replicate ponding water scenarios.

**Figure 3-1: Currie Barracks Permeable Pavement Installations (UNI Eco-Stone® in foreground, porous asphalt in background))**
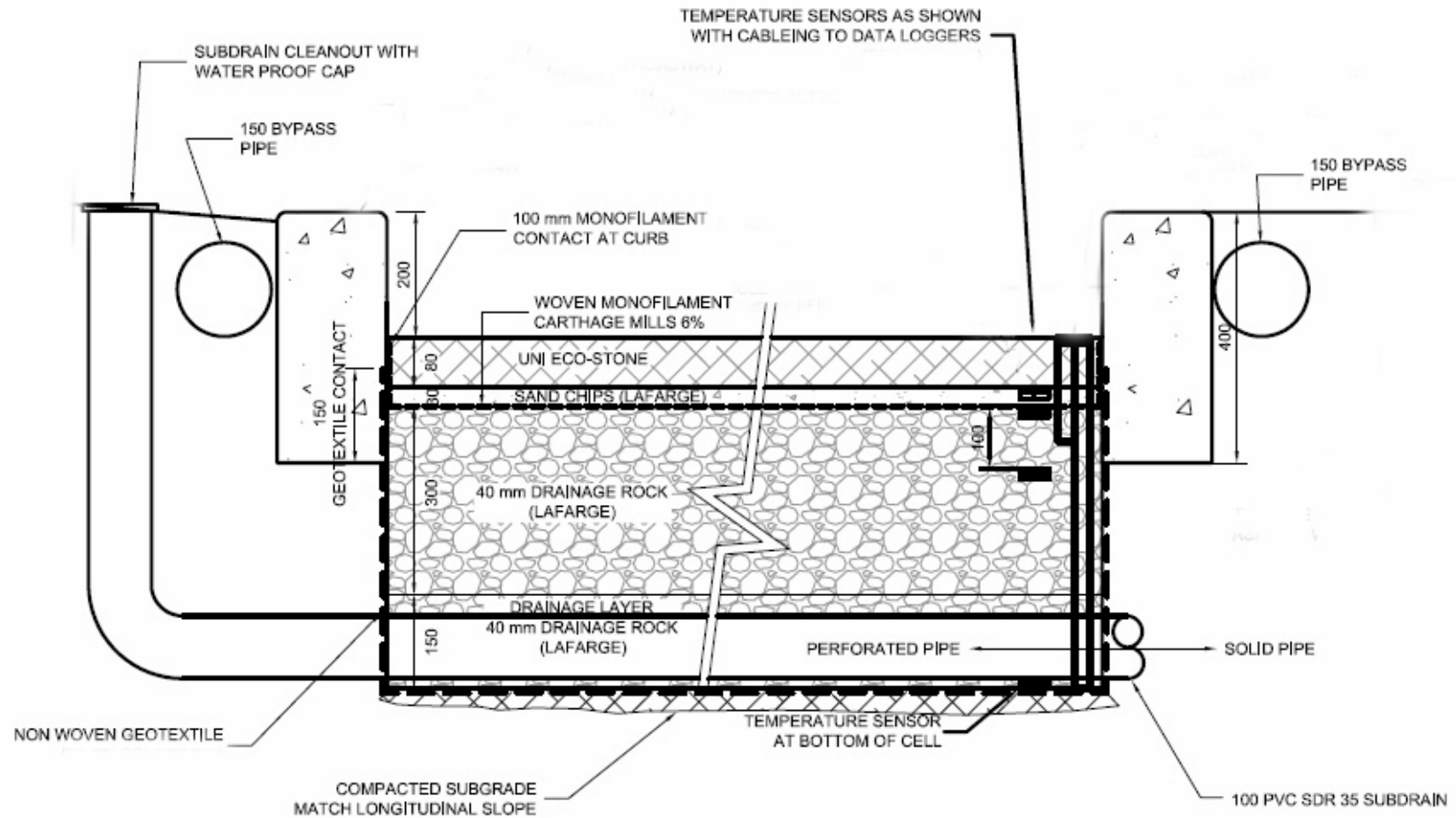
**Figure 3-2: Currie Barracks Permeable Pavement Cross-Section (Eco-Stone® installation shown. Porous Asphalt installation is identical except for the surface course) (Courtesy of Westhoff Engineering Resources, Inc.)**
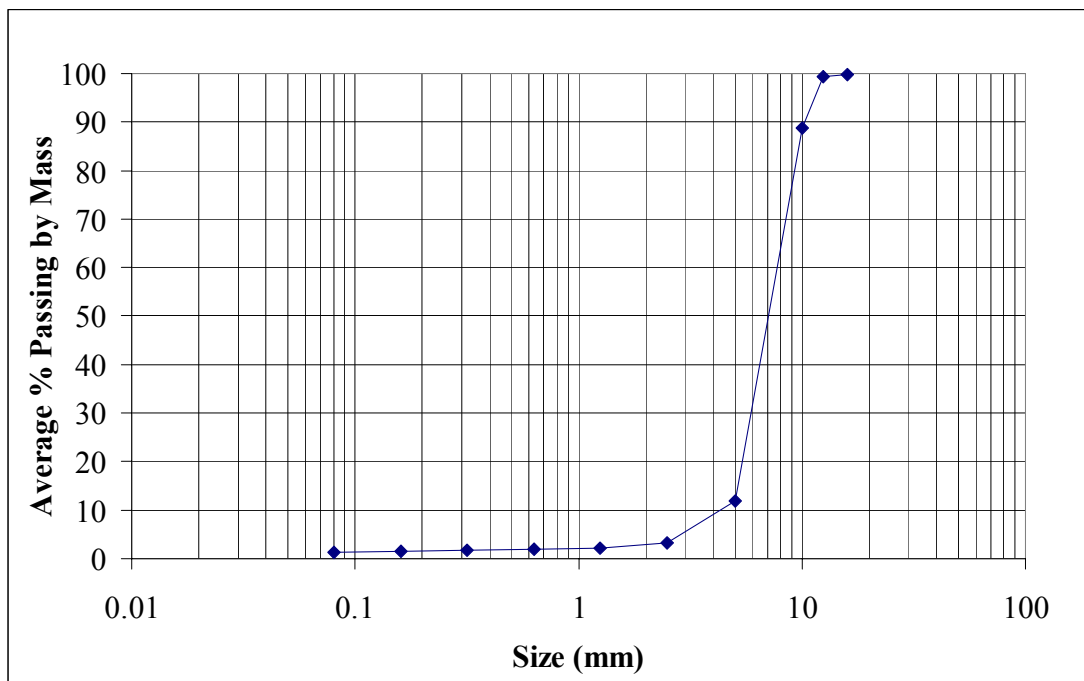
**Figure 3-3: Gradation Analysis of Bedding Course for Eco-Stone® and Porous Asphalt (and joint fill material for Eco-Stone®)**
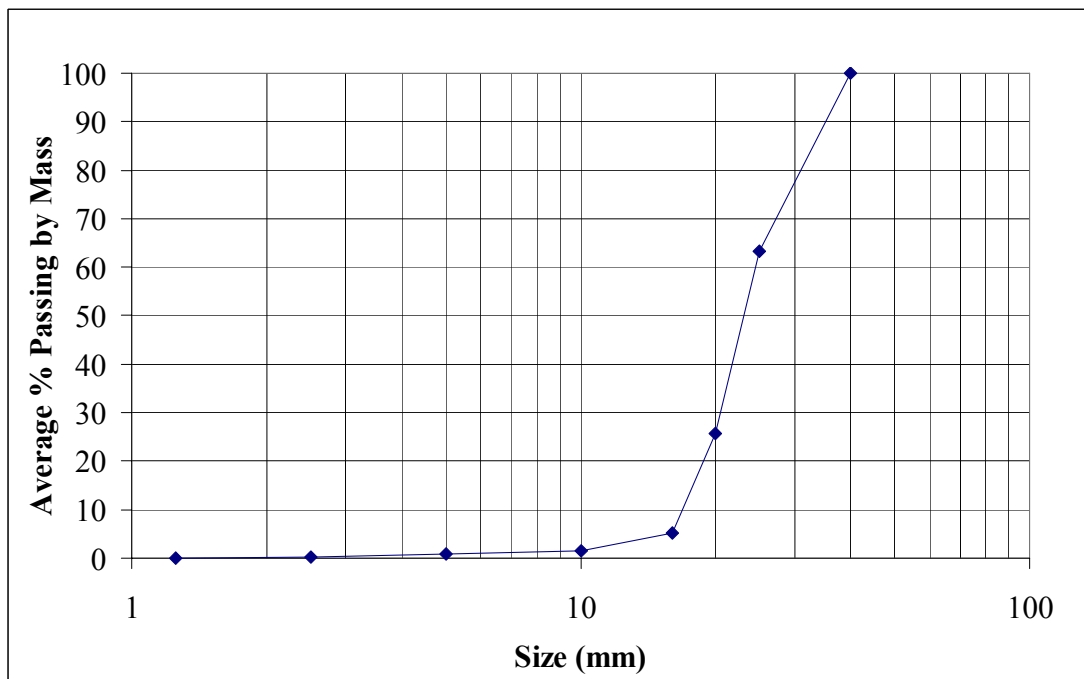


**Figure 3-4: Gradation Analysis of Base Course for Eco-Stone® and Porous Asphalt**

### *3.1.1 Field Runoff Distribution Equipment*

There are two water storage tanks at the Currie Barracks field site, each approximately 5,000 L in capacity (see Figure 3-5). During experiments, water was pumped from these tanks using a gas-powered pump to the pavement through 2" hose that was connected with cam-locks to the field runoff applicator. The field runoff applicator, shown in Figure 3-6, consists of a 2" ABS pipe header fitted with five 2" outlets, dispersed evenly across the width of the pavement. Note that in Figure 3-6 the water application is uneven due to rutting and deformations on the pavement surface. These flow patterns would also occur in natural runoff situations.



**Figure 3-5: Water Storage Tanks at Currie Barracks**

**Figure 3-6: Field Runoff Application Device**

### *3.1.2 Field Monitoring Equipment*

The monitoring equipment at Currie Barracks, all of which was located in the monitoring manhole, consisted of a v-notch weir, a Hach Sigma 900 autosampler, a Hach Sigma 950 flow meter, and a Hach Sigma 75 KHz ultra sonic flow sensor which measures the level behind the weir. The specifications of this equipment are given in Appendix A.

### 3.2 DESCRIPTION OF LABORATORY MODELS

Three different lab-scale permeable pavement models were constructed in the Hydraulics Laboratory at The University of Calgary to test solids removal, long-term

decline in infiltration capacity, characteristics of particles retained and removed from the pavement structures, and the effects of winter sanding activities on infiltration capacity.

### 3.2.1 Standard Models

Figure 3-7 and Figure 3-8 show the two standard-sized models used for long-term laboratory experimentation of both the porous asphalt and UNI Eco-Stone® pavements. The structures had cross sectional areas of 465 mm X 465 mm. The frame of the models was constructed of ¾" plywood and 2x4's because of the structural integrity and ease of construction with these materials. The layer depths of the pavements for the laboratory models were almost identical to the layers at the field installations at Currie Barracks, with the exception that the base course depth was reduced to 300 mm in order to minimize the overall weight of the model. Additionally, there was no geotextile below the base course since effluent collected in an underdrain in a field installation would be above this geotextile. All aggregate used in the models was washed thoroughly to remove any fines, so as not to interfere with the parameters being measured. There were very few fines in the base course aggregate to begin with, so the gradation of the material used in the laboratory was virtually identical to that used at Currie Barracks (Figure 3-4). In the case of the bedding course aggregate, however, there were some fines in the original material, and the gradation of the aggregate measured after washing differed slightly from Figure 3-3 in that there were zero particles below 500 μm. Several base effluent readings of 0 mg/L TSS were taken after construction of the pavement models, verifying the absence of any fines in the aggregate. To ensure even distribution of the aggregate within the structure, the base and bedding courses were levelled and compacted using an

aggregate compactor (Figure 3-10). The pavement courses were supported by a perforated stainless steel underdrain support which rested on a ledge around the inside of the bottom of the wooden frame. Below the underdrain support, there was a 200 mm clearance to allow for effluent sample collection. Effluent was collected by sliding a plastic tray under the frame. The tray was sized such that it was large enough to collect all of the effluent discharged from the bottom of the pavement models (see Figure 3-9). The cross sectional area of the pavements was chosen as 465 mm X 465 mm because it conveniently fits a square pattern of UNI Eco-Stone® interlocking blocks, allowing for a small clearance. Furthermore, this size was judged to be large enough to allow for the spatial variability that would be seen in reality and yet small enough to be constructed in the given laboratory space. The inside of the wooden frame structures were coated with a water sealant to prevent any potential effects of water absorption into the wood. Additionally, all cracks and corners of the models were sealed with silicone to prevent leakage of water. The geotextile was folded up the sides of the structure, stapled and sealed with polyurethane glue to ensure no water bypassed down the edges of the fabric. Situated above the surface course of the pavement models was a laboratory runoff applicator, which will be described in Section 3.2.3.
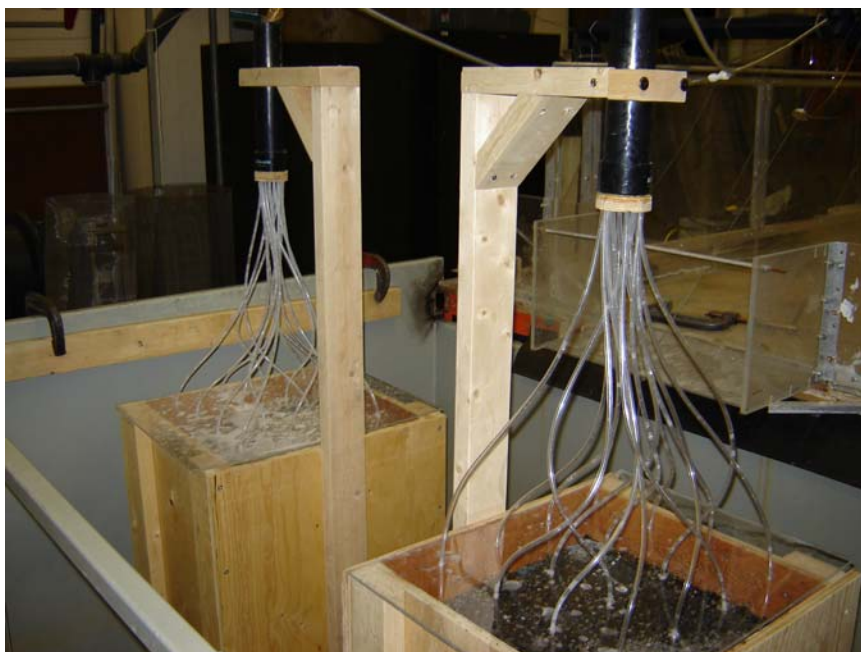
**Figure 3-7: Standard-Sized Laboratory Models**



**Figure 3-8: Laboratory Runoff Model (Detail)**

**Figure 3-9: Effluent Collection Tray**



**Figure 3-10: Aggregate Compactor**

*3.2.2 Miniature Model*

A third, smaller structure was used to investigate the effect of winter sanding on long-term surface infiltration capacities for both pavement surfaces (Figure 3-11). The model had a cross sectional area of 465 mm X 235 mm (approximately half the area of the standard models), and did not contain a base course. The smaller structure and streamlined design were used to simplify the construction process and eliminate redundant components of the model. The structure was used solely for infiltration measurements; solids removal characteristics were not investigated. As mentioned previously, clogging in permeable pavements occurs primarily because of the accumulation of solids in the top portion of the pavement structure, and not because of migration of solids to the interior of the pavement (Balades *et al*, 1995). Thus, clogging occurs mostly above the upper geotextile, and this smaller-scale structure was sufficient for replicating the decline in long-term surface infiltration capacity due to the presence of winter sanding material. The bedding course and joint fill material was thoroughly washed prior to installation. Similar to the standard models, positioned above the miniature model was a laboratory runoff applicator, as will be described in Section 3.2.3.

**Figure 3-11: Miniature Laboratory Model**

### 3.2.3 Laboratory Runoff Distribution Equipment

Located above the surfaces of the pavement models were removable laboratory runoff applicators, as shown in Figure 3-7 and Figure 3-11. The runoff applicator was designed to distribute sediment-loaded water uniformly across the pavement surfaces. The applicator consisted of an ABS pipe reservoir, connected to an array of vinyl distribution tubes (ID 0.17" (4.3 mm)) that were fastened through a ¼" firm plexiglass sheet. The tubes were connected to the sheet through tight-fitting drilled holes, and the sheet was supported on the top of the wooden frame, approximately 10 mm above the pavement surfaces. For the standard sized models, there was an array of 16 distribution tubes, while for the miniature model there was an array of 8 tubes. The spacing for the

tubes was such that for the Eco-Stone® blocks, the outlet of each tube sat directly over the center of the impermeable areas of a block. This was so as to disperse the water evenly to all of the pavement area and to dissipate the energy of the droplets so that any potential long-term effects of impact from falling water were reduced. For porous asphalt, the same design was used for the runoff applicator. The ABS pipe reservoir was held in place by a large wooden bracket constructed over the pavement model, which is visible in Figure 3-7. Water was fed into the ABS pipe reservoir from a mixing tank via a 0.17" (5.4 mm) ID clear vinyl conveyance tube. The water was pumped through the conveyance tube from a 1/6 HP submersible sump pump that was located in the mixing tank. The mixing tank had a 575 L capacity tank and consisted of 4 mixing blades controlled by a variable speed DC Motor (see Figure 3-12). The tank itself was a ¾" plywood structure lined with 8 mil (0.2 mm) polyethylene sheeting. Originally designed for mixing sand slurries, the mixing blades were capable of keeping large particles (up to 1 mm) in suspension. Clear vinyl tubing enabled visual observation to determine whether any settling was occurring in the conveyance tube at low flow rates. There was a valve installed in the tubing from the reservoir to the pavement models to allow flexibility in the rate of application. All laboratory models were situated in a large pan in the hydraulics laboratory where effluent water was allowed to drip freely from the perforated underdrain support. Waste drainage water was pumped from the flume pan into a nearby sink using a second submersible pump.

**Figure 3-12: Laboratory Sand Slurry Mixing Tank**

## 3.3 SIMULATED SEDIMENT FOR STORMWATER RUNOFF

Experiments in both the laboratory and field required simulated stormwater runoff to be applied to the pavement surfaces. Two types of simulated runoff were used; one consisting of synthetic sediment, and the other consisting of naturally-occurring sediment collected from Calgary streets.

### *3.3.1 Sil-co-sil 106 (Synthetic Sediment)*

For some experiments a synthetic sediment mixture was used. Synthetic sediment is desirable for research purposes because it has consistent particle size distribution and chemical properties, whereas naturally occurring sediment is highly variable depending on sampling location. The consistent properties of synthetic sediment allow for unbiased comparisons of solids removal efficiency between the two pavement types. Washington State Department of Ecology (2004) recommended using U.S. Silica Company's "sil-co-sil 106" ground silica for laboratory experiments to investigate solids removal. According to Ed O'Brien and Mieke Hoppin of Washington State Department of Ecology Water Quality Program (2006), this recommendation was based on comparative data from Washington State Department of Transportation tests on highway runoff in the Pacific Northwest, which is dominated by fine silts and fine sands. Sil-co-sil 106 is a single grain with consistent chemical properties, high specific gravity and consistent PSD, and was therefore thought to work better for lab-scale testing of stormwater treatment devices. Although on the conservative side in terms of particle sizes (O'Brien and Hoppin, 2006), it was assumed that if Sil-co-sil 106 could be removed then likely larger silt and sand particles could also be removed. Sil-co-sil may behave differently than actual stormwater because of the absence of different sized particles, organics, and colloidal materials, but it provides a good method of comparison between multiple permeable pavement types. Sil-co-sil 106 was used only in laboratory experiments. The average particle size distribution for sil-co-sil 106 is shown in Figure 3-13.
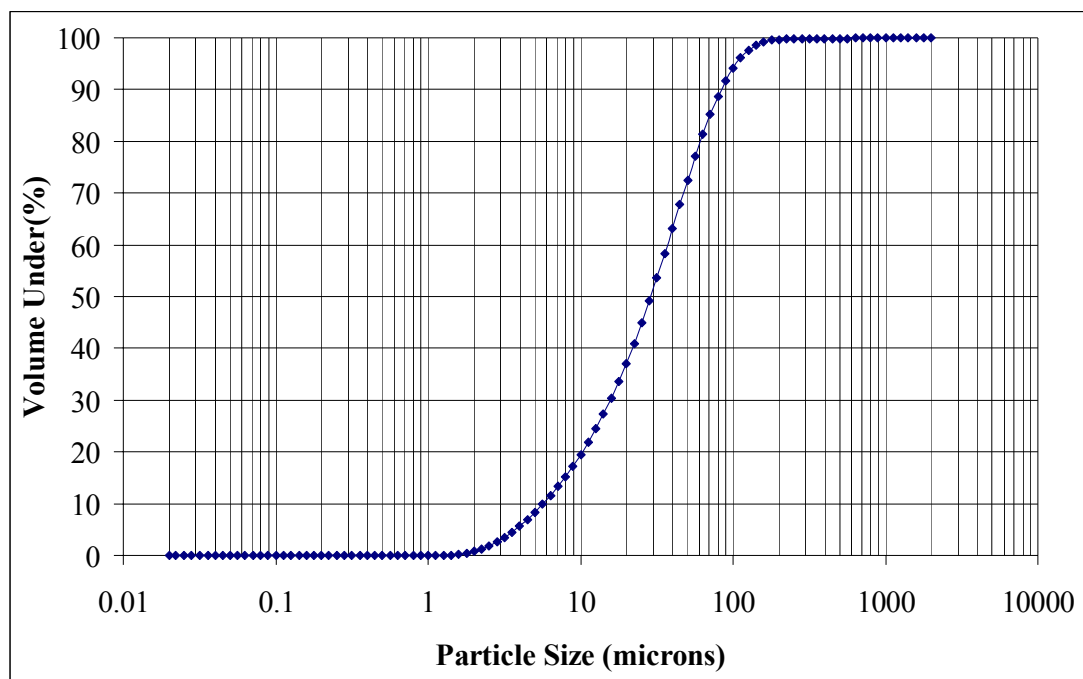
**Figure 3-13: Average Particle Size Distribution, sil-co-sil 106**

### *3.3.2 Natural Sediment (Sub-250 µm Street Sweepings)*

In addition to synthetic sediment, some experiments were performed with sediment collected from Calgary roads in order to observe more realistic long-term performance of the pavement structures. Street sweepings from City of Calgary Schwarze A8000 vacuum sweeping vehicles were collected and sieved to a size of 250 µm and below. The collection procedure consisted of manually brushing the bulk material from the sweepings pile at The City of Calgary's District 5 Roads Compound through a 2 mm mesh sieve onto a collection board (Figure 3-14), in order to reduce the volume of sediment. Following this, the sediment was transported to The University of Calgary, where it was dried by spreading the sediment on a tarp on particularly hot and clear days, occasionally turning the material to expose it to air (Figure 3-15). Once the sediment had

been sufficiently dried, it was further sieved through a No. 60 Sieve Size screen (250µm) with a Sweco vibratory separator. It was ensured that enough sediment was collected and sieved for the duration of experimentation (approximately 0.3 m$^3$).
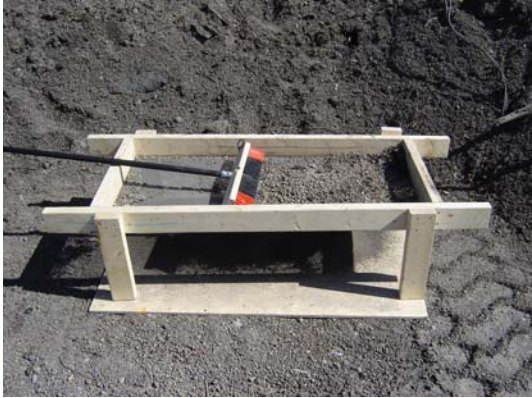


**Figure 3-14: Sieving at District 5 Roads**



**Figure 3-15: Sun-drying the street sweepings sediment**

The sediment was sieved to 250 μm because this represents the finer portion of material that would typically be found on Calgary streets (for a brief investigation of local stormwater PSDs, refer to Appendix E). The finer portion was desired since this is typically the material that is ultimately responsible for the clogging of permeable pavements (Gerrits, 2001). Also, with regards to filtration capabilities, it is presumed that if the pavements are capable of removing the sub-250 μm particles, they would be capable of removing larger particles as well. It is also the size range that is of particular importance in stormwater treatment because of its association with particular pollutants and the relative ease of which it can be mobilized and transported in stormwater discharges (Barnes *et al*, 2001). Research has shown that finer particulates (< 250 μm) are more efficient in the adsorption of pollutants, including phosphates, heavy metals, and pesticides, and as such will carry a higher pollutant concentration (Sartor *et al*, 1974; Roger *et al*, 1998; Andral, 1999). Although these particular pollutant loads were not monitored in this study, it is still of importance to monitor the solids of this size range and their removal through the pavement structures. Another reason for using this size range was that anything coarser than 250 μm was difficult to keep consistently mixed in the laboratory mixing tank, and anything larger than 250 μm would not normally be mobilized during typical runoff events in Calgary. Refer to Appendix C for a mathematical evaluation of the particle sizes that are typically mobilized during Calgary runoff events. The street sediment was used for both laboratory and field experiments.

### 3.3.3 Sediment Concentration in Simulated Stormwater

For all field and laboratory experiments involving simulated stormwater runoff, the target concentration of sediment applied to the surfaces was 500 mg/L. This value was chosen based on other research, physical observations, and specific experimental goals. It was desired to use a total suspended solids (TSS) concentration that was high enough to allow the effective hydraulic life of the pavements to be tested in a laboratory setting in a reasonable amount of time, and yet still be within the range of feasible TSS concentrations for the Calgary area. Several grab samples were taken at various established residential catchbasins throughout the city during storm events, and the TSS was found to range from approximately 20-550 mg/L (see Appendix E). Although 500 mg/L is at the higher end of the spectrum for runoff in Calgary, it is not an unrealistic value. The same concentration was used for both laboratory experiments and experiments at Currie Barracks so that accurate comparisons could be made.

As for research literature on the topic of appropriate TSS concentrations for stormwater, much of it is not directly applicable because the characteristics of stormwater runoff vary greatly depending on geographic location and storm event. However, there has been substantial research that has shown that 500 mg/L is not an unreasonable value to be found in stormwater runoff in established residential areas. (Sansalone and Buchberger, 1995; Pratt, 2001; Ehlers, 2003; Rankin and Ball, 2004; Taebi and Droste, 2004; Memon and Butler, 2005).

In the laboratory, the concentration was kept as close to 500 mg/L as possible using the sand slurry mixing tank. Grab samples of inflow concentration were taken consistently throughout all experimental runs. Due to turbulence within the mixing tank,

the instantaneous TSS concentration of the inflow varied considerably. However, the overall average over the course of experiments remained almost exactly 500 mg/L, as shown in Figure 3-16 and Figure 3-17.

For field experiments at Currie Barracks, the sediment was applied manually to the pavement surface by evenly dispersing 500 g of sediment over the pavement for every 1000 L of continuously applied water from the storage tanks through the field runoff applicator (Figure 3-18). The sediment was applied in this manner because it would have been very difficult to keep the sediment in suspension through mixing in a field situation. The limitations of this application method are that there are inconsistencies in the instantaneous concentrations of the applied water. However, given that the experiments at Currie Barracks were intended to represent ponding situations, the average concentration of water infiltrating the pavements, or the event mean concentration (EMC), would have been very close to 500 mg/L. Event Mean Concentration can be defined as:

$$EMC = \frac{M}{V} \qquad\qquad (3.1)$$

where:

$EMC$ = event mean concentration (mg/L)
$M$ = total mass of a constituent over entire event duration (mg)
$V$ = total volume of flow over entire event duration (L)

For future research, a portable mixing tank similar to the one in the laboratory could be constructed.
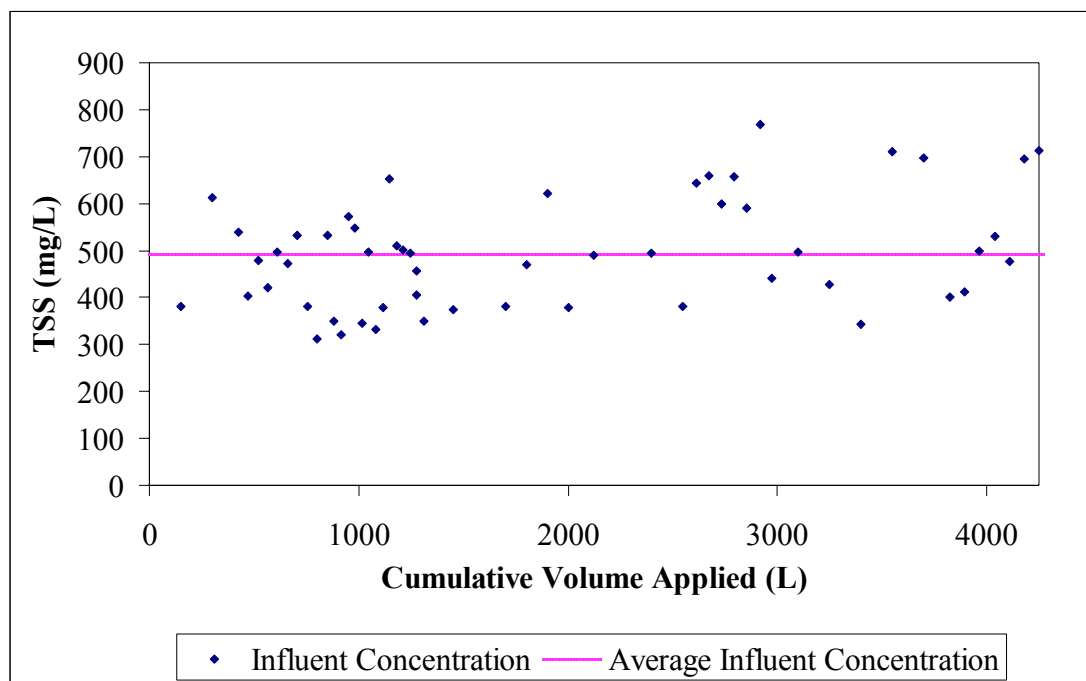
**Figure 3-16: Influent TSS Concentration, sil-co-sil 106**
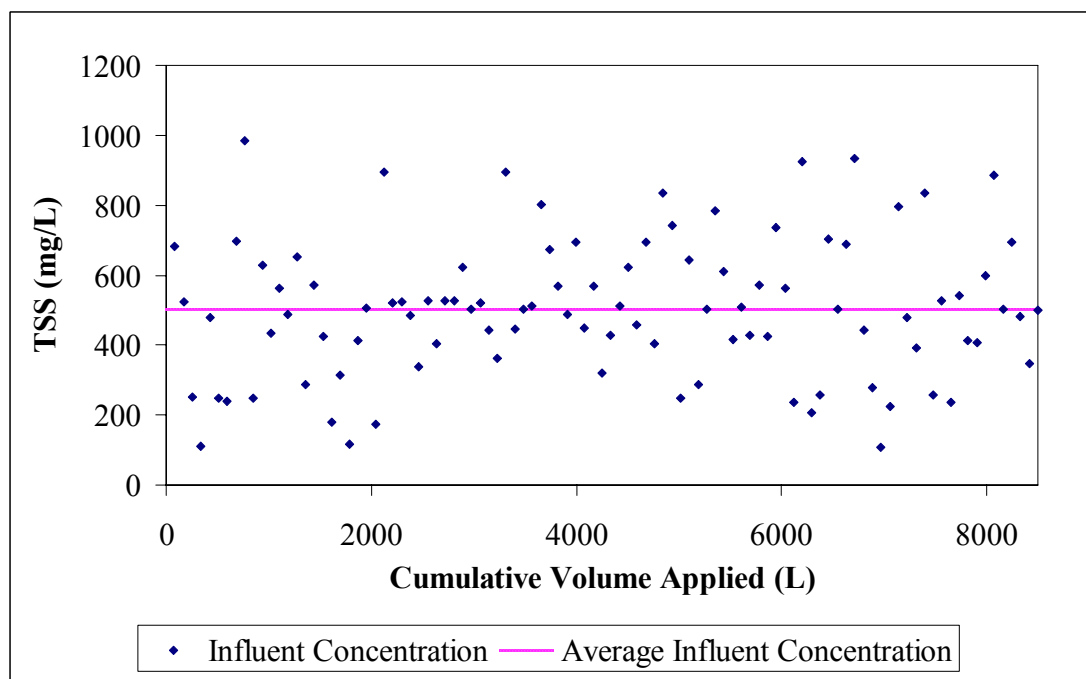


**Figure 3-17: Influent TSS Concentration, Sub-250 μm Street Sweepings**

**Figure 3-18: Sediment Application at Currie Barracks**

## 3.4 EXPERIMENTS

### 3.4.1 Field Experiments

#### 3.4.1.1 Simulated Runoff Experiments

The experiments at the Currie Barracks field installations consisted of the application of a known volume of water (approximately 8400 L) to the pavement surfaces at a constant flow rate and with constant TSS concentration. The application water was hauled from the 69th Street Storm Pond and discharged into the storage tanks before being applied to the pavement surfaces. Storm pond water was used so that the natural stormwater chemistry (pH, conductivity, chemical constituents, etc.) and any possible biological activity were preserved as much as possible. The storm pond water was

withdrawn from the outlet of the 69th St. storm pond. There was minimal disturbance of the sediments in the pond during removal, and the background suspended solids concentration of the water was extremely low. Frequent analysis of the raw stormwater showed the TSS concentrations averaged 0 – 10 mg/L. The overall target concentration of 500 mg/L was not significantly impacted by the background TSS in the storm pond water.

The TSS concentration was kept as close to 500 mg/L as possible by the manual addition of sediment to the inflow water as described in Section 3.3.3. Outflow rates from the subdrain system were monitored in the manhole with the weir and Sigma 950 flow meter, and samples were collected with the Sigma 900 autosampler for laboratory measurement of effluent TSS concentrations and particle size distributions. For details and specifications on the monitoring equipment, see Appendix A. A six meter long wooden beam was installed and sealed at the downstream end of each pavement section to allow all water to be captured behind the beam, causing a ponding situation. The beams were sealed to the pavement surface using polyurethane expanding foam, which was very effective in preventing any leakage under the beams. In total, six experiments of this type were carried out from the period of July to September 2006; 3 for each pavement surface type.

Water was pumped from the storage tanks to the pavement surface, at an average flow rate of 5.87 L/s (equivalent to 1211 L/s/ha for the pavement area, or 242 L/s/ha for an I/P ratio of 4). For the purposes of this study, an I/P ratio of 4 was chosen throughout this thesis. This is based on an approximation of the types of situations in which these pavements would be installed under the request of Canada Lands Company. The

equivalent rainfall intensity for this flow rate is found using a variation of the rational method:

$$Q = Q_{incident} + Q_{runoff}$$

$$= 0.000278iA + 0.000278Ci(I/P)A$$

( **3.2** )

where:

$Q$ = flow rate (L/s)
$i$ = rainfall intensity (mm/hr)
$A$ = permeable pavement area (m$^2$)
$C$ = runoff coefficient (dimensionless)
$I/P$ = impervious to pervious area ratio (dimensionless)

In this set of experiments, the average applied flow rate was 5.87 L/s, and the average application time was 23 minutes. The area of each pavement surface is 48.48 m$^2$, and the runoff coefficient C for a pavement surface ranges from 0.7 to 0.95 (The City of Calgary Wastewater & Drainage, 2000). If C is taken as 0.9 and I/P is 4, the equivalent rainfall intensity for the simulated runoff application is about 95 mm/hr. According to the Intensity-Duration-Frequency curve from the City of Calgary Stormwater Manual (2000), for 20 minute duration, this is slightly greater than the 1-in-100 year storm event value of ~80 mm/hr. Although this is a very intense simulated storm for the Calgary area, the intent of these pavement installations, as mentioned previously, was to test their performance when pushed to the maximum possible limits. Of course, the equivalent intensity would drop for higher assumed I/P ratios as well.

The amount of artificial runoff applied in one experimental run (~8400 L) was equivalent to approximately 34.65 mm of rainfall for an I/P ratio of 4. The City of

Calgary receives an average of 400 mm of precipitation per year. Each experimental simulated runoff application was the equivalent of a total of approximately 0.09 years (10% of the annual local precipitation) of additional surface runoff.

Manually collected influent samples, as well as effluent samples collected by the Sigma 900 autosampler were then taken to the Environmental Laboratory at The Department of Civil Engineering at The University of Calgary and analyzed for total suspended solids and particle size distribution in an attempt to understand solids removal processes within the pavement. In the case of the influent samples, grab samples of the raw influent stormwater were taken and mixed with proportions of the sub-250 μm street sweeping sediment equal to those applied in the simulated runoff experiments. The influent sample collection procedure was done in this manner so as to capture the background TSS in the pond water which, although minimal, was still important to represent in the PSD analysis to maintain accuracy. The influent and effluent samples were then centrifuged to separate the solids, and analyzed for particle size distribution as will be described in Section 3.5.2.

Additionally, the total time that standing water remained on the surface (ponding time), as well as the maximum depth of ponding, were recorded to give an appreciation of how standing water would behave on the permeable pavements. Figures 3-19 to 3-22 show some typical field experimental procedures at Currie Barracks.

**Figure 3-19: Typical Simulated Runoff Experiment (shown for porous asphalt)**



**Figure 3-20: Typical Simulated Runoff Experiment (shown for Eco-Stone$^{®}$)**

**Figure 3-21: Ponding Beam, Sealed with Polyurethane Expanding Foam**



**Figure 3-22: Measuring Maximum Ponding Height**

**3.4.1.2 Surface Infiltration Capacity and Maintenance Experiments**

As mentioned previously, clogging of permeable pavements takes place primarily in the upper layers of the pavement structure. Consequently, the concept behind maintenance of permeable pavements is to remove a portion of the material from the upper few centimetres of the pavement structure to restore the infiltration capacity. For open-jointed paving blocks such as the UNI Eco-Stone® used in this study, this entails removing the joint fill material itself, whereas for porous asphalt the goal is to try to remove the fine material trapped in the voids of the upper layers of the asphalt.

Between the dates of May 25 and October 23, 2006, periodic surface infiltration capacity measurements were performed both before and after two separate maintenance attempts using a City of Calgary Schwarze Model A8000 vacuum sweeper (Figure 3-23) Specifications for the sweeper are shown in Appendix F. The first maintenance attempt, which was carried out on June 5, 2006, consisted of a single dry pass of each pavement, i.e., without the aid of adding water for cleaning purposes. The second maintenance attempt, which was carried out on October 23, 2006, consisted of three passes with simultaneous application of water for dust control. Surface infiltration capacity measurements were made using 30-cm diameter, 25 cm high galvanized steel rings (ring infiltrometers), which were sealed to the pavement surfaces with Plumber's Putty as suggested by Bean *et al* (2004) (see Figure 3-24). The initial water level in the rings was recorded, and the time to completely drain the rings was observed (a falling-head measurement). This is essentially a "surface inundation test", as described by Bean *et al* (2004) , and only gives a rough approximation of the actual surface infiltration capacity. It is less accurate than a double ring infiltrometer test because of the potential for

horizontal migration of infiltrating water (Bean *et al*, 2004). However, given the available time and resources, the surface inundation test was judged to be sufficient to provide relative approximations of surface infiltration capacity for this study. Three trials were done for each measurement, and this data was then used to compute the average surface infiltration capacities in mm/hr. In all, 15 locations were sampled: 7 on the porous asphalt and 8 on the Eco-Stone® paving blocks. It is important to note that between surface infiltration capacity measurements, in addition to naturally occurring rainfall-runoff processes, the simulated runoff from the solids removal and flow attenuation experiments described in Section 3.4.1.1 were applied. In total, from the time of the first infiltration capacity measurement in late May to the last one in late October, a total of 3 artificial applications were applied for each pavement section. Each application was approximately equivalent to a 1-in-100 year storm for 20 minute duration (80-100 mm/hr intensity).

**Figure 3-23: City of Calgary Vacuum Sweeper (Schwarze A8000)**



**Figure 3-24: Ring Infiltrometer Sealed With Plumber's Putty**

The locations of the infiltrometers on the pavement surfaces are shown in Figure 3-25. The same precise locations were used consistently throughout all infiltration measurements.
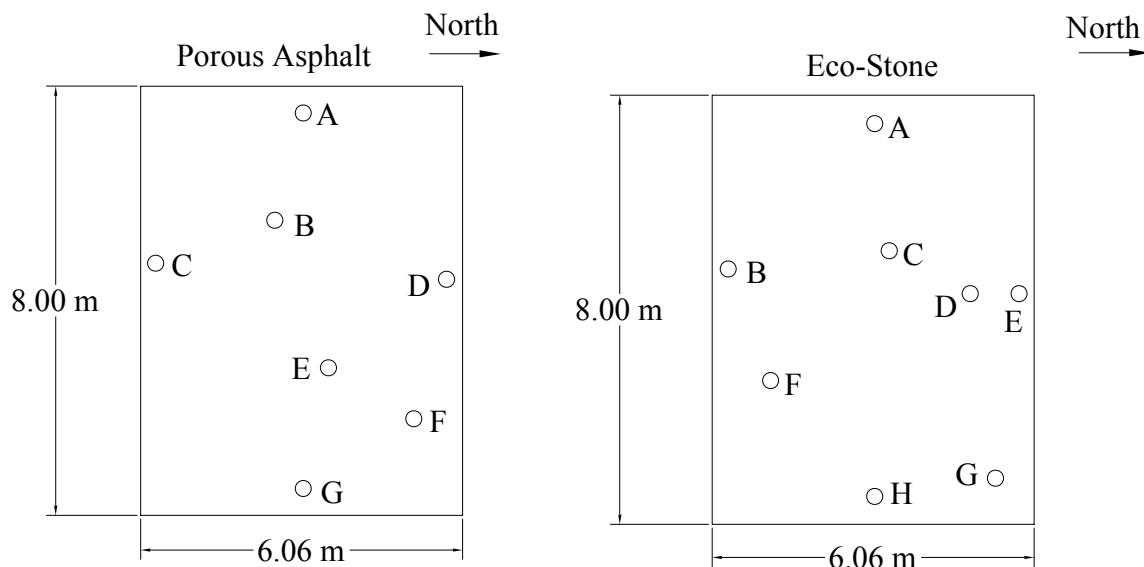


**Figure 3-25: Infiltrometer Locations**

## *3.4.2 Laboratory Experiments*

## 3.4.2.1 Long-term Solids Removal Characteristics (Standard-Sized Models)

For this series of experiments, sediment-loaded water was applied to the standard-sized pavement models for a simulated period of time. Grab samples for the influent and effluent were frequently taken for TSS and particle size distribution analysis. Experiments were conducted using both the synthetic silica sediment and the sub-250 μm street sweepings.

For laboratory experiments using both synthetic and natural sediments, the following relationship was used to calculate the necessary applied volume for an equivalent simulated year:

$$V = dA(I/P + 1)$$ ( **3.3** )

where:

$V$ = equivalent volume of annual precipitation (m$^3$)
$d$ = yearly depth of precipitation in Calgary (m)
$A$ = permeable pavement area (m$^2$)
$I/P$ = impervious to pervious area ratio (dimensionless)

For the standard-sized pavement models, the total surface area was 0.216 m$^2$, the average yearly precipitation for Calgary is approximately 400 mm, and an I/P ratio of 4 was assumed, as was assumed for the field experiments. Therefore the application of approximately 0.423 m$^3$, or 432 L of water (rounded down to 425 L for sake of simplicity), loaded with 500 mg/L of sediment as described in Section 3.3.3, was required to simulate one year of stormwater runoff for each standard-sized laboratory model.

Effluent samples were collected from beneath the structures with the collection tray. It was ensured that the collection tray was thoroughly washed between sample collections to avoid cross contamination. TSS grab samples of 500 mL were collected from each pavement structure after every 85 L of applied water per pavement, which is equivalent to 0.2 simulated years. In general, between 0.4 and 0.6 simulated years were performed per day, which was the equivalent of approximately 5-8 hours of actual experimental time. The pavements were left overnight without any water application. Although there was no closely-monitored "drying time" allowed for the pavements, there were certain periods where the pavement structures would go several days without any

water application. Given the indoor, humid setting, this is not sufficient time to allow for any drying within the pavement structure.

*Ground Silica Experiments*

The primary objective of experimenting with ground silica was to observe solids removal capabilities for a fine, inert sediment, excluding any chemical or biological effects that may occur within the permeable pavement structures. As such, the silica was dispersed with tap water in the mixing tank, and this mixture was pumped to the runoff applicators through a clear vinyl conveyance tube separated with a Y-connector to both pavement surfaces.

Initially several different flow rates were applied to observe the effects on TSS results, with the ultimate goal being to determine the maximum rate that simulated runoff could be applied without affecting solids removal characteristics. It was discovered that higher flow rates caused rapid flushing of ground silica solids through the pavement structure with limited solids retention. Through trial and error it was determined that a flow rate of 0.009 L/s (416 L/s/ha) was an optimal flow rate for a balance between a reasonably rapid application rate and minimal flushing of solids. Referring to Equation 3.2, this flow rate is equivalent to a rainfall intensity of 33 mm/hr when assuming an I/P ratio of 4. The runoff in these experiments was applied continuously for several hours at a time, and was not based on any design storm, so it is not practical to determine an equivalent return frequency based on an intensity-duration-frequency curve. A total of 10 years' runoff application was simulated for the long-term ground silica experiment.

*Sub-250 μm Street Sweepings Experiments*

While the long-term ground silica experiment focused on the application of a chemically and biologically inert substance, the sub-250 μm street sediment experiments focused on attempting to simulate urban runoff as closely as possible. The laboratory models were disassembled and re-assembled with new, washed material prior to the street sweepings experiments. Periodically, bulk sediment samples of 5-10 kg were separated into 212.5 gram samples by riffling, which is a sample splitting technique to retain equal particle size distributions for sub-samples. A chute riffler, or chute riffle, is a device consisting of a series of chutes that are alternately directed to opposite sides and into pans. Rifflers have an estimated maximum error for equal splitting of particle size distributions of approximately 3.4% (Allen, 1981). For every half-year of simulated runoff on both pavements, 212.5 grams of sub-250 μm street sediment, after being dried in an oven at 120 °C overnight, was mixed in the laboratory with 425 L of water obtained from the 69th St. storm pond. As with the field experiments at Currie Barracks, storm pond water was used in order to replicate the biological and chemical properties of stormwater runoff, which may play a role in solids and pollutant removal processes in permeable pavements (Shackel and Pearson, 2003). The water was collected from the outlet of the pond, transported to The University of Calgary, and stored in a 16000 L aerated storage tank in the hydraulics laboratory. Water was pumped from the storage tank to the 575 L mixing tank as needed for experimentation.

There is a y-connector in the conveyance tube such that water from the mixing tank can be applied continuously to the runoff applicators for both pavement models at the same flow rate of 0.009 L/s. As with the ground silica, several flow rates were tested

for the rapid flushing of solids, and 0.009 L/s was found to exhibit no flushing. The flow rate for the outlets to both pavements was frequently monitored by timing the filling of a graduated cylinder to ensure it remained at this value. A total of 20 years' runoff and sediment application was simulated for the experiments with the sub-250 μm street sweepings, for both pavement types.

Upon completion of the 20 year simulated application, the pavement models were carefully disassembled, and samples of accumulated sediment were collected from various layers of both pavement models so that particle size distribution could be analyzed throughout the structures. Data from this analysis was desired to give an appreciation of the solids filtration locations within the pavement structures. For the Eco-Stone® model (Figure 3-26), sediment was collected from the top 25 mm of joint fill material (Location A on Figure 3-26), from the bottom 55 mm of joint fill material (Location B), from the bedding course (Location C), from on top of the geotextile (Location D), and from three separate depths of the base course (Locations E, F, and G). For the porous asphalt model (Figure 3-27), samples were collected from the asphalt surface itself (Location A on Figure 3-27), from the bedding course (Location B), from on top of the geotextile (Location C), and from three separate depths of the base course (Locations D, E, and F). As discussed in Section 3.2.1, the washed bedding course and base course materials did not contain any particles finer than 500 μm. Similarly, it was known that the applied sediment was all passed through a 250 μm sieve. Consequently, the sediment at the various layers of the pavement structures was obtained by gently washing the aggregate from each location through a 500 μm sieve and collecting the wash water and sediment from beneath the sieve. All accumulated street sweepings

sediment passed through the sieve, while any material from the courses within the pavement structures themselves was retained on the sieve. The collected samples were then centrifuged, separated, and analyzed as will be described in Section 3.5. This allowed a direct comparison of the sediment removal characteristics to be made for each layer of the pavement structures, without any interference on the analysis from the pavement aggregates themselves. For the porous asphalt surface course, the sediment was somewhat more difficult to collect. The sediment was obtained by removing the asphalt slab from the model, turning it upside down and washing sediments through the asphalt from the bottom, collecting them in a collection tray that was placed underneath the slab.
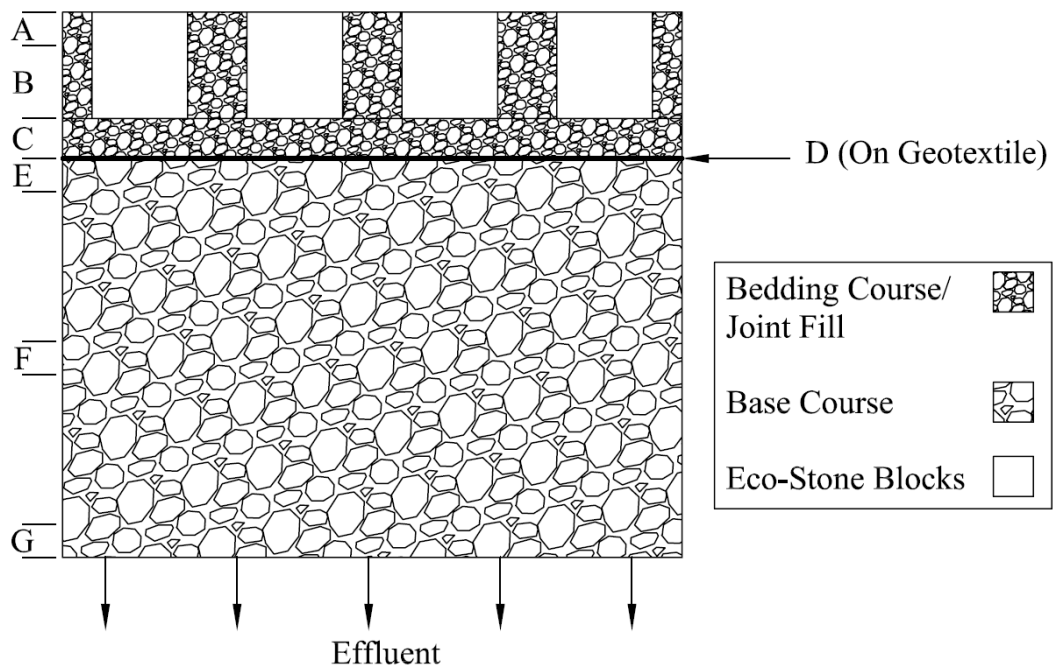


**Figure 3-26: Sampling Locations for Analysis of PSD at Various Layers of Standard-Sized Laboratory Eco-Stone® Model After 20 Years of Simulated Runoff**

A

B

C (On Geotextile)

D

E

F

Bedding Course

Base Course

Porous Asphalt

Effluent
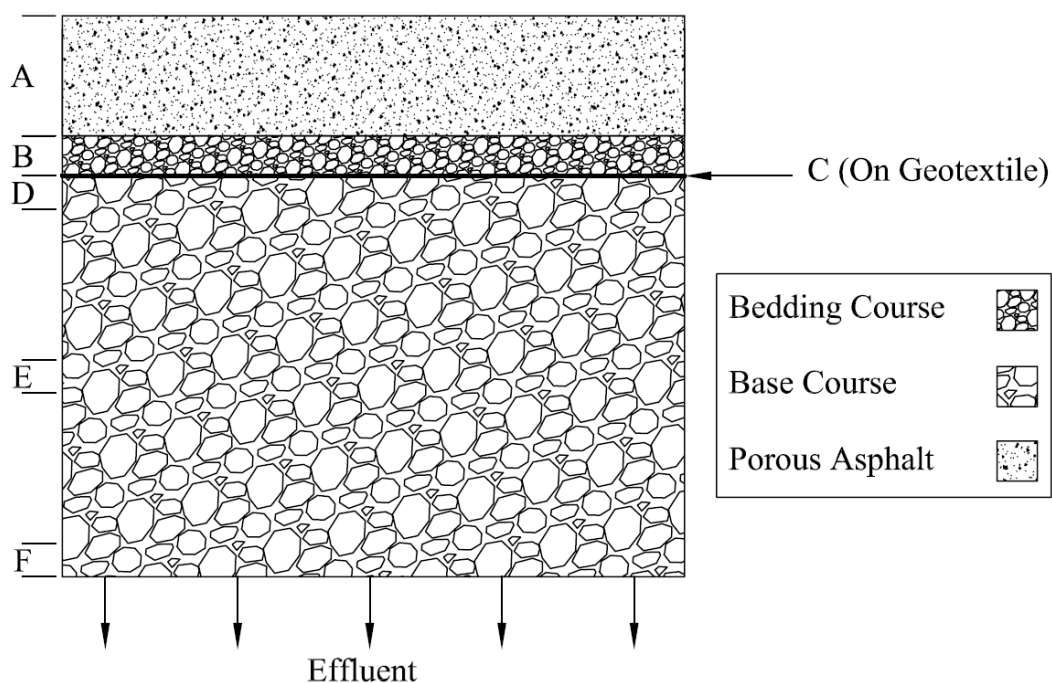
**Figure 3-27: Sampling Locations for Analysis of PSD at Various Layers of Standard-Sized Laboratory Porous Asphalt Model After 20 Years of Simulated Runoff**

**3.4.2.2 Long-term Decline in Laboratory Surface Infiltration Capacities**

Concurrently with the long-term simulated runoff applications explained in Section 3.4.2.1, the surface infiltration capacity of the pavements was measured at the end of each simulated year. This was done to evaluate the long-term hydraulic performance of the pavements for both the ground silica experiments, as well as the street sediment experiments. The same galvanized steel ring that was used for the field measurements was also used in the laboratory measurements (see Figure 3-28). The ring was sealed to precisely the same location for every measurement, again using plumber's putty, and a falling head measurement was made. The area within the ring was equal to a large portion of the pavement model areas (33%), so it was a fair representation of the

overall infiltration capacity of the surface. Three trials of each falling head measurement were executed. The infiltrometer rings in the laboratory were filled by standard tap water. Since only relatively small volumes of this water were applied, any potential interference between the chemistry of the tap water and the storm pond water was believed to be negligible. The maximum measurable infiltration capacity in the laboratory was limited by the flow rate of the hose used for water application, and was determined to be approximately 30,000 mm/hr. The infiltration capacity of the pavement surfaces (for the 10-year runs of ground silica as well as the 20-year runs for the street sediment) was measured at the end of every simulated year.

**Figure 3-28: Ring Infiltrometer Measurement (shown with ground silica sediment on the Eco-Stone® model)**

### 3.4.2.3 The Effects of Winter Sanding Material on Surface Infiltration Capacity (Miniature-Sized Model)

The effect of the presence of winter sanding material on the long-term surface infiltration capacity of both permeable pavement surfaces was investigated in the laboratory using the miniature model described in Section 3.2.2. The sanding material was obtained from the same source as the material that was used for sanding the streets at Currie Barracks. The material differs only slightly from that used by The City of Calgary on most of Calgary's roads. The gradation analyses for both The City of Calgary and Currie Barracks winter sanding materials are shown in Figure 3-29. Due to the existence of only one miniature model, the pavement surfaces were studied in succession, with the Eco-Stone® being examined first. After collecting approximately 0.1 m³ of bulk winter

sanding material, the sample was split using a sample splitter to maintain equal particle size distribution between sub samples. The equivalent of one year of material was applied to the surface. The amount of material required to simulate one year's worth of winter sanding was calculated as shown in Appendix D.

In practice, new sanding material is applied every year, and then a portion of this material is recovered by street sweepers in the spring. According to Sutherland and Martin (2006), street sweeping vehicles have average pickup efficiencies between 86.3% and 99.1% for particles 0-2000 μm. Presumably, a large percentage of winter sanding material would thus be recovered during spring cleaning. In the case of the laboratory study, overall long-term effect of the presence of the material was observed, without adding new material or removing old material for each simulated year. Another factor to consider for winter sanding material is that it appears to be readily broken down into smaller particles by vehicular traffic. The percentage of particles that are broken down, and the degree to which they are broken down, is highly variable and almost impossible to quantify. However, to give a rough approximation of the proportion of crushing of winter sanding material, brief breakage-load experiments were done for a cross section of winter sanding particles, and these results were compared to vehicular loads likely to occur. The procedure for these experiments, as well as the results, are detailed in Appendix D. Based on the results of the breakage load tests, in addition to qualitative observations of the broken down winter sanding material, it was decided to manually crush 20% of the material by applying a point load until fracture. Following this, the material was dispersed onto the pavement surface.

After the crushing and dispersion of the winter sanding aggregate over the pavement surface, simulated runoff application proceeded in much the same way as the prior long-term experiments, using the same TSS concentration. The procedure differed in that, since the surface area was of a smaller size than the standard sized models, a proportionately smaller volume of runoff (215 L) was used to simulate an equivalent year. Additionally, the infiltration capacity was measured by installing and sealing a temporary beam across the pavement, creating an "infiltration box" of precisely the same surface area as that of the infiltrometer ring. Falling head measurements were then taken as before. Infiltration measurements had to be done in this manner because the area of the miniature model restricted the placement of the infiltrometer ring.
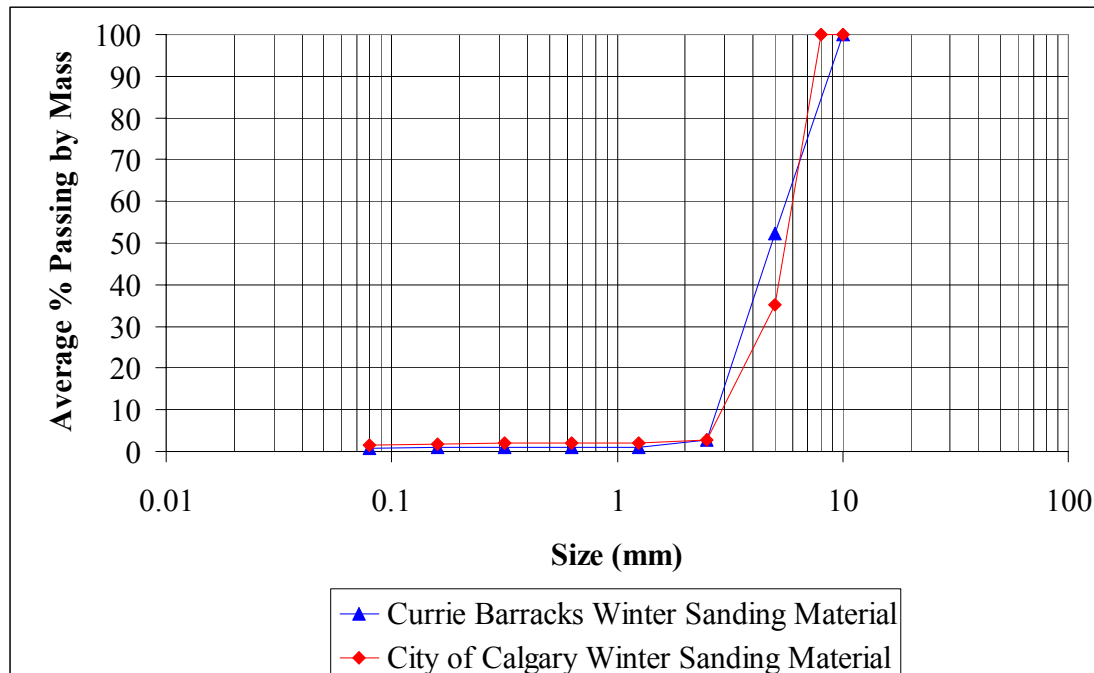


**Figure 3-29: Winter Sanding Material Gradation Analysis**

**3.5 ANALYTICAL METHODS**

*3.5.1 Total Suspended Solids*

Total Suspended Solids was analyzed according to the procedures described in Standard Methods for the Examination of Water and Wastewater (Clescerl *et al*, 1999), using a filter flask and Whatman 934-AH filter papers.

*3.5.2 Particle Size Distribution Analysis*

Particle size analysis was performed with a Malvern Mastersizer 2000 laser diffraction particle size analyzer. The details of the theoretical principles behind this method of particle size distribution analysis are described in Appendix B.

A bulk sample of approximately 0.5 – 1 gram of sediment was required for an accurate analysis using the laser diffraction analyzer. To collect this mass of sediment, a considerable volume of effluent was required, in some cases more than 10 L. This liquid sample was centrifuged using a Damon/IEC CRU-5000 centrifuge, at 4000 rpm for 15 minutes in four 1 L bottles per cycle. After removal from the centrifuge, the liquid supernatant was poured off, and the sludge was removed using a spoon.

Once the sediment had been collected, it was dried in an oven at 105 deg C for several hours. It was then separated into the appropriate target mass of 0.1-0.3 grams (depending on the prevalence of various-sized particles) using a chute-riffler, which maintains PSD between subsamples. This 0.1-0.3 gram subsample was then soaked overnight in hydrogen peroxide to dissolve organic bonds and allow better separation of particles. This naturally dissolves a portion of the organic content, but for low-organic-

content samples such as those used in this study (0% for ground silica, measured as 4% for street sweeping sediment), removal of the organic content likely does not have a significant impact on the particle size distribution. Following this, the sample is soaked overnight in Calgon to properly disperse the particles. The sample was then ready to be applied into the PSD analyzer, the operation of which is described in Appendix B.

**Chapter Four: Results and Discussion**

Results are presented and discussed under two main sections: Field Results and Laboratory Results, with the individual experiments for each setting existing as sub-sections. For field tests, the following experiments were performed:

- Flowrate and attenuation response

- TSS removal performance

- TSS removal characteristics (PSD analysis)

- Surface infiltration capacities/maintenance operations

For laboratory tests, the following experiments were performed:

- TSS removal performance and characteristics for both synthetic (sil-co-sil 106) and natural (sub-250 μm street sweepings) sediment

- Long-term surface infiltration capacities

- The effects of the presence of winter sanding material on long-term surface infiltration capacities.

## 4.1 Field Results

### *4.1.1 Flowrate and Attenuation*

Three simulated runoff events were applied to each permeable pavement field installation over the period of July 20 to September 7, 2006. The results for outflow rate (recorded at the monitoring manhole) versus inflow rate for both pavement surface types

are shown in Figure 4-1, in addition to the daily precipitation data from the nearby City of Calgary Lincoln Park monitoring station. The flow rates are shown on a L/s/ha basis in order to compare the findings with storm sewer design guidelines; an I/P ratio of 4 was assumed. The time for applied water to flow through the entire pavement structure to the monitoring manhole (the lag time), as well as surface ponding duration, and the proportion of flow-through water, are shown in Table 4-1 and Table 4-2 for the Eco-Stone® and porous asphalt respectively.

There was a moderate level of flow rate attenuation for both pavement types, with the peak flow rate being reduced from the inflow in all cases except for that of the Eco-Stone® on August 17, with peak rate reductions from the inflow ranging from 30 – 85% for all other experimental dates. It is important to observe the ponding time on Figure 4-1, indicated for each simulated runoff experiment by a large marker icon. In some cases, especially for the porous asphalt on August 24, 2006, there is the illusion of exaggerated sub-surface attenuation within the pavement substructure. However, in reality the extended detention time and reduced flow rate is due to the much lower surface infiltration capacity for the pavement, which can be seen from the extremely long ponding time. This lowered surface infiltration capacity was due to the comparatively rapid clogging of the porous asphalt surface that was observed over the first year of its installation, as will be explained further in Section 4.1.4. The surface ponding time for the Eco-Stone® was considerably less than that for the porous asphalt pavement throughout all experiments, which is also indicative of the lower surface infiltration capacity of the porous asphalt installation.

Peak flow rate, flow duration, and the proportion of water observed to flow to the manhole is quite variable for both pavements across all experimental dates. This can likely be attributed to the level of antecedent moisture in the pavement structure. Figure 4-1 shows that on August 17, the hydrograph for the Eco-Stone® displayed a much higher peak flow rate, almost reaching that of the inflow rate. Looking at the precipitation patterns over the testing period, one observes that there was approximately 23 mm of rain in the week prior to the August 17 experiment, which is three times more than the amount of precipitation received in the next wettest pre-experiment week over all experiments. Although 12.6 mm of precipitation was received on August 3, this occurred in the late afternoon, after the simulated runoff experiment for that day had finished.

Despite the moderate attenuation and peak flow reductions observed for the permeable pavements at Currie Barracks, additional flow control measures would likely have to be installed for full-scale installations in Calgary. The soils in the Calgary region are generally very impermeable, with a high clay content. The uncompacted sub-grade soils at the Currie Barracks installation, for example, showed average pre-construction infiltration rates of 0 to 10 mm/hr at a depth of approximately 600 mm in summer/fall climate conditions. These values are too low to safely accommodate storms that would be typically experienced in Calgary. As such, permeable pavement installations in this region would likely have to incorporate an underdrain system, similar to the one installed in the Currie Barracks installations, to convey detained stormwater to traditional storm sewer systems. With regards to design release rates for storm sewer systems in Calgary, The City of Calgary (2000) states that storm sewers should be designed for a minimum unit area release rate of 70 L/s/ha, and that 120 L/s/ha should be used for designing high

release areas with little storage and steep slopes. The peak outflow rates seen in Figure 4-1 exceed this range in most instances, and therefore a flow control device would likely be required for full scale installations of permeable pavements in Calgary in order to provide the appropriate outflow rates and detention times.
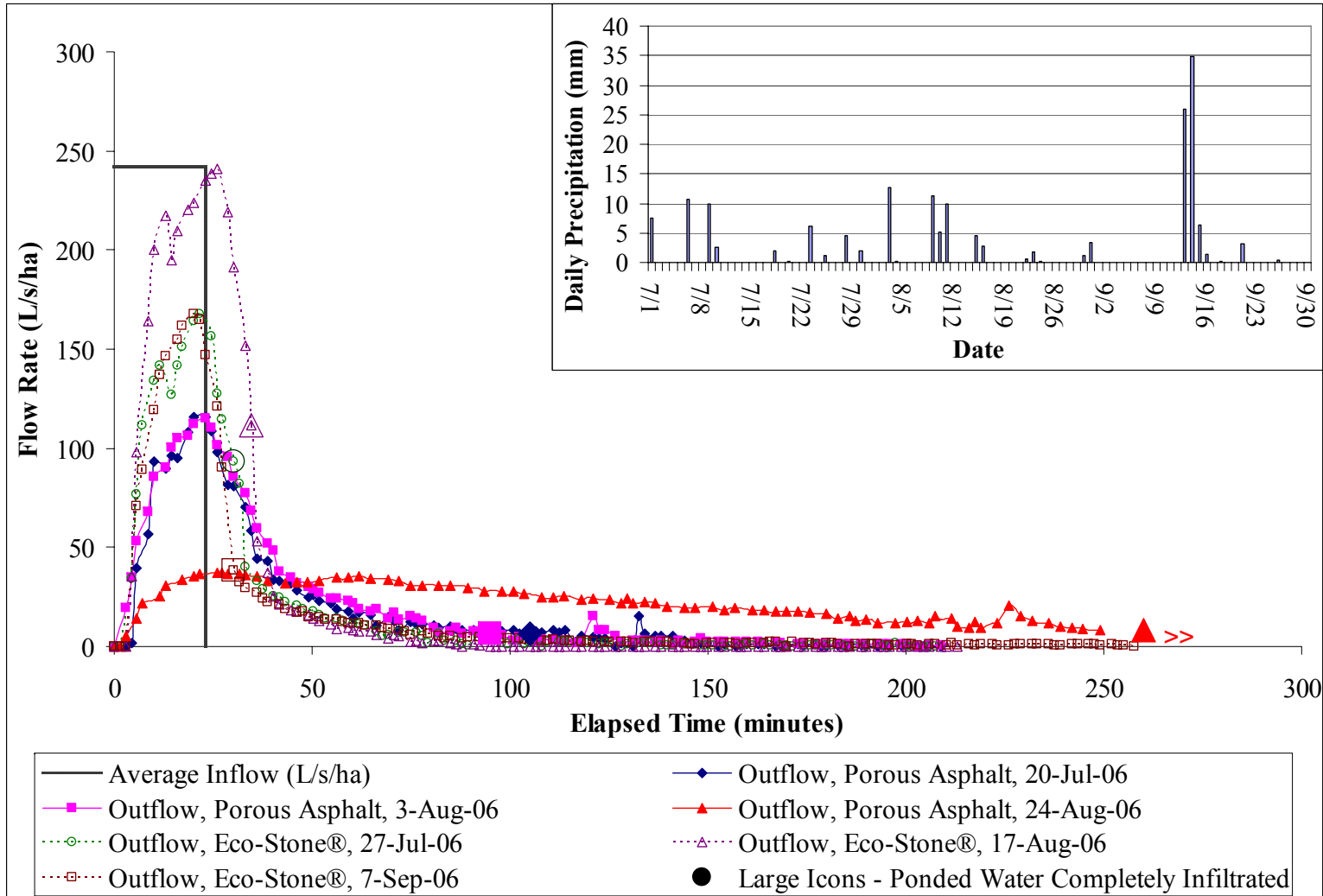
**Figure 4-1: Flow Data for Field Tests Assuming I/P Ratio of 4 (Daily Precipitation Data Superimposed in Top Corner)**

**Table 4-1: Flow Data for UNI Eco-Stone®**

| Experiment Date | Lag Time to Manhole (seconds) | Ponding Time (minutes) | Proportion Through Outlet (% of Applied Volume) |
|---|---|---|---|
| 27/7/06 | 66 | 30 | 78 |
| 17/8/06 | 59 | 35 | 99 |
| 7/9/06 | 72 | 29 | 88 |

**Table 4-2: Flow Data for Porous Asphalt**

| Experiment Date | Lag Time to Manhole (seconds) | Ponding Time (minutes) | Proportion Through Outlet (% of Applied Volume) |
|---|---|---|---|
| 20/7/06 | 60 | 105 | 84 |
| 3/8/06 | 65 | 94 | 72 |
| 24/8/06 | 63 | >200 | 99 |

On Figure 4-1, no precise value is shown for the ponding time of the porous asphalt on August 24 because the water did not completely drain on this date, even after more than three hours. Eventually, the beam had to be removed to allow traffic through at the end of the day, and the remaining water drained downstream through the Eco-Stone® blocks. Therefore, the accuracy of the measured outflow rates for this date is unreliable after 200 minutes.

Table 4-1 and Table 4-2 show the percentage of total applied water that was observed to flow to the outlet in the monitoring manhole. These results varied quite widely from experiment to experiment, ranging anywhere from 72% to 99%. The reason for this variation is likely to do with recent storm events and the degree of antecedent moisture in the pavement structure, as well as the level of saturation of the sub-grade soil

beneath the pavement. August 17, which was preceded by the most precipitation in the week prior to experimentation compared to other experimental dates, was also the experiment with the highest flow-through percentage. The experiment on August 24, which also had a high flow-through, was not preceded by a high level of precipitation, which appears to contradict this. However, flow-through data from this particular event may not be accurate because the ponded water was eventually allowed to drain onto the Eco-Stone® blocks as already described. Further investigation into the potential for preceding storm events and the antecedent moisture conditions in the pavement structure affecting the proportion of flow-through water is recommended.

### 4.1.2 TSS Removal Performance - Field

Results for total suspended solids removal efficiencies observed at the Currie Barracks permeable pavement installations are shown in Figure 4-2 and Figure 4-3, as well as in Table 4-3 and Table 4-4. For the first 2000 L of outflow volume, there appears to be an initial flushing of solids, which would explain the higher initial TSS concentrations observed during this period. On October 12, 2006, a "clean run" was performed; in which only clean water was applied to the Eco-Stone® pavement surface. The results showed that there was a TSS spike for the first 2000 L, indicating that the flushing occurs regardless of whether solids are present in the influent. The flushing effect is likely a combination of naturally occurring street sediment that accumulated on the pavement surface between experiments, as well as some solids that had settled out in the underdrain outlet pipe during low flows towards the end of previous runoff events, either natural or experimental.
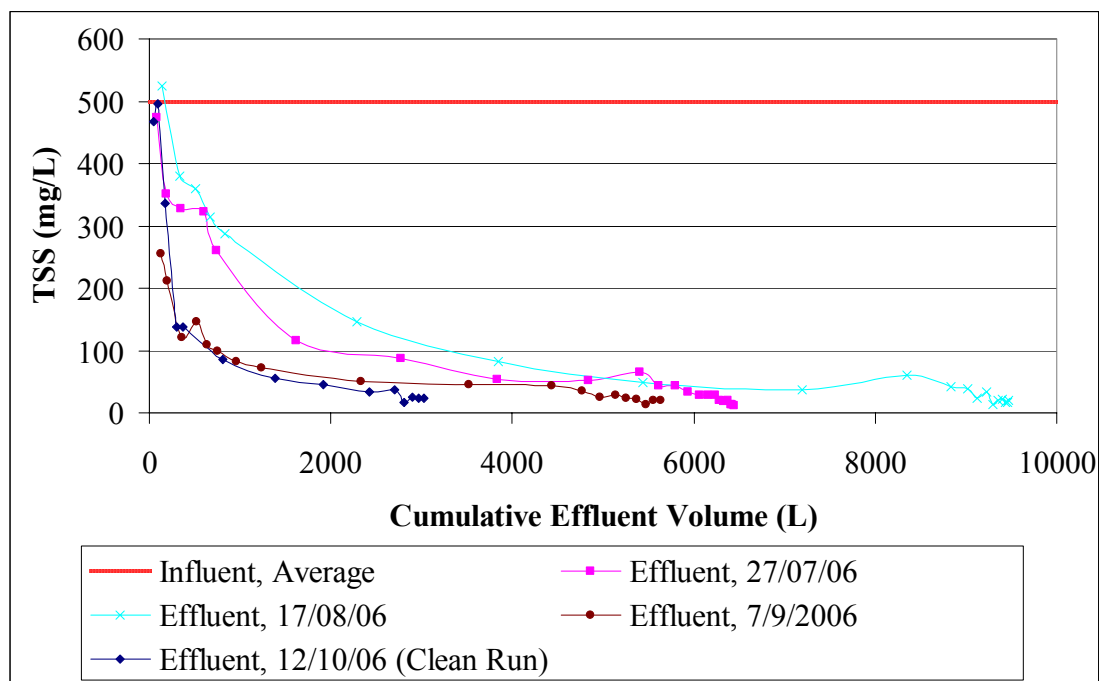
**Figure 4-2: TSS Removal at Currie Barracks for Eco-Stone®**
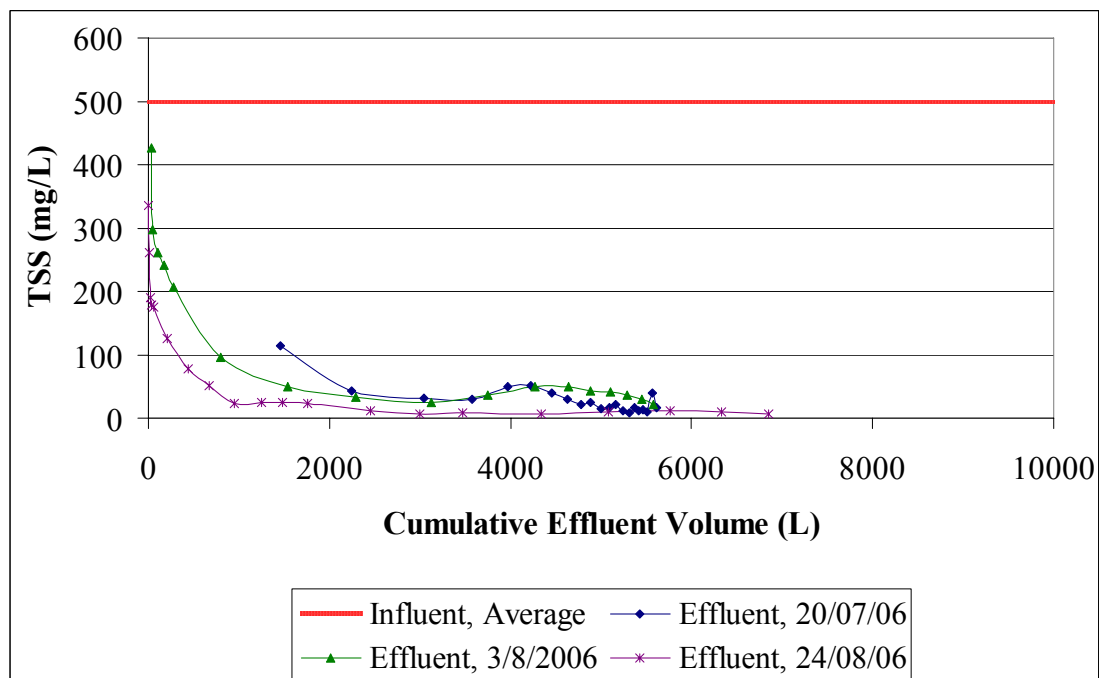


**Figure 4-3: TSS Removal at Currie Barracks for Porous Asphalt**

Table 4-3 and Table 4-4 show overall solids removal efficiencies both including and excluding the initial 2000 L flush. The efficiency after the initial flush is a more realistic representation because during the flush it is unknown what concentration of solids is being applied due to naturally occurring road sediment. Once the existing solids have flushed through, the influent TSS concentration is a known value and therefore the experimental conditions are more controlled.

**Table 4-3: UNI Eco-Stone® Average TSS Removal Efficiencies, Field Installation**

|  | 7/27/06 | 8/17/06 | 9/7/06 | Overall Average |
|---|---|---|---|---|
| **Average TSS Removal** | 78 % | 75 % | 85 % | 79% |
| **Average TSS Removal, after initial 2000 L flush** | 93 % | 92 % | 94 % | 93% |

**Table 4-4: Porous Asphalt Average TSS Removal Efficiencies, Field Installation**

|  | 7/20/06 | 8/3/06 | 8/24/06 | Overall Average |
|---|---|---|---|---|
| **Average TSS Removal** | 94 % | 77 % | 84 % | 85% |
| **Average TSS Removal, after initial 2000 L flush** | 95 % | 93 % | 98 % | 95% |

Both pavement surface types displayed very similar TSS removal efficiencies after the first 2000 L flush, with 92-98% of applied TSS removed from the simulated runoff influent. When the 2000 L flush is included in removal efficiency calculations, the rates vary more, but again, the exact influent TSS concentration is not known during this

flush and the results have reduced reliability. A constant influent concentration of 500 mg/L was used to calculate removal efficiencies.

### *4.1.3 TSS Removal Characteristics - Particle Size Distribution of Influent and Effluent*

Total suspended solids removal efficiency for permeable pavement is very dependent on the size of particles applied to the pavement surface. Since it acts as a filter, a larger proportion of coarse material will be retained in comparison to fine material, while finer material is more likely to pass through the structure. It is therefore very important to consider the particle size distribution of both influent and effluent when investigating the pavements' capabilities for removing solid matter. Furthermore, the current guidelines for The City of Calgary state that 85% of particles over 75 μm must be removed by stormwater treatment methods (The City of Calgary Wastewater & Drainage, 2000). In recent years there has been some debate in the region over the current pollutant loading criteria, and changes in regulations will likely occur in the future. This further increases the need for reliable regional data regarding the capability of permeable pavements for removing various size ranges of particles; this data can then be used to determine the acceptability of these BMPs for whatever future regulations may stipulate.

Figure 4-4 and Figure 4-5 show the particle size distributions of the influent and effluent at Currie Barracks for the Eco-Stone® and porous asphalt, respectively, on the dates when simulated runoff experiments were performed. Substantially finer solids were observed in the effluent when compared to the influent. The repeatability of the PSD data for influent and effluent between experiments was quite high, and there was negligible difference seen between the PSD data of both pavement types. When multiple data sets

were able to be collected for effluent on the same experimental date, this is indicated by #X in the legends of Figure 4-4 and Figure 4-5, with the higher numbered data sets representing the PSD for effluent collected at a later time than lower numbered data sets during the same experimental run. Based on this, the effluent PSD did not appear to show any consistent patterns of change over the course of a single experiment, or from experiment to experiment. The reason that multiple data sets for the effluent were not collected on every experimental date is that in some cases there were data processing errors, and in other cases there was not enough bulk sediment to perform multiple PSD analyses.
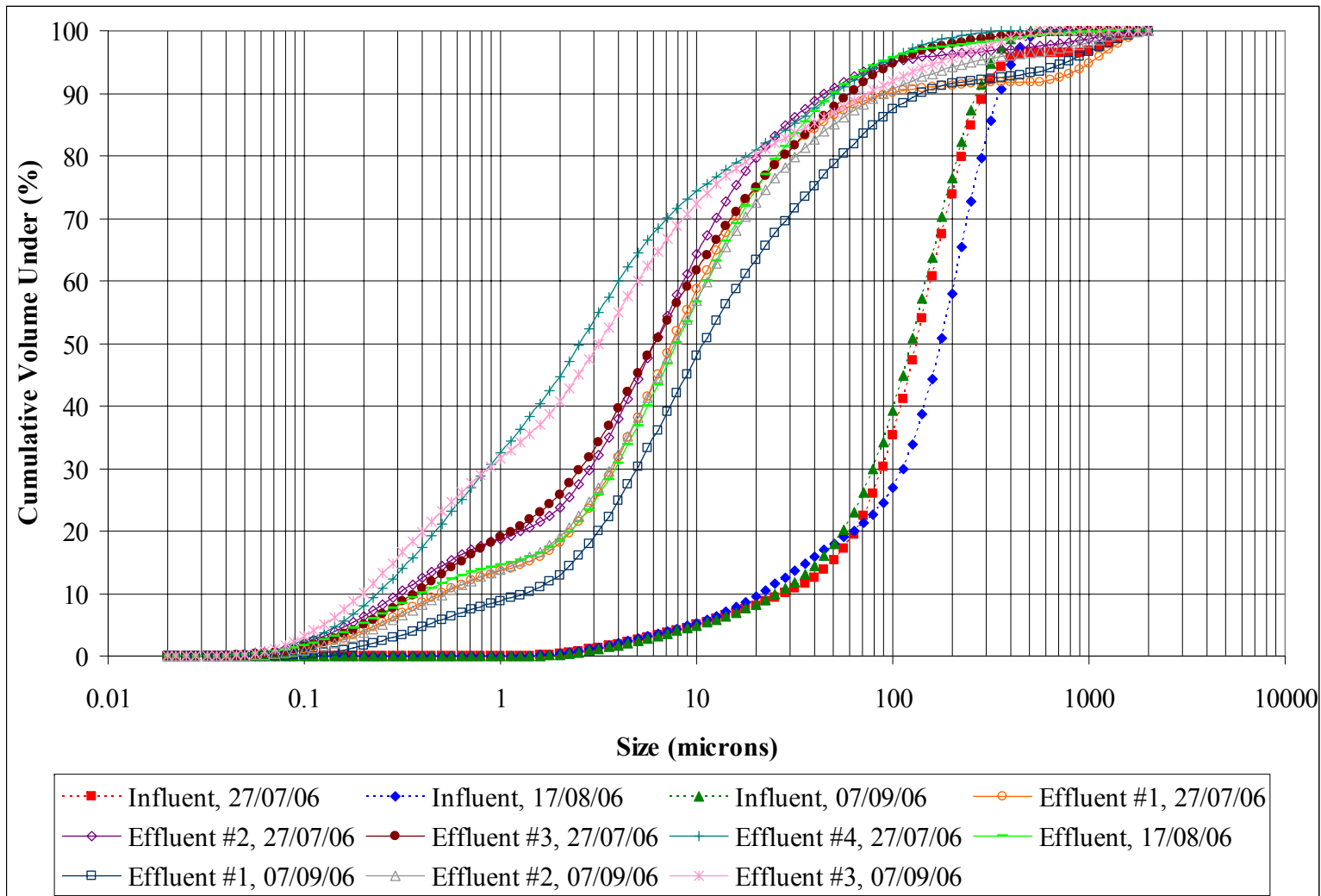
**Figure 4-4: Particle Size Distributions, Eco-Stone®, Currie Barracks**
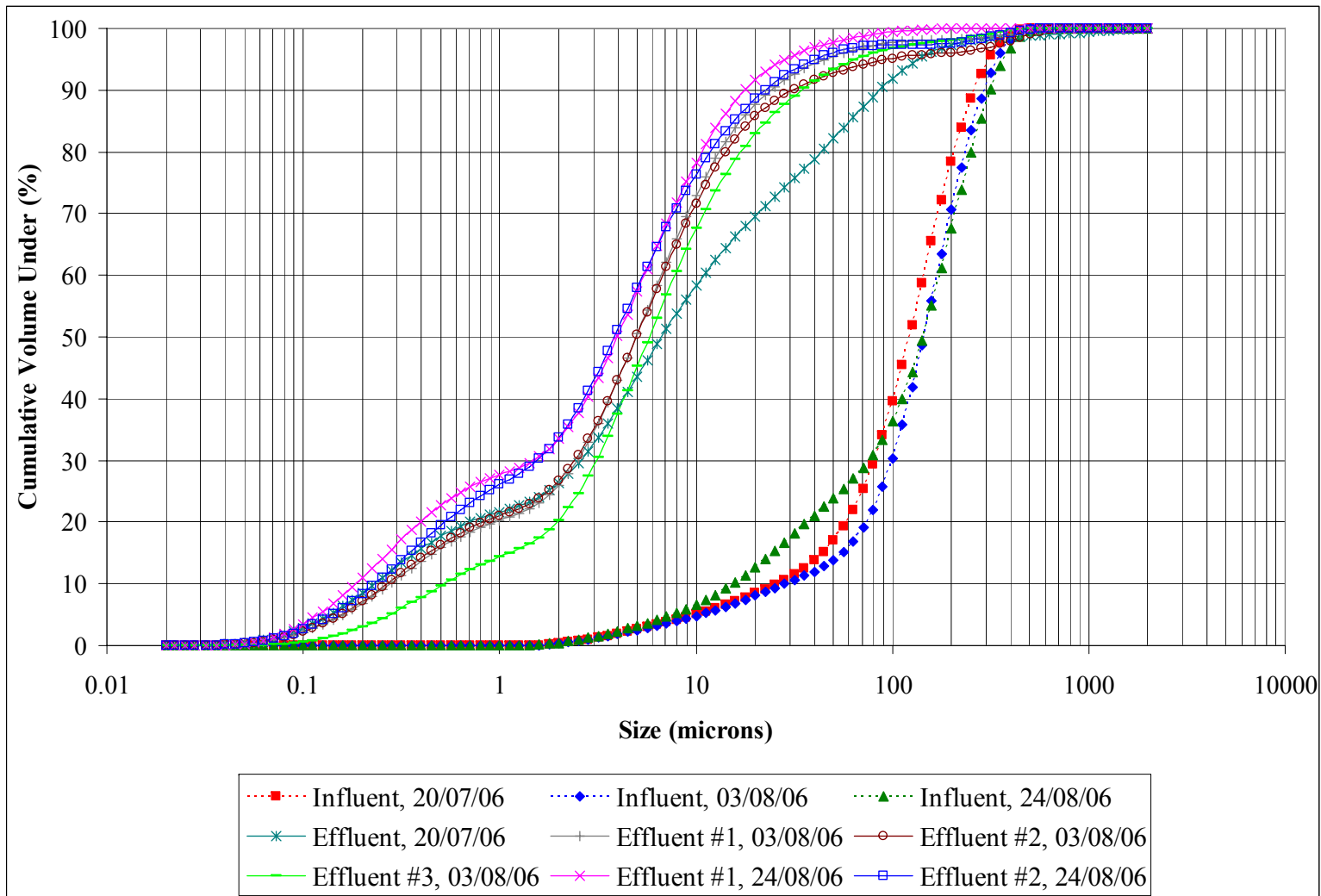
**Figure 4-5: Particle Size Distributions, Porous Asphalt, Currie Barracks**

Based on average particle size distribution data for all experimental dates and overall average total suspended solids removal rates (i.e., after the 2000 L flush) for a particular pavement, one can arrive at approximations of removal efficiency for various size fractions within the pavement. Since there is good repeatability with all PSD and TSS data (Table 4-7 and Table 4-8), the errors associated with using mean values are low. The formulas used to calculate removal efficiency of particular size fractions are as follows:

$$
\begin{aligned}
\beta_{\leq x} &= \frac{TSS_{in(\leq x)} - TSS_{eff(\leq x)}}{TSS_{in(\leq x)}} \\
&= \frac{TSS_{in}\alpha_{in} - TSS_{eff}\alpha_{eff}}{TSS_{in}\alpha_{in}} \\
&= \frac{TSS_{in}\alpha_{in} - (1-\xi)TSS_{in}\alpha_{eff}}{TSS_{in}\alpha_{in}} \\
&= \frac{\alpha_{in} - \left[(1-\xi)\alpha_{eff}\right]}{\alpha_{in}}
\end{aligned}
\tag{4.1}
$$

where:

$\beta_{\leq x}$ = removal efficiency for all particles less than or equal to X μm
$TSS_{in(\leq x)}$ = TSS in the influent that are less than or equal to X μm (mg/L)
$TSS_{eff(\leq x)}$ = TSS in the effluent that are less than or equal to X μm (mg/L)
$TSS_{in}$ = TSS in the influent (total)
$\alpha_{in}$ = proportion of influent that is less than or equal to X μm
$TSS_{eff}$ = TSS in the effluent (total)
$\alpha_{eff}$ = proportion of effluent that is less than or equal to X μm
$\xi$ = average overall removal efficiency of all TSS

$$\begin{aligned}
\beta_{\geq x} &= \frac{TSS_{in(\geq x)} - TSS_{eff(\geq x)}}{TSS_{in(\geq x)}} \quad\quad (4.2) \\[2mm]
&= \frac{TSS_{in}\left(1 - \alpha_{in}\right) - TSS_{eff}\left(1 - \alpha_{eff}\right)}{TSS_{in}\left(1 - \alpha_{in}\right)} \\[2mm]
&= \frac{TSS_{in}\left(1 - \alpha_{in}\right) - \left(1 - \xi\right)TSS_{in}\left(1 - \alpha_{eff}\right)}{TSS_{in}\left(1 - \alpha_{in}\right)} \\[2mm]
&= \frac{\left(1 - \alpha_{in}\right) - \left[\left(1 - \xi\right)\left(1 - \alpha_{eff}\right)\right]}{\left(1 - \alpha_{in}\right)}
\end{aligned}$$

where:

$\beta_{\geq x}$ = removal efficiency for all particles greater than or equal to X µm.
$TSS_{in(\geq x)}$ = TSS in the influent that are greater than or equal to X µm (mg/L)
$TSS_{eff(\geq x)}$ = TSS in the effluent that are greater than or equal to X µm (mg/L)

Using Equations 4.1 and 4.2, the calculated removal efficiencies are shown in Table 4-5 and Table 4-6 for particle size fractions above and below 200 µm, 100 µm, 75 µm, 50 µm, 25 µm, and 10 µm for both pavement types. It should be noted that these fractional removal efficiencies are valid only for the specific influent that was used in these simulated experiments. If an influent with a different PSD was applied to the pavements, the removal efficiencies for the various size fractions would vary accordingly. Since there is such a high proportion of the influent sediment in the coarser range, and a large percentage of the influent sediment overall is removed by the pavements, the "fraction above" removal efficiencies are very high. As an illustration, consider that, as one approaches the removal efficiency for $\geq 0$ µm, the fractional removal efficiency would be at their minimum at 92% in the case of the Eco-Stone[®], or 95% in the case of the porous asphalt, as these are the overall TSS removal efficiencies. For the "fraction below" removal efficiencies, this bias is not present.

**Table 4-5: Particle Size Fractional Removal Efficiencies for the Eco-Stone®
Installation at Currie Barracks**

| Size Fraction | Proportion of Influent Under Size Fraction, Average Across All Eco-Stone® Experiments (%) | Std. Deviation | Proportion of Effluent Under Size Fraction, Average Across All Eco-Stone® Experiments (%) | Std. Deviation | % Removal for Size Fraction |
|---|---|---|---|---|---|
| *Greater Than* | | | | | |
| ≥200 | 30.53 | 8.18 | 4.54 | 2.56 | 99 |
| ≥100 | 66.18 | 5.19 | 7.10 | 2.80 | 99 |
| ≥75 | 75.36 | 2.48 | 9.03 | 3.13 | 99 |
| ≥50 | 82.93 | 1.29 | 12.54 | 3.70 | 99 |
| ≥25 | 89.75 | 0.92 | 20.74 | 4.81 | 98 |
| ≥10 | 94.94 | 0.16 | 37.81 | 7.82 | 97 |
| *Less Than* | | | | | |
| ≤200 | 69.47 | 8.18 | 95.46 | 2.56 | 90 |
| ≤100 | 33.82 | 5.19 | 93.31 | 2.80 | 80 |
| ≤75 | 24.64 | 2.48 | 90.97 | 3.13 | 74 |
| ≤50 | 17.07 | 1.29 | 87.46 | 3.70 | 64 |
| ≤25 | 10.25 | 0.92 | 79.26 | 4.81 | 45 |
| ≤10 | 5.06 | 0.16 | 62.19 | 7.82 | 13 |

**Table 4-6: Particle Size Fractional Removal Efficiencies for the Porous Asphalt Installation at Currie Barracks**

| Size Fraction | Proportion of Influent Under Size Fraction, Average Across All Porous Asphalt Experiments (%) | Std. Deviation | Proportion of Effluent Under Size Fraction, Average Across All Porous Asphalt Experiments (%) | Std. Deviation | % Removal for Size Fraction |
|---|---|---|---|---|---|
| *Greater Than* | | | | | |
| ≥200 | 27.84 | 4.54 | 2.10 | 1.17 | 99 |
| ≥100 | 64.60 | 3.83 | 3.62 | 2.35 | 99 |
| ≥75 | 74.18 | 3.91 | 4.83 | 3.49 | 99 |
| ≥50 | 81.73 | 4.21 | 7.07 | 5.11 | 99 |
| ≥25 | 88.48 | 2.70 | 12.80 | 6.92 | 99 |
| ≥10 | 94.49 | 0.78 | 29.15 | 6.57 | 99 |
| *Less Than* | | | | | |
| ≤200 | 72.16 | 4.54 | 97.90 | 1.17 | 94 |
| ≤100 | 35.40 | 3.83 | 96.38 | 2.35 | 87 |
| ≤75 | 25.82 | 3.91 | 95.17 | 3.49 | 83 |
| ≤50 | 18.27 | 4.21 | 92.93 | 5.11 | 76 |
| ≤25 | 11.52 | 2.70 | 87.20 | 6.92 | 64 |
| ≤10 | 5.51 | 0.78 | 70.85 | 6.57 | 40 |

Of particular importance from the perspective of stormwater treatment in Calgary are the particles over 75 μm. As shown in Table 4-5 and Table 4-6, the removal efficiency for particles greater than or equal to 75 μm is above 99% for both pavement types for sub-250 μm street sweeping influent. For particles finer than 75 μm, the removal rates were 74% for the Eco-Stone® and 83% for the porous asphalt. As the size range decreases from 75 μm, the removal rate begins to drop drastically for both pavement types. From a water quality standpoint, the performance of both pavement types in this study for removing solids is exceptional. Again, it must be stressed that these

values are only valid for the influent used for this study. For future studies it would be very informative to apply influents with different PSDs and observe the changes in removal efficiencies for various influent size ranges.

**Table 4-7: Repeatability for PSD Data**

| Data | Average Standard Deviation Across All Size Fractions (%) | Maximum Standard Deviation for a Single Size Fraction (%) |
|---|---|---|
| All Currie Barracks Eco-Stone® Influent PSD Data | 1.19 | 8.56 |
| All Currie Barracks Eco-Stone® Effluent PSD Data | 4.33 | 11.02 |
| All Currie Barracks Porous Asphalt Influent PSD Data | 1.06 | 4.74 |
| All Currie Barracks Porous Asphalt Effluent PSD Data | 2.97 | 7.14 |

**Table 4-8: Repeatability for TSS Removal Efficiency**

| Data Set | Average TSS Removal (%) | Standard Deviation |
|---|---|---|
| Eco-Stone®, 7/27/06 | 92.99% | 4.15% |
| Eco-Stone®, 8/17/06 | 91.73% | 6.68% |
| Eco-Stone®, 9/7/06 | 94.02% | 2.33% |
| Overall Eco-Stone® Average Across Experiments | 92.91% | 0.93% |
| Porous Asphalt, 7/20/06 | 94.97% | 2.61% |
| Porous Asphalt, 8/3/06 | 92.74% | 1.83% |
| Porous Asphalt, 8/24/06 | 98.18% | 0.37% |
| Overall Porous Asphalt Across Experiments | 95.30% | 2.23% |

*4.1.4 Surface Infiltration Capacity and Maintenance Experiments*

The surface infiltration capacities of the installations at Currie Barracks were monitored at various intervals from May 25 to October 6 2006, both before and after two separate maintenance operations. As surface infiltration capacity for permeable pavements is highly spatially variable (Kresin *et al*, 1997), multiple locations were tested on both pavement surfaces, with the locations chosen to represent a fairly random spatial distribution. Precisely the same locations were monitored for every measurement; these locations are shown in Figure 4-6.
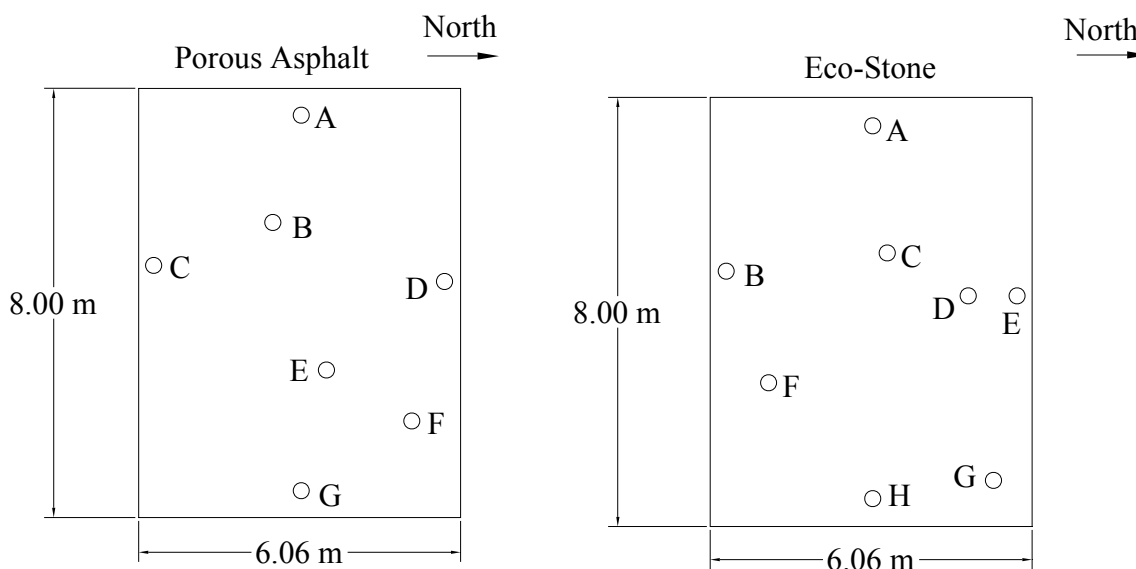


**Figure 4-6: Infiltrometer Locations for Porous Asphalt and Eco-Stone® Installations at Currie Barracks**

Unfortunately, initial surface infiltration capacities of the pavement surfaces were not measured immediately after installation in 2005 due to the fast onset of freezing temperatures and winter conditions. However, on November 24, 2005, very shortly after

installation, water was applied to the pavement surfaces to observe and demonstrate their functionality. From videos and photographs taken on this date, very rough approximations of surface infiltration capacity can be deduced. Water was applied to the pavement surfaces at a very high rate (~8 L/s), and judging from the videos and photos, there was a wetting area of approximately 1 m$^2$ for both pavement surfaces (Figure 4-7 and Figure 4-8). The water infiltrated almost instantaneously. Using this rudimentary data it can be estimated that the initial surface infiltration capacity of both permeable pavements was in the range of 25,000 – 40,000 mm/hr.



**Figure 4-7: Initial Surface Infiltration Capacity of the Eco-Stone® at Currie Barracks, November 24, 2006 (8 L/s Application Rate)**



**Figure 4-8: Initial Surface Infiltration Capacity of the Porous Asphalt at Currie Barracks, November 24, 2006 (8 L/s Application Rate)**

The results for all surface infiltration capacity measurements throughout the spring to fall of 2006 are shown in Figure 4-9 and Figure 4-10 (Error bars are shown to indicate the average deviations, based on percentage, across all multiple-trial measurements). In most cases, on the first measurement dates (taken place over May 25 to June 1, 2006), the surface infiltration capacity had substantially decreased since the

initial estimation. There were some exceptions to this, and interestingly there appears to be a general pattern of higher surface infiltration capacities at the very edges of the pavements. This is likely because of the negative impact that traffic has on surface infiltration capacity (Ferguson, 2005), and the fact that very little vehicular traffic would travel across the extreme outer edges of the pavement surfaces. Other than this, there does not to appear to be any consistent patterns in decline from the initial estimation to the first measurement date. There is a high degree of spatial variability, though, which supports the findings of Kresin *et al* (1997).

The remaining surface infiltration capacities were made before and after two separate maintenance activities. Discussion of the maintenance results and their implications follows.
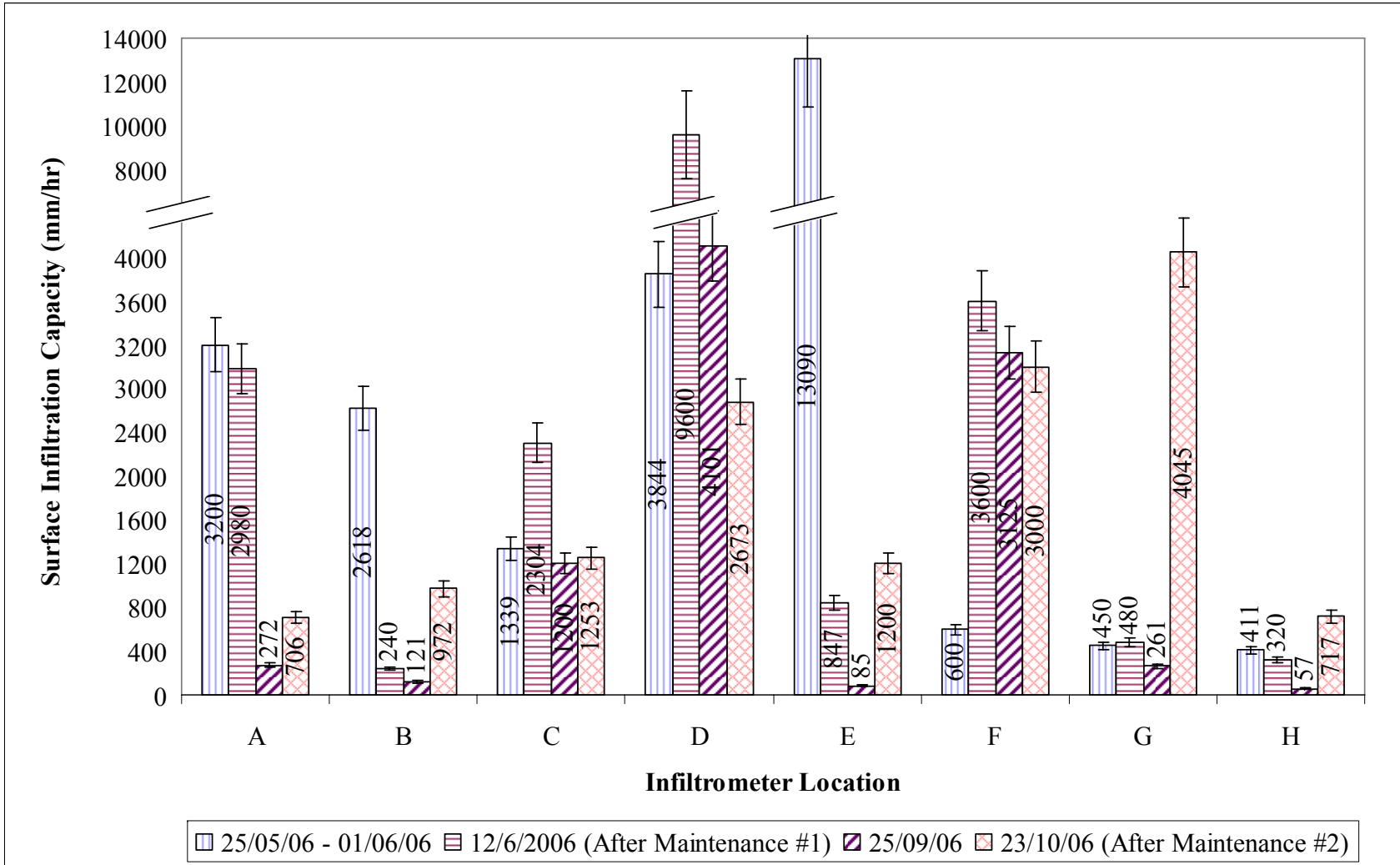
**Figure 4-9: Surface Infiltration Capacities for Eco-Stone® at Currie Barracks from 25/05/06 - 23/10/06**
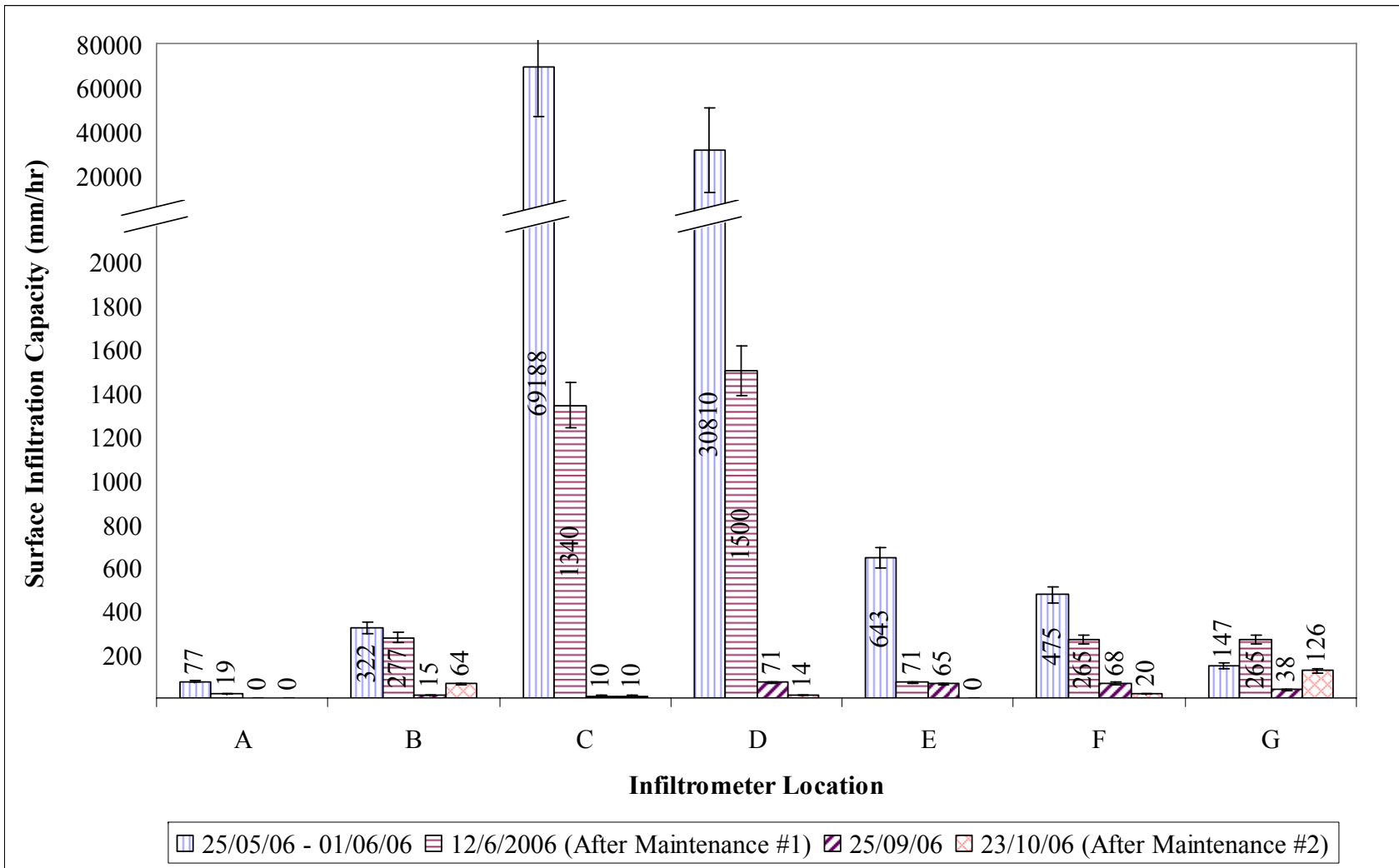
**Figure 4-10: Surface Infiltration Capacities for Porous Asphalt at Currie Barracks from 25/05/06 - 23/10/06**

*Maintenance #1 – Single Dry Pass, Schwarze A8000*

For the porous asphalt, all but one of the monitored locations showed a substantial decrease in surface infiltration capacity after the first vacuum sweeping maintenance. For the Eco-Stone®, certain locations showed an improvement, while some showed hardly any change at all and still others showed a decrease in infiltration capacity.

The poor results of the first vacuum sweeping maintenance can possibly be attributed to a few factors. The pavement surface (especially the porous asphalt) was already substantially clogged in certain areas. As suggested by Balades *et al* (1995) vacuum sweeping is ineffective for porous asphalt if the infiltration rate is below 3600 mm/hr, which is the case for many of the locations. The negative effects can possibly be attributed to a "grinding and crushing" effect, that is, loose surface fines being spread out and ground more permanently into the pavement surface by the vacuum sweeping equipment, and coarser solids being broken down into finer solids. This phenomenon, which would increase the potential for clogging, is certainly reported to occur over time from vehicular traffic (Kresin, 1996), so it is possible that the vacuum sweeping equipment in this case applied a similar action.

It is also important to note that, between the first pre-maintenance measurements on May 25, the pass of the vacuum sweeper, and the post-maintenance measurements on June 12 (a period of about 3 weeks), there was a total of approximately 50 mm of rainfall. Although it seems unlikely, it is possible that the reduced infiltration rates could be due to additional clogging caused by the runoff during this period.

The amount of saturation in the pavements should not have been a highly significant factor, because all infiltration measurements were done after the pavement

area surrounding the infiltrometer locations had been soaked with water for several minutes. Furthermore, multiple repeats of every infiltration measurement were taken, with excellent repeatability and no clear trend of increases or decreases between trials.

For the Eco-Stone®, the locations that showed an improvement in infiltration rates had a visibly higher volume of joint fill material removed from the vacuum sweeper than those locations which showed no improvement or degradation in infiltration rate (Figure 4-11 and Figure 4-12). Those locations that showed no improvement or degradation still contained most of their joint fill material, and the material was visibly held in by a "crust" of fine material. The amount of joint fill material removed appeared to be highly influential on the degree to which (or whether) improvement in infiltration was observed. This is in agreement with the observations by Kresin *et al* (1997) and James and Gerrits (2003). It is possible that additional passes of the vacuum sweeper would have shown further improvement for the UNI Eco-Stone®.

In the case of the porous asphalt, it is possible that no amount of additional passes with the vacuum sweeper would have shown any improvement in infiltration because the average infiltration rate of the entire surface was already too low to be able to benefit from the maintenance procedure (Balades *et al*, 1995). This needs further investigation.
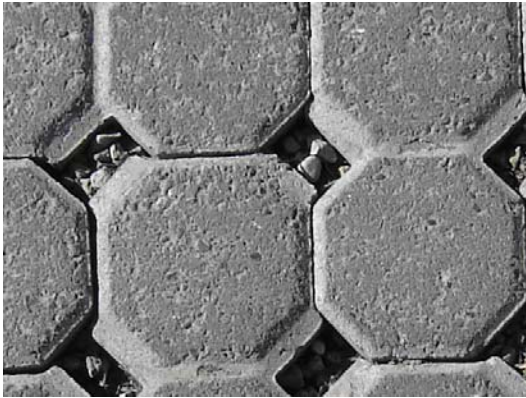
**Figure 4-11: Post-Maintenance Eco-Stone®, Infiltrometer 'D' (Significant Joint Fill Material Removed)**



**Figure 4-12: Post-Maintenance Eco-Stone®, Infiltrometer 'B' (Little Joint Fill Material Removed)**

*Maintenance #2 – Three wet passes, Schwarze A8000*

The measured infiltration capacities before and after the second maintenance attempt are also shown on Figure 4-9 and Figure 4-10. For the porous asphalt, virtually no improvement was observed, and by that point in time all locations for the porous asphalt appeared to be irreversibly clogged. Even the location with the highest measured infiltration capacity, 126 mm/hr observed at Location "G", is barely acceptable for stormwater management purposes in Calgary. The rapid clogging and resulting decline in surface infiltration capacity over the initial 10 months of the porous asphalt's lifespan is likely due to a combination of factors, including application of winter sanding materials, compression of the asphalt (and thus reduction in void spaces) due to high traffic loads, and the grinding and crushing action of traffic, as mentioned by Kresin *et al* (1997). It is possible that the specific porous asphalt mix used is not ideal for the conditions and climate in which it was installed. Further investigation into all of these factors is needed for future studies.

The Eco-Stone®, on the other hand, showed very positive results after the second maintenance attempt. Almost all locations showed significant improvement in infiltration capacity, and all locations have infiltration capacities well above 500 mm/hr, which is sufficient for a permeable pavement to handle almost all Calgary storms if the I/P ratio is at 4, as assumed throughout this study. The improved infiltration recovery after the second maintenance, in comparison to the first maintenance, is possibly due to the increased number of passes removing a deeper depth of joint fill material from the Eco Stone surface, rather than the presence of water application. The reason for this conclusion is that, as with the first maintenance, improvement in infiltration capacity appeared to be proportional to the depth to which joint fill material was removed. In addition, Balades *et al* (1995) found that moistening followed by sweeping actually has a negative effect on the infiltration capacity of permeable pavements. The fact that depth of joint fill material removed is proportional to the improvement in surface infiltration capacity is interesting in that it may provide a visual indication for the adequacy of maintenance activities. Repeated passes could be made until a satisfactory amount of joint fill removal (and thus corresponding recovery in infiltration capacity) had been accomplished.

## 4.2 Laboratory Results

While field experiments mostly focused on the performance of permeable pavements in a realistic setting, as well as general short-term observations of newly installed field installations, the laboratory experiments were designed to simulate long-

term capabilities of the pavements, and to observe trends in solids removal efficiency and characteristics, as well as clogging and solids accumulation locations throughout the pavement structures.

### 4.2.1 TSS Removal Performance, Synthetic Sediment

Figure 4-13 shows the long-term results for effluent solids concentration for both the Eco-Stone® and the porous asphalt over 10 simulated years using 500 mg/L sil-co-sil 106 as the applied influent. Over the course of 4250 L of applied simulated runoff, the average effluent TSS concentration was 192 mg/L for the Eco-Stone® and 190 mg/L for the porous asphalt, which corresponds to TSS removal efficiencies of approximately 62 % for both pavement types. The effluent concentration for both pavements fluctuated considerably, with standard deviations of 85 mg/L and 106 mg/L for the Eco-Stone® and porous asphalt, respectively, and it became more highly variable as the total applied volume of simulated runoff increased. This is likely due to a "flushing effect", whereby solids that had partially accumulated throughout the pavement's sub-structure are washed through once the hydraulic head reaches a certain point. As more solids accumulate throughout the pavement structure, the likelihood of instantaneous flushes of partially retained solids increases, which explains the increased fluctuations seen towards the later portions of Figure 4-13.
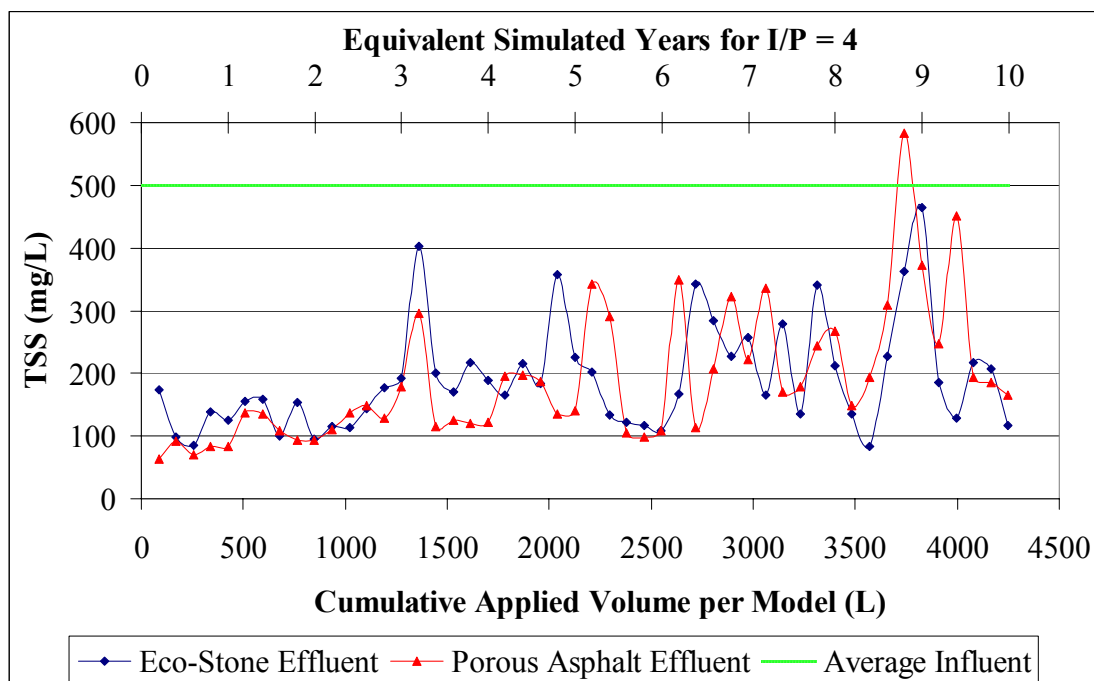
**Figure 4-13: Long-term Influent and Effluent TSS for Eco-Stone® and Porous Asphalt When Using 500 mg/L sil-co-sil 106 Ground Silica as Influent**

After 10 simulated years, experimentation with ground silica was discontinued due to lack of realistic long-term representation. Infiltration measurements were taken at the end of every simulated year, and no reduction in infiltration (and thus no clogging) was observed throughout 10 simulated years of sediment application. The surface infiltration capacity was greater than the maximum measurable surface infiltration capacity in the laboratory (approximately 30,000 mm/hr) for every measurement, and thus the data is not shown as a figure in this thesis. The lack of any decreases in surface infiltration capacity over time deviates from what would be expected, and has been observed, in field installations, and thus it was determined that although the silica influent illustrates the capability of new permeable pavements for removing inert spherical solids

in the 0-150 μm range, it was not realistic in representing the long-term performance of permeable pavements subjected to actual street sediments..

### *4.2.2 TSS Removal Characteristics - Particle Size Distributions, Influent and Effluent, Synthetic Sediment*

Figure 4-14 and Figure 4-15 show the particle size distributions for the influent and effluent of the Eco-Stone® and porous asphalt, at various stages of the long-term simulated runoff experiment using sil-co-sil 106. There are negligible difference between PSDs for both influent and effluent regardless of either pavement surface type or total volume of sediment applied. This implies that all size ranges of sediment in the influent are permitted to pass through the entire pavement structure and that the "equivalent sieve size" of the layers of the pavement structures is larger than the largest particle in the sil-co-sil 106 mix (approximately 150 μm). This also gives some insight into the mechanism of solids removal in the case of the silica. Although there was no "sieving action" through various layers of the pavement, there was still a significant degree of solids removal as shown previously in Section 4.2.1. The reason for this is likely that there were certain areas where the silica was temporarily trapped (i.e. small pockets or divots throughout the structure created by the orientation or surface characteristics of the various aggregates), and there may also have been weak adhesion between the silica and certain aggregate particles, along with some sedimentation. The flow pattern of the simulated runoff, which would be quite random as it passed through the multiple layers of aggregate, would then in some cases wash these temporarily trapped portions of silica through to the effluent.

These findings are significant for two reasons: they indicate the size of particles that are potentially permitted to pass through the permeable pavement systems used in this study (at least 150 μm), and additionally they suggest that the process of clogging is more complex than simply the accumulation of fine solids throughout the structure. With natural sediment, there are numerous physical, chemical, and biological properties present that are not present in the ground silica; for example, the presence of organic materials, colloidal materials, volatile chemicals, and potentially cohesive particles. The essentially spherical shape of the silica and its inert properties allow it to pass through the pavement layers much easier than oblong-shaped or chemically and biologically active materials would. The silica's PSD did not change from influent to effluent throughout the course of the experiment, partly because it never formed a "crust", i.e. a layer or series of layers of conglomerated solids. These crusts, which are typically observed with natural road sediment, essentially act as finer-grained filters, and thus would prohibit certain solids from passing through the structure. What this all suggests is that the TSS removal efficiency observed with the synthetic "sil-co-sil 106" sediment was purely mechanical filtration and sedimentation; i.e., the capability of the pavements to filter inert, spherical, non-cohesive particles less than 150 μm in size. This is certainly not a realistic measurement of the filtration or sieving capabilities of the pavements in a natural scenario, but it does provide some information about the solids removal process.
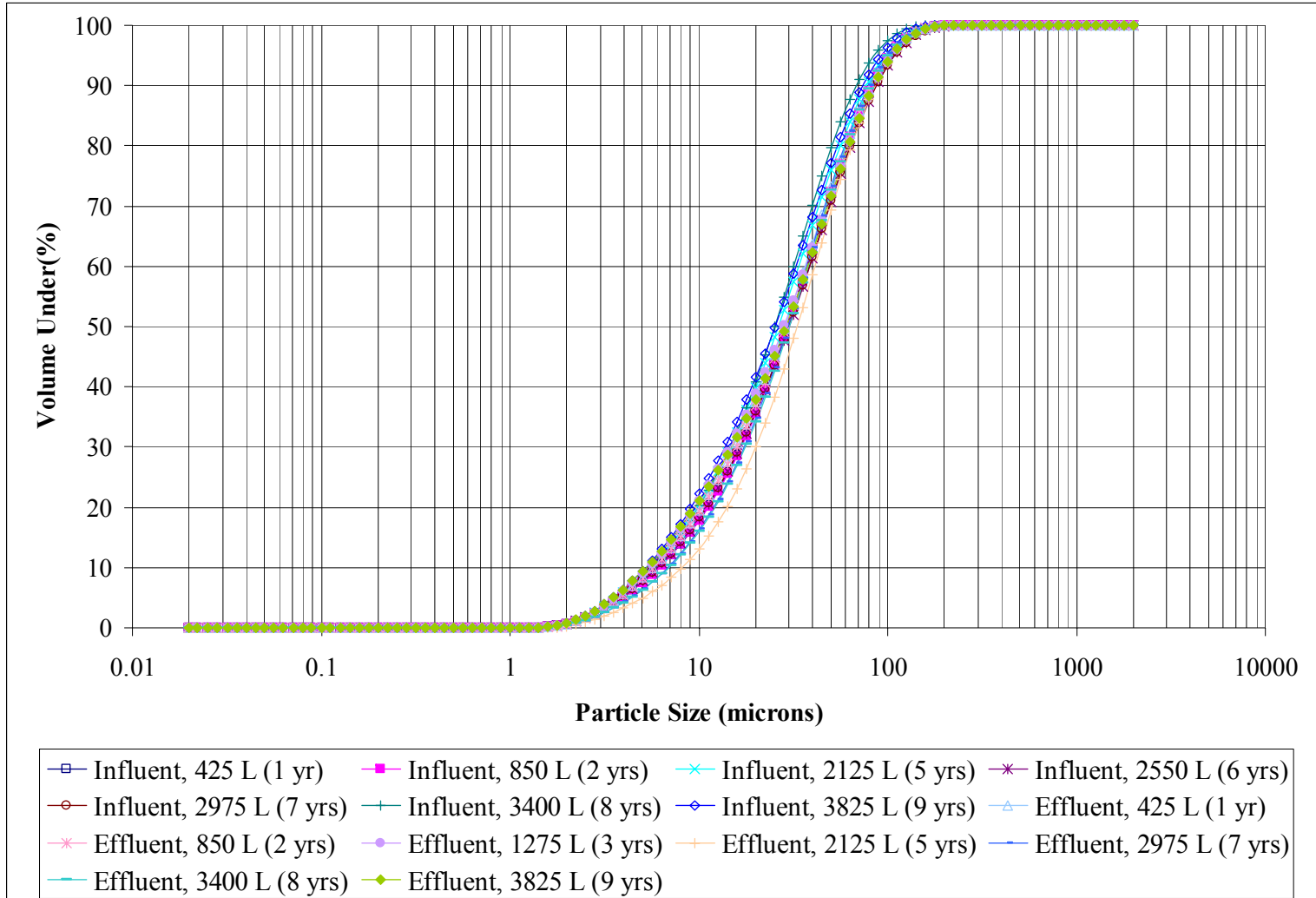
**Figure 4-14: Particle Size Distribution for the Influent and Effluent of the Laboratory Eco-Stone® Model for sil-co-sil 106**
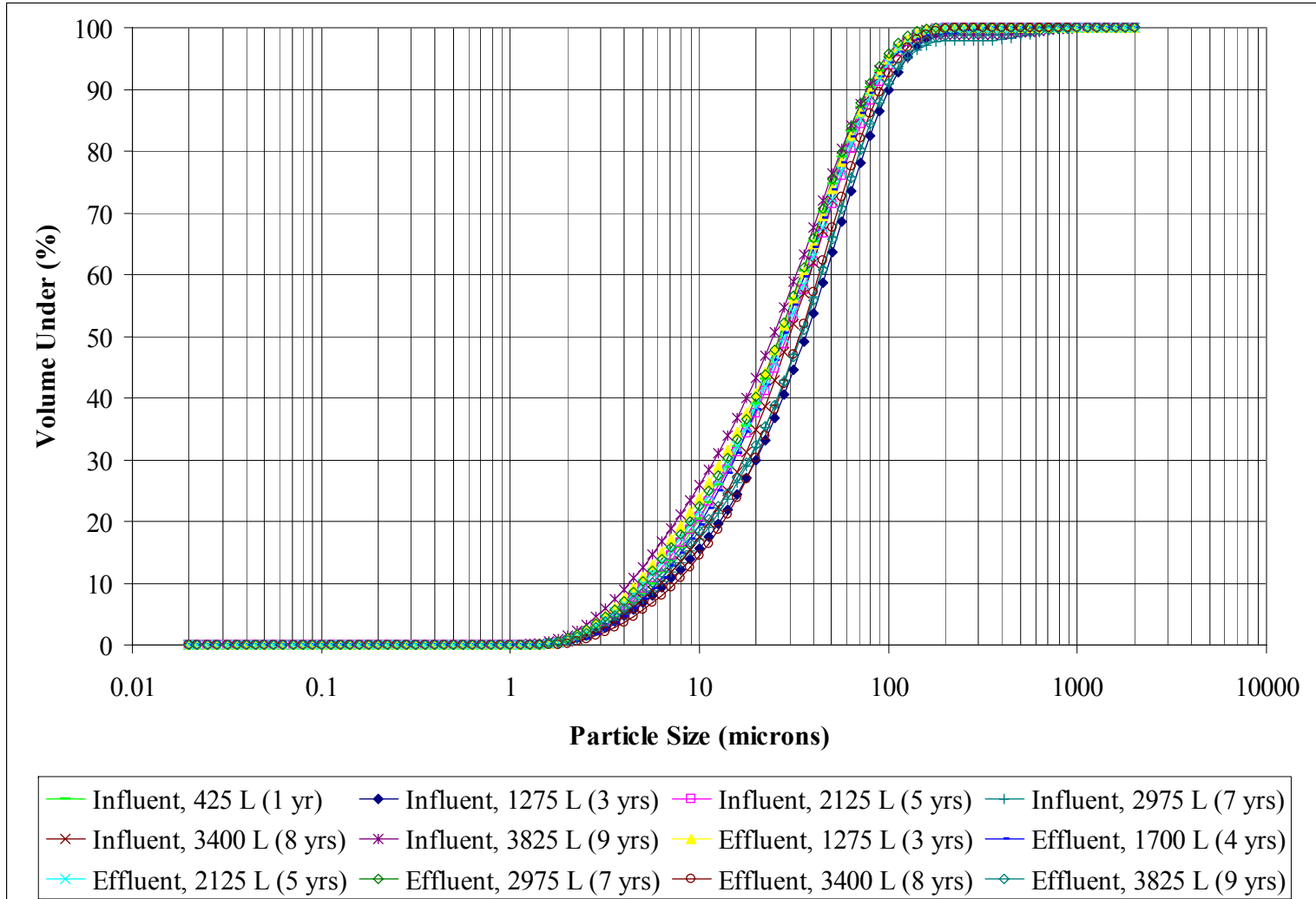
**Figure 4-15: Particle Size Distribution for the Influent and Effluent of the Laboratory Porous Asphalt Model for sil-co-sil 106**

### *4.2.3 TSS Removal Performance, sub-250 µm Street Sweepings*

The long-term effluent TSS concentrations for both pavements when using 500 mg/L sub-250 µm street sweepings as an influent are shown in Figure 4-16, as compared to the average influent concentration. The Eco-Stone® effluent had an average TSS concentration of 21 mg/L with a standard deviation of 14 mg/L. The porous asphalt effluent had an average TSS concentration of 20 mg/L with a standard deviation of 18 mg/L. Removal efficiencies for both surface types were 96%, with a standard deviation of 2.75% and 3.56% for the Eco-Stone® and porous asphalt models, respectively. That the removal efficiencies were so similar for both pavement surface types (which was also the case for the ground silica experiments) suggests that the surface itself, in the case of sub-250 µm material, may be less of a factor in solids removal than the sub-surface courses, because the sub-surface courses for both pavements were identical. However, it is important to note that very little surface crusting occurred in the laboratory models. In field installations where surface crusting is observed, the surface may then play a more predominant role in solids removal.

The difference in removal efficiencies for the synthetic sediment and street sweeping sediment is likely due to a combination of factors. Firstly, the maximum size of the street sediment is larger than the maximum size of the silica, so there may be more retention of solids due to "sieving action" through the layers of the pavement sub-layers. Additionally, the street sediment, upon visual qualitative observation of the material's behaviour when combined with water, is much more cohesive than the silica, and as a result it has a greater tendency to conglomerate and form crusts within the pavement structure. The street sweeping sediment is also more likely to contain particles that are

oblong or otherwise non-spherical. These particles would have a greater tendency to interlock with one another and resist flow through the pavement, thus causing greater accumulation within the pavement structure. And finally, the street sweeping sediment is not chemically and biologically inert, as the silica is, and this may play a role in the behaviour of the particles and their tendency to adhere to one another or to the surfaces within the pavement structure.
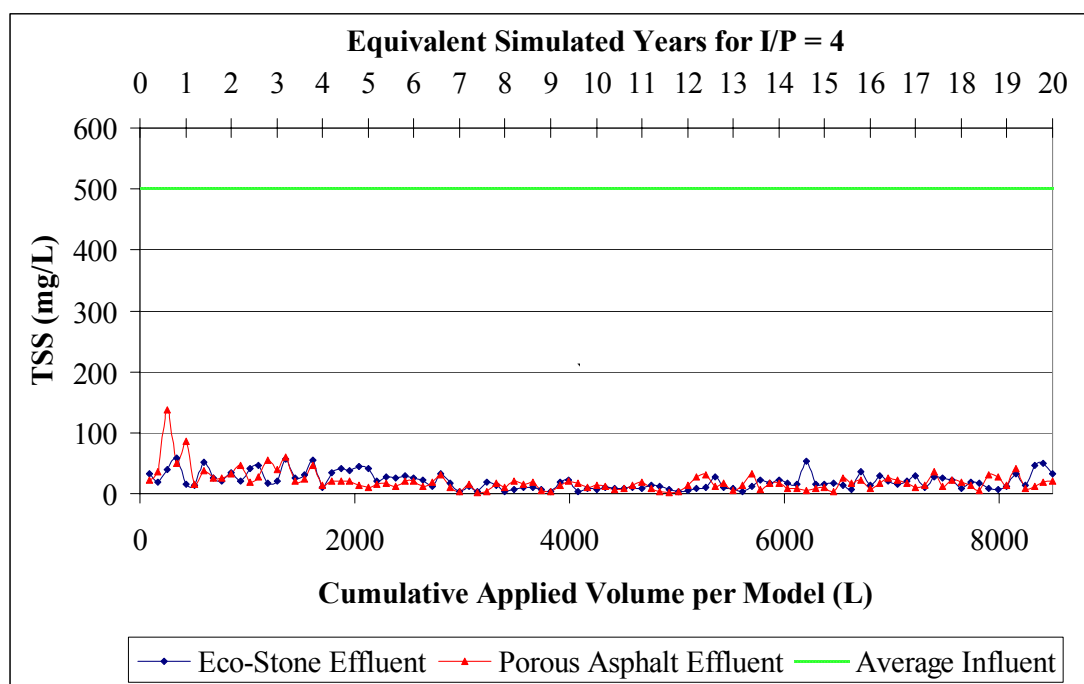


**Figure 4-16: Long-term Influent and Effluent TSS for Eco-Stone® and Porous Asphalt When Using 500 mg/L sub-250 µm Street Sweepings as Influent**

### 4.2.4 TSS Removal Characteristics - Particle Size Distributions, Influent and Effluent, Natural Sediment

The particle size distributions of the influent and effluent for the sub-250 µm street sweeping long-term simulated runoff experiments for the laboratory Eco-Stone®

and porous asphalt models are shown in Figure 4-17 and Figure 4-18. The influent PSDs were taken by collecting 2 L samples at the outlets of the conveyance tubes, centrifuging, and collecting the sediment. Since there was such close agreement between the PSDs of the influents from both conveyance tubes, they are combined on Figure 4-17 and Figure 4-18 to show the excellent repeatability in the PSD measurements.

The effluent particle size distribution results for the sub-250 μm street sweepings were very similar for both pavement types, and were also very similar for the laboratory and field experiments at Currie Barracks. The surfaces for the field installations were subjected to considerably different conditions than the surfaces in the laboratory, such as traffic loadings, real storm events, temperature fluctuations, and changes in antecedent moisture levels within the pavement, but the sub-structure design and composition were almost identical. It is difficult to determine the locations in which solids were removed in the field versus the locations that they were removed in the laboratory, but it does appear that, overall, very similar solids removal rates were achieved, and very similar size ranges of particles were removed from both laboratory models and field installations.
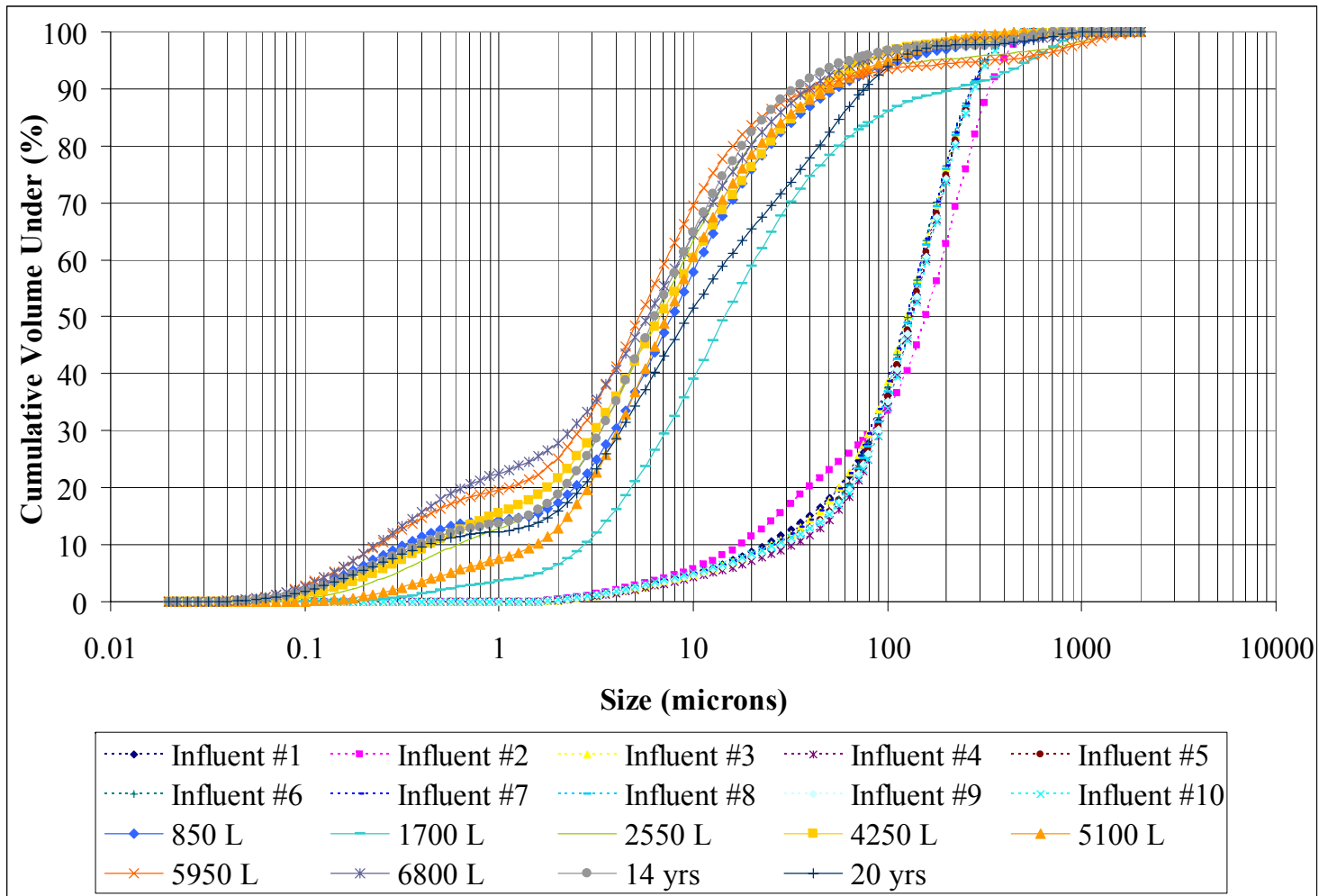
**Figure 4-17: Particle Size Distribution for the Influent and Effluent of the Standard-Sized Eco-Stone® Model for Long-term Laboratory Simulation for sub-250 μm Street Sweepings**
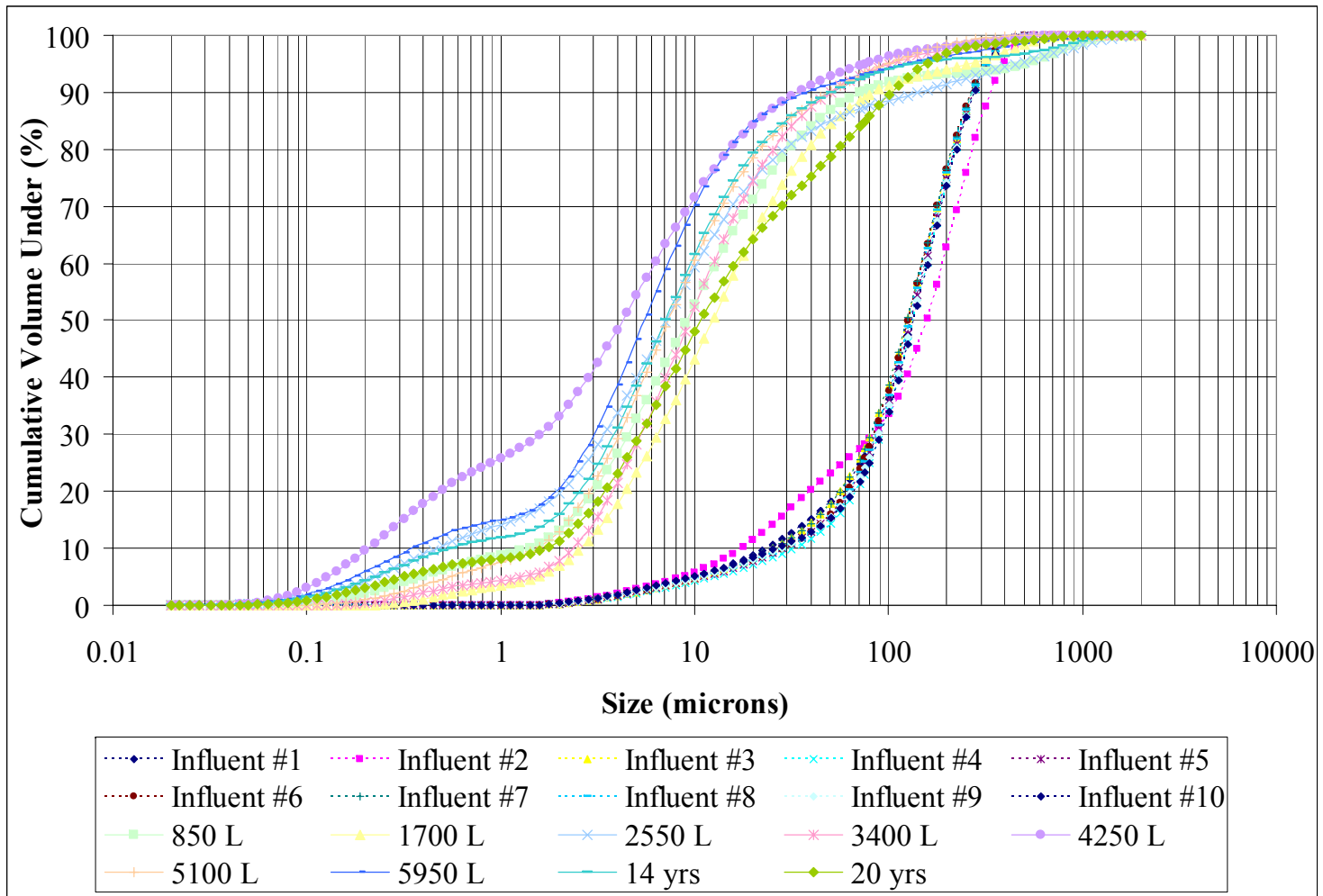
**Figure 4-18: Particle Size Distribution for the Influent and Effluent of the Standard-Sized Porous Asphalt Model for Long-term Laboratory Simulation for sub-250 µm Street Sweepings**

The fractional removal efficiencies, as described previously in Section 4.1.3, for the laboratory installations are shown in Table 4-9 and Table 4-10. The results are very similar to those observed in the field installations. Again, the removal efficiency decreases for the finer fractions, and is extremely high for all "greater than" fractions due to the coarse bias of the influent PSD, as discussed in Section 4.1.3.

**Table 4-9: Particle Size Fractional Removal Efficiencies for the Standard-Sized Eco-Stone® Model for Long-term Laboratory Simulation**

| Size Fraction | Proportion of Influent Under Size Fraction, Average Across All Eco-Stone® Experiments (%) | Std. Deviation | Proportion of Effluent Under Size Fraction, Average Across All Eco-Stone® Experiments (%) | Std. Deviation | % Removal for Size Fraction |
|---|---|---|---|---|---|
| *Greater Than* | | | | | |
| **>200** | 24.70 | 3.89 | 3.79 | 2.65 | 99 |
| **>100** | 61.96 | 3.77 | 7.13 | 2.54 | 99 |
| **>75** | 72.88 | 3.34 | 7.71 | 3.55 | 99 |
| **>50** | 82.16 | 2.80 | 11.08 | 4.78 | 99 |
| **>25** | 89.83 | 1.38 | 20.07 | 7.18 | 99 |
| **>10** | 95.06 | 0.37 | 40.95 | 8.51 | 98 |
| *Less Than* | | | | | |
| **<200** | 75.30 | 3.89 | 96.21 | 2.65 | 95 |
| **<100** | 38.04 | 3.77 | 92.87 | 2.54 | 90 |
| **<75** | 27.12 | 3.34 | 92.29 | 3.55 | 86 |
| **<50** | 17.84 | 2.80 | 88.92 | 4.78 | 79 |
| **<25** | 10.17 | 1.38 | 79.93 | 7.18 | 68 |
| **<10** | 4.94 | 0.37 | 59.05 | 8.51 | 51 |

**Table 4-10: Particle Size Fractional Removal Efficiencies for the Standard-Sized Porous Asphalt Model for Long-term Laboratory Simulation**

| Size Fraction | Proportion of Influent Under Size Fraction, Average Across All Porous Asphalt Experiments (%) | Std. Deviation | Proportion of Effluent Under Size Fraction, Average Across All Porous Asphalt Experiments (%) | Std. Deviation | % Removal for Size Fraction |
|---|---|---|---|---|---|
| *Greater Than* | | | | | |
| **>200** | 24.70 | 3.89 | 4.28 | 2.24 | 99 |
| **>100** | 61.96 | 3.77 | 7.13 | 2.54 | 99 |
| **>75** | 72.88 | 3.34 | 9.02 | 3.12 | 99 |
| **>50** | 82.16 | 2.80 | 12.26 | 4.16 | 99 |
| **>25** | 89.83 | 1.38 | 20.73 | 6.22 | 99 |
| **>10** | 95.06 | 0.37 | 42.29 | 9.01 | 98 |
| *Less Than* | | | | | |
| **<200** | 75.30 | 3.89 | 95.72 | 2.24 | 95 |
| **<100** | 38.04 | 3.77 | 92.87 | 2.54 | 90 |
| **<75** | 27.12 | 3.34 | 90.98 | 3.12 | 86 |
| **<50** | 17.84 | 2.80 | 87.74 | 4.16 | 80 |
| **<25** | 10.17 | 1.38 | 79.27 | 6.22 | 68 |
| **<10** | 4.94 | 0.37 | 57.71 | 9.01 | 52 |

For fractional removal efficiencies in the very fine range (i.e., <10 μm), the accuracy of this method becomes unreliable. To illustrate the reason behind this, consider that, in the influent, there were consistently zero particles detected below 1 μm, whereas for the effluent, the average fraction below 1 μm was as high as 25%. It would appear as though fines are appearing in the effluent that were not present in the influent. However, this is not the case, since all aggregate used in the pavement models was thoroughly washed, their gradations were measured and shown to contain zero particles under 500 μm, and the initial base flow from the pavement structure was 0 mg/L. The reason for this

apparent slight discrepancy for small particle sizes is likely due to the precision of the PSD analyzer. The effluent is much finer than the influent, and is also only 5% of the influent concentration. Therefore, very fine elements that may have been below detectable levels, or obscured due to very low absolute quantities of particles in the influent, are observed in the effluent because of an "amplification effect" of the finer particles. The particles were present in the influent, but they were in such minute quantities that they were below the detectable limits of the analyzer, or otherwise obscured due to low particle numbers.

**4.2.4.1 Size Distribution of Particle Accumulation Throughout Structure**

Figure 4-19 and Figure 4-20 show the results for the PSD analyses of the various layers of the pavement models, with the layer locations superimposed in the upper corner of the figures. For both pavement models, the layers above the geotextile appear to have very little influence on the sieving of specific particle sizes, while the geotextile itself appears to be most influential. The PSD of the sediment changes very little through the surface course and bedding course, although it is followed by a relatively drastic change above and below the geotextile (Locations D and E for Figure 4-19, and Locations C and D for Figure 4-20). The material is substantially finer below the geotextile compared to above. Interestingly, there also appears to be a change from the top to the bottom of the base course material. It is difficult to determine whether this is due to the sieving properties of the layer itself, or due to cross-contamination at the geotextile layer, whereby some of the larger particles may migrate through larger holes in the geotextile and influence the PSD of the aggregate directly below it. It seems unlikely that the base

course, which consists of the largest aggregate and void spaces, would have sieving properties greater than those in the other layers of the pavement models. Regardless, these findings are significant in that they demonstrate the role the geotextile can have in filtration for permeable pavements.
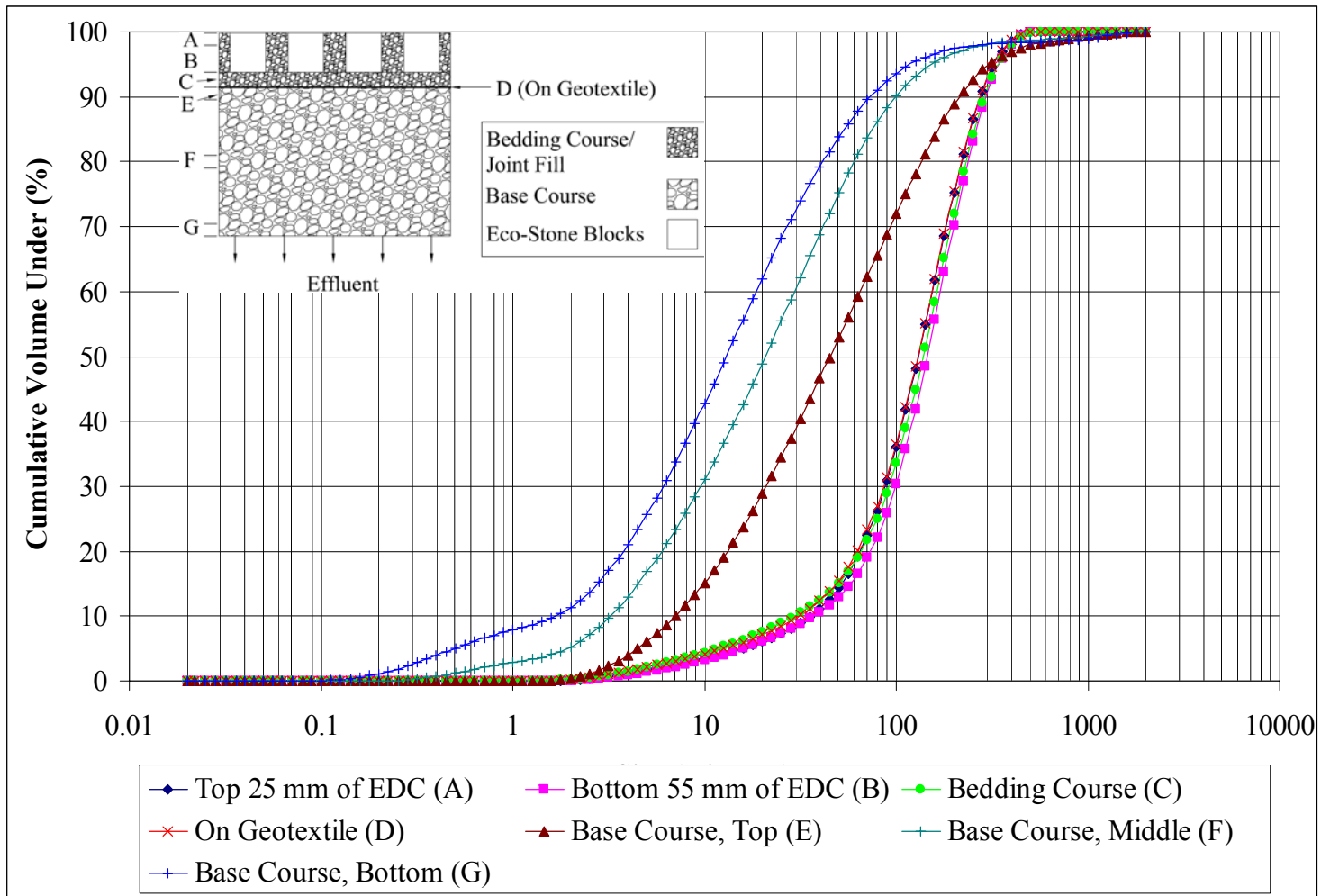
**Figure 4-19: Particle Size Distributions for Eco-Stone® Layers Throughout Pavement Model After 20 Years of Simulated Runoff (Layer Locations Superimposed in Upper Left Corner)**
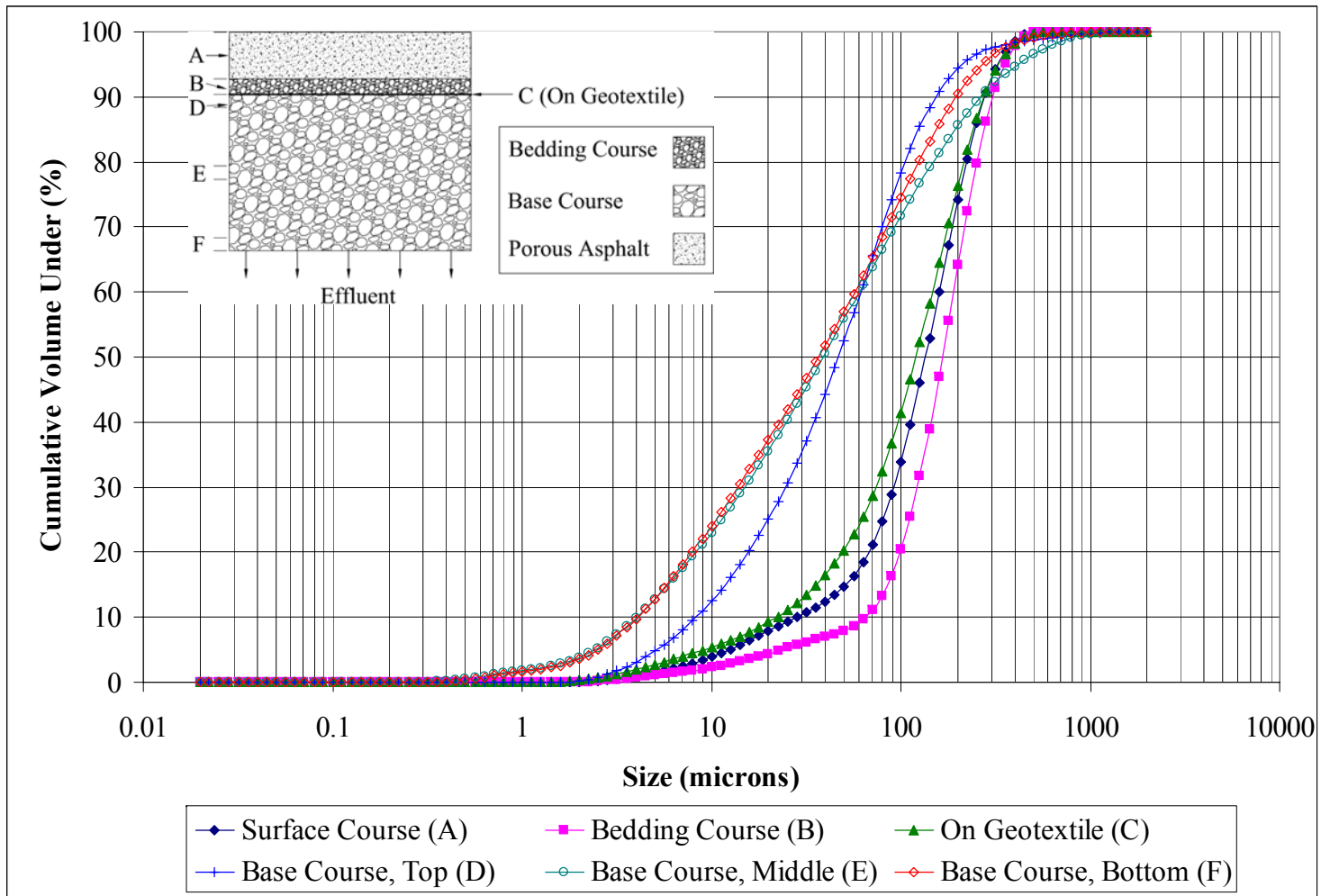
**Figure 4-20: Particle Size Distributions for Porous Asphalt Layers Throughout Pavement Model After 20 Years of Simulated Runoff (Layer Locations Superimposed in Upper Left Corner)**

### *4.2.5 Long-term Surface Infiltration Capacity*

The results of the long-term surface infiltration capacity measurements are shown in Figure 4-21. The first several years of data in Figure 4-21 were found through linear extrapolation due to limitations in the maximum measurable infiltration capacity in the laboratory setting. Therefore, the accuracy of the data in this figure is reliable only below an infiltration capacity of 30,000 mm/hr.

Both pavement surface types showed a gradual decline over the 20 simulated years of runoff application. However, the decline was much slower than was observed in the field installations at Currie Barracks. Additionally, in the laboratory, the porous asphalt showed higher infiltration capacities than the Eco-Stone® throughout the course of the experiment, which was also different than that which was observed at Currie Barracks. The most likely reason for these discrepancies was the absence of vehicular traffic for the laboratory models. Porous asphalt, by its very nature, is compressible. It is believed that heavy loads on the asphalt may cause a significant degree of compression, and consequently a reduction in the void space of the material. This in turn would lead to lower infiltration capacities and a more rapid decline in infiltration capacity. This reasoning is supported by the following excerpt from Ferguson (2005): "The heavy traffic load of…busy city streets can reduce porous asphalt's porosity and infiltration rate soon after construction". Unfortunately, this was not able to be tested for this thesis because the early onset of cold winter conditions made it difficult to conduct any further research on the asphalt at Currie Barracks. For future studies, it would be interesting to take cores of the porous asphalt and analyze both qualitatively and quantitatively the level of overall compression and compaction that had taken place since installation.

Another possible reason for the discrepancy between laboratory and field infiltration capacity results is the effect of "drying time", or long periods of exposure to sunlight without any precipitation. It is possible that these periods could perpetuate the formation of non-permeable crusts due to the drying and subsequent solidification of conglomerations of moisture-laden sediment within the pavement structure. These "drying time" conditions could not be simulated in the laboratory because of time and feasibility constraints. Periods of several days or weeks would be required to realistically dry out the inner and surface layers of the pavement models, and this would cause long-term laboratory simulation to take an impractically long period of time. In addition, by its very nature, the laboratory had a level of humidity because of the continuous flow of water. Furthermore, ideally one would incorporate direct natural sunlight into these types of experiments. For future studies, it is recommended to attempt to construct outdoor models for the purpose of observing the effects of drying time on the rate of clogging of permeable pavement surfaces.
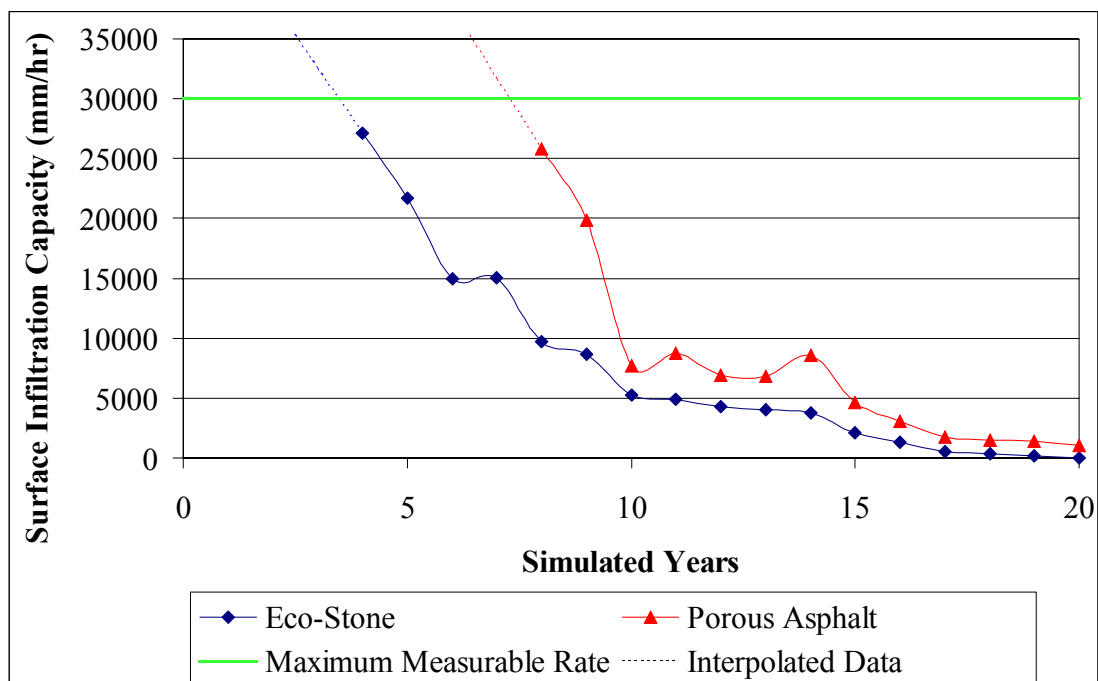
**Figure 4-21: Long-term Laboratory Surface Infiltration Capacities for Porous Asphalt and Eco-Stone®**

One final factor that likely would have been responsible for the differences in results in the field and laboratory is the presence of winter sanding materials. The field installations at Currie Barracks did receive winter sanding material through the winter of 2005-2006, although the precise amount is uncertain because during some sanding activities the pavements were avoided while during others they were not. The addition of material due to tire tracking is also unpredictable. Nonetheless, in an attempt to further test this in a laboratory setting, the final set of experiments that was carried out in the laboratory was a simulation to determine the effects of winter sanding material on long-term infiltration capacity of both pavement surface types.

*4.2.6 Effects of Winter Sanding Material on Long-term Surface Infiltration Capacity*

The effects of the presence of winter sanding material on the long-term surface infiltration capacities of the permeable pavement surfaces were investigated in the laboratory using the miniature model described in Section 3.2.2. For details on the calculations used to determine the characteristics and quantities of the sanding material that was used, refer to Appendix D. 1 kg/m$^2$ was applied to the surface, with approximately 20% of the material crushed under a point load to simulate the breakdown into smaller particles that would occur in reality (see Appendix D for details).

Figure 4-22 shows the results of the laboratory winter sanding experiments compared to the standard laboratory long-term surface infiltration capacity experiments. The winter sanding experiments were only run for 10 simulated years due to time constraints, but there is a clear trend showing that the surface infiltration capacities were substantially decreased for both pavement types when winter sanding material was present, regardless of the presence of vehicular traffic. Similar to the standard long-term infiltration capacity experiments, the first several years of data were extrapolated due to limitations in the maximum measurable infiltration capacity in the laboratory setting. Table 4-11 shows the year-by-year comparison of data for the surface infiltration capacities with and without the presence of winter sanding material for 10 simulated years. The Eco-Stone's$^®$ infiltration capacity was reduced on a yearly average by 951%, with the value after 10 years being 962% lower when winter sanding material was present. The porous asphalt's infiltration capacity was reduced on a yearly average by 103%, with the value after 10 years being 62% lower when winter sanding material was present. The porous asphalt's surface infiltration capacity remained significantly above

that of the Eco-Stone[®], and the effects of winter sanding material were less pronounced. These findings are, again, contradictory to the results seen in the field, where the surface infiltration capacity of the porous asphalt declined much more rapidly than that of the Eco-Stone[®]. This suggests that the presence of vehicular traffic is a very significant factor for the long-term hydraulic performance of porous asphalt surfaces, because this was one of the only significant variables that was absent from laboratory testing. Despite the discrepancies, this set of experiments does show that the presence of winter sanding material on permeable pavement surfaces substantially decreases the surface infiltration capacity and as such would likely lead to more rapid clogging and ultimate failure of the pavements. These findings agree with those of St. John and Horner (1997).
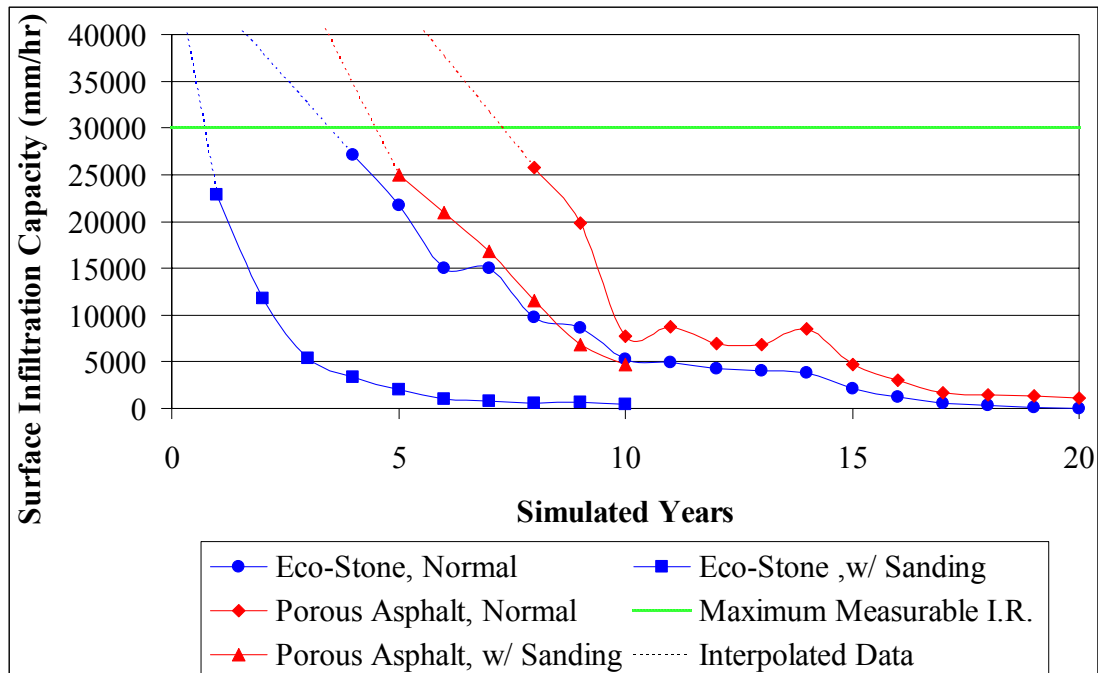


**Figure 4-22: Long-term Laboratory Surface Infiltration Capacity of Porous Asphalt and Eco-Stone[®] With and Without the Presence of Winter Sanding Material**

**Table 4-11: Percent Difference Between Surface Infiltration Capacity With and Without The Presence of Winter Sanding Material**

| Cumulative Applied Solids per Area (kg/m$^2$) | Equivalent Simulated Years | Surface Infiltration Capacities (mm/hr) | | | | | |
| --- | --- | --- | --- | --- | --- | --- | --- |
| | | UNI Eco-Stone$^®$ | | | Porous Asphalt | | |
| | | Normal | w/ Sanding Material | % Decrease | Normal | w/ Sanding Material | % Decrease |
| 0 | 0 | x | x | x[1] | x | x | x[1] |
| 0.98 | 1 | 43413[2] | 22856 | -90 | x | x | x[1] |
| 1.96 | 2 | 37991[2] | 11769 | -223 | x | x | x[1] |
| 2.95 | 3 | 32568[2] | 5400 | -503 | x | x | x[1] |
| 3.93 | 4 | 27144 | 3375 | -704 | x | x | x[1] |
| 4.91 | 5 | 21721 | 2000 | -986 | 43540[2] | 24960 | -74 |
| 5.90 | 6 | 15000 | 1064 | -1310 | 37623[2] | 20942 | -80 |
| 6.88 | 7 | 15068 | 759 | -1885 | 31706[2] | 16793 | -89 |
| 7.87 | 8 | 9746 | 588 | -1557 | 25790 | 11576 | -123 |
| 8.85 | 9 | 8638 | 622 | -1289 | 19873 | 6780 | -193 |
| 9.83 | 10 | 5259 | 495 | -962 | 7684 | 4750 | -62 |
| | | | **AVG** | -951 | | **AVG** | -103 |

---

[1] In cases where both the Normal and Winter Sanding values were above maximum measurable limit, no % Decrease was calculated

[2] Values obtained by linear extrapolation of the first two measurable data points

**Chapter Five: Conclusion**

**5.1 Conclusions**

The primary objectives of this research were to determine the performance of two types of permeable pavement with respect to hydraulics and water quality, and to try to gain a better understanding of the mechanisms and processes behind solids removal and clogging within permeable pavement structures.

The following observations and conclusions can be drawn from this study:

1) Although both permeable pavement types showed a moderate level of attenuation, the peak discharge rate was still higher than what would typically be accepted as part of conventional storm sewer system design practice for storm sewer systems, and as such some form of flow rate control would likely be required.

2) The porous asphalt surface in the field was found to clog substantially faster than the Eco-Stone® within the first year of operation. If installed in a similar setting, the porous asphalt would not be suitable for long-term use due to its poor hydraulic performance, whereas the Eco-Stone®, after one year, was still functioning sufficiently.

3) Both permeable pavement types exhibited excellent total suspended solids removal efficiencies both in a laboratory and field setting, typically ranging from 90-96%.

4) Solids removal occurs even when there is no "sieving action", as was demonstrated by the application of sil-co-sil 106, in which the influent and effluent PSDs were identical, and yet there was still solids removal of

approximately 62%. This was likely due to sedimentation and partial trapping of solids in the aggregates throughout the pavement structure.

5) In the case of natural sediment, the effluent was found to be considerably finer than the influent, and the "sieving action" was found to occur most predominantly at the geotextile layer. Although this is somewhat contradictory to the findings of other studies in which overall clogging took place in the upper portions of the pavement structure, this may be due to the influent characteristics. The findings in this study are significant in that they highlight the importance of choosing materials for the various courses and geotextiles in the pavement.

6) Both pavement types showed remarkably similar solids removal efficiencies and characteristics, suggesting that their sub-surface courses play more of a role in solids removal for sub-250 μm sediment than the surfaces themselves. This is somewhat contradictory to previous studies, but this is likely due to the types and sizes of sediment used in the influent for those studies.

7) 99% of particles sized 75 microns and over were removed by the pavement structures, whereas 74-86% of particles under 75 microns were removed. These fractional removal efficiencies are true only for the sub-250 μm sediment used in this study. Nonetheless, they show that the pavements meet current City of Calgary TSS removal guidelines.

8) Using vacuum sweeping as maintenance, the effective hydraulic life of the Eco-Stone® pavements can be substantially extended, whereas the porous asphalt did not show substantial improvement.

9) In a laboratory setting, both pavements were capable of lasting an equivalent of 15-20 years of sediment application while still maintaining hydraulic functioning. Vehicular traffic appears to have a highly degrading effect on infiltration capacity, since field installations showed remarkably faster clogging than those in the laboratory.

10) The application of winter sanding material, and its subsequent breakage into finer materials by vehicular traffic, has a very significant impact on the long-term surface infiltration capacity of both permeable pavement types. In the laboratory, the infiltration capacity was shown after 10 years to be 103% lower than the infiltration capacity without winter sanding material in the case of the Eco-Stone®, and 951% lower in the case of the porous asphalt.

## 5.2 Recommendations for Future Study

1) It would be highly informative to do a study on the fractional solids removal efficiencies of these pavement structures using a variety of influent sediments, with multiple particle size distributions.

2) The influence of drying time by direct sunlight, as well as vehicular traffic, on the long-term surface infiltration capacities would provide more data on the hydraulic performance of these systems, as well as appropriate installation locations.

3) Experimenting with different joint fill and bedding materials, as well as different geotextiles, as well as geotextile locations throughout the pavement structure, may provide more insight into what combination provides the best balance between solids removal and long-term hydraulic performance.

4) Other potential maintenance activities, especially for the porous asphalt, need to be researched.

5) Devising a realistic method to simulate the motion and impact of vehicular traffic would allow more realistic long-term laboratory experiments to be performed.

# References

Allen, T. Particle size measurement, 3rd edition, Chapman & Hall. 1981

American Society for Testing Materials. "C 131 standard test method for resistance to degradation of small-size coarse aggregates by abrasion and impact in the los angeles machine." ASTM. 1989.

Andersen, C. T., D. L. Foster, C. J. Pratt. "The role of urban surfaces (permeable pavements) in regulating drainage and evaporation: Development of a laboratory simulation experiment." Hydrological Processes 13(4): 597-609, 1999.

Andral, M. C. "Particle size distribution and hydrodynamic characteristics of solid matter carried by runoff from motorways." Water Environment Research 71(4): 398-407, 1999.

Ashley, R. M., J. L. Bertrand-Krajewski, T. Hvitved-Jacobsen, M. Verbanck. Solids in sewers - characteristics, effects and control of sewer solids and associated pollutants, IWA Publishing. 2004

Backstrom, M. "Ground temperature in porous pavement during freezing and thawing." Journal of Transportation Engineering 126(5), 2000.

Backstrom, M., A. Bergstrom. "Draining function of porous asphalt during snowmelt and temporary freezing." Canadian Journal of Civil Engineering 27(3): 594, 2000.

Balades, J. D., M. Legret, H. Madiec. "Permeable pavements: Pollution management tools." Water Science and Technology 32(1): 49-56, 1995.

Barnes, K. B., J. M. Morgan III, M. C. Roberge. "Impervious surfaces and the quality of natural and built environments." Baltimore: Towson University. 2001.

Bayon, J. R., D. Castro, X. Moreno-Ventas, S. J. Coupe, A. P. Newman. Pervious pavement research in spain: Hydrocarbon degrading microorganisms. 10th International Conference on Urban Drainage, Copenhagen, Denmark, 2005.

Bean, E. Z. A field study to evaluate permeable pavement surface infiltration rates, runoff quantity, runoff quality, and exfiltrate quality. Biological and Agricultural Engineering. Raleigh, North Carolina, North Carolina State University. **Master of Science**, 2005.

Bean, E. Z., W. F. Hunt, D. A. Bidelspach. Study on the surface infiltration rate of permeable pavements. Critical Transitions in Water and Environmental Resources Management. 2004 World Water and Environmental Resources Congress, Salt Lake City, Utah, USA, 2004.

Bond, P. C., C. J. Pratt, A. P. Newman. <u>A review of stormwater quantity and quality performance of permeable pavements in the uk</u>. 8th International Conference on Urban Storm Drainage, Sydney, Australia, 1999.

Booth, D. B. "Urbanization and the natural drainage system - impacts, solutions, and prognosis." <u>The Northwest Environmental Journal</u> **7**: 93-118, 1991.

Booth, D. B., J. Leavitt. "Field evaluation of permeable pavement systems for improved stormwater management." <u>Journal of the American Planning Association</u> **65**(3): 314-325, 1999.

Borgwardt, S. "Expert opinion." University of Hannover, Institute for Planning Green Spaces and for Landscape Architecture. 1994.

Brady, N. C., R. R. Weil. <u>The nature and properties of soils, thirteenth edition</u>. New Jersey, Pearson Education, Inc. 2002

Brattebo, B. O., D. B. Booth. "Long-term stormwater quantity and quality performance of permeable pavement systems." <u>Water Research</u> **37**(18): 4369-4376, 2003.

Briggs, J. F., J. P. Houle, R. M. Roseen, T. P. Ballestero. <u>Hydraulic and hydrologic performance of porous asphalt pavement</u>. StormCon 2005, Orlando, Florida, 2005.

Cahill Associates Inc. Comprehensive stormwater management: Structural bmps. <u>Pennsylvania stormwater best management practices manual - 2nd draft</u>. West Chester, PA**:** 197-276, 2005.

Cahill, T. "Technical note #21: A second look at porous pavement/underground recharge." <u>Watershed Protection Techniques</u> **1**(2): 76-78, 1994.

Cao, Z., G. Pender, J. Meng. "Explicit formulation of the shields diagram for incipient motion of sediment." <u>Journal of Hydraulic Engineering</u> **132**(10): 1097-1099, 2006.

Clausen, J. C. "Annual report: Jordan cove urban watershed section 319 national monitoring program project." Department of Natural Resources Management and Engineering College of Agriculture and Natural Resources, University of Connecticut. 2004.

Clescerl, L.S., A.E. Greenberg, A.D. Eaton. "Standard Methods for Examination of Water & Wastewater, 20th Edition." American Public Health Association, January 1999.

Colandini, V., M. Legret, Y. Brosseaud, J. D. Balades. "Metallic pollution in clogging materials of urban porous pavements." <u>Water Science and Technology</u> **32**(1): 57-62, 1995.

Collins, K. A., W. F. Hunt, J. M. Hathaway. Evaluation of various types of permeable pavement with respect to water quality improvement and flood control. StormCon 2006, Denver, Colorado, 2006.

Coupe, S. J., H. G. Smith, A. P. Newman, T. Puehmeier. "Biodegradation and microbial diversity within permeable pavements." European Journal of Protistology **39**(4): 495-498, 2003.

Davies, J. W., C. J. Pratt, M. A. Scott. Laboratory study of permeable pavement systems to support hydraulic modelling. 9th International Conference on Urban Drainage, Portland, Oregon, 2002.

Dierkes, C., A. Holte, W. F. Geiger. Heavy metal retention within a porous pavement structure. 8th International Conference on Urban Storm Drainage, Sydney, Australia, 1999.

Dierkes, C., L. Kuhlmann, J. Kandasamy, G. Angelis. Pollution retention capability and maintenance of permeable pavements. 9th International Conference on Urban Drainage, Portland, Oregon, 2002.

Dierkes, C., M. Lohmann, M. Becker, U. Raasch. Pollution retention of different permeable pavements with reservoir structure at high hydraulic loads. 10th International Conference on Urban Drainage, Copenhagen, Denmark, 2005.

Dunlop Tires. "Care & maintenance - tire repair." http://www.dunloptire.com/care/replacement.html, 2006.

Ehlers, P. F. "Lognormal distribution of pollutants." STATCAR. Report Prepared for The City of Calgary, 2003.

Environment Australia. "Introduction to urban stormwater management in australia." Department of the Environment and Heritage, Prepared under the Urban Stormwater Initiative of the Living Cities Program 2002. 2002.

Fach, S., W. F. Geiger. "Effective pollutant retention capacity of permeable pavements for infiltrated road runoffs determined by laboratory tests." Water Science and Technology **51**(2): 37-45, 2005.

Fancher, S., S. Townsen, et al. "Sustainable infrastructure alternative paving materials subcommitte report." City of Portland, Bureau of Environmental Sciences. 2003.

Ferguson, B. K. Porous pavements, CRC Press. 2005

Ferguson, B. K. Progress in porous pavements. StormCon 2006, Denver, Colorado, 2006.

Field, R., H. Masters, M. Singer. "An overview of porous pavement research." <u>Water Resources Bulletin (American Water Resources Association)</u> **18**(2): 265-270, 1982.

Fwa, T. F., S. A. Tan, Y. K. Guwe. "Laboratory evaluation of clogging potential of porous asphalt mixtures (paper no. 99-0087)." <u>Transportation Research Record: journal of the Transportation Research Board</u> **No. 1681**: 43-49, 1999.

Gerrits, C. Restoration of infiltration capacity of permeable pavers. <u>School of Engineering</u>. Guelph, Ontario, Canada, University of Guelph. **Master of Science**, 2001.

Hamzah, M. O., Hardiman. "Characterization of the clogging behaviour of double layer porous asphalt." <u>Journal of the Eastern Asia Society for Transportation Studies</u> **6**: 968-980, 2005.

Hogland, W., J. Niemczynowicz, T. Wahlman. "The unit superstructure during the construction period." <u>The Science of the Total Environment</u> **59**: 411-424, 1987.

Hossain, M., L. A. Scofield, W. R. Meier. "Porous pavement for control of highway runoff in arizona: Performance to date." <u>Transportation Research Record No. 1354</u>: 45-54, 1992.

Hun-Dorris, T. "Advances in porous pavement." <u>Stormwater - The Journal for Surface Water Quality Professionals</u> **March/April 2005**, 2005.

Hunt, B., S. Stevens, D. Mayes. <u>Permeable pavement use and research at two sites in eastern north carolina</u>. 9th International Conference on Urban Drainage, Portland, Oregon, 2002.

James, W. "Studies on the environmental design of permeable concrete block pavement for reducing stressors and contaminants in an urban environment." 2002.

James, W. Clogging of permeable concrete block pavement by street particulates and rain. <u>Innovative modeling of urban water systems, monograph 12</u>. Guelph, Canada, 2004.

James, W., C. Gerrits. Maintenance of infiltration in modular interlocking concrete pavers with external drainage cells. <u>Practical modeling of urban water systems, monograph 11</u>. Guelph, Canada, 2003.

James, W., H. Langsdorff. <u>The use of permeable concrete block pavement in controlling environmental stressors in urban areas</u>. 7th International Conference on Concrete Block Paving (PAVE AFRICA 2003), Sun City, South Africa, 2003.

Kindsvater, C. E., R. W. C. Carter. "Discharge characteristics of rectangular thin-plate weirs." Journal of the Hydraulics Division - Proceedings of the American Society of Civil Engineers 83(HY6), 1957.

Kresin, C. Long-term stormwater infiltration through concrete pavers. School of Engineering. Guelph, Ontario, Canada, University of Guelph. **Master of Science**, 1996.

Kresin, C., W. James, D. Elrick. Observations of infiltration through clogged porous concrete block pavers. Advances in modeling the management of stormwater impacts - vol. 5. Guelph, Canada, 1997.

Kuang, S., J. Sansalone. Filtration and clogging of cementitious permeable pavement by particles in runoff. StormCon 2006, Denver, Colorado, 2006.

Lane, E. W. "Progress report on studies on the design of stable channels of the bureau of reclamation." Proceedings from the American Society of Civil Engineering **79**, 1953.

Legret, M., V. Colandini. "Effects of a porous pavement with reservoir structure on runoff water: Water quality and fate of heavy metals." Water Science and Technology **39**(2): 111-117, 1999.

Legret, M., V. Colandini, C. Le Marc. "Effects of a porous pavement with reservoir structure on the quality of runoff water and soil." The Science of the Total Environment **189/190**: 335-340, 1996.

Legret, M., M. Nicollet, P. Miloda, V. Colandini, G. Raimbault. "Simulation of heavy metal pollution from stormwater infiltration through a porous pavement with reservoir structure." Water Science and Technology **39**(2): 119-125, 1999.

Malvern Instruments, "Brochure for Mastersizer 2000 Particle Size Analyzer", 2006

McNally, C., C. Philo, T. B. Boving. "Porous pavement and groundwater quality technical bulletin." University of Rhode Island Cooperative Extension - Nonpoint Education for Municipal Officials. 2005.

Memon, F. A., D. Butler. "Characterisation of pollutants washed off from road surfaces during wet weather." Urban Water Journal **2**(3): 171-182, 2005.

Newman, A. P., S. J. Coupe, T. Puehmeier, J. A. Morgan, J. Henderson, C. J. Pratt. Microbial ecology of oil degrading porous pavement structures. 9th International Conference on Urban Drainage, Portland, Oregon, 2002a.

Newman, A. P., C. J. Pratt, S. J. Coupe, N. Cresswell. "Oil bio-degradation in permeable pavements by microbial communities." Water Science and Technology **45**(7): 51-56, 2002b.

O'Brien, E., M. Hoppin. Personal communication**:** Washington State Department of Ecology Water Quality Program, 2006.

Pagotto, C., M. Legret, P. Le Cloirec. "Comparison of the hydraulic behaviour and the quality of highway runoff water according to the type of pavement." Water Research **34**(18): 4446-4454, 2000.

Pratt, C. J. "Sustainable urban drainage - a review of published material on the performance of various suds devices." Prepared for The Environment Agency, Coventry University. 2001.

Pratt, C. J., J. D. G. Mantle, P. A. Schofield. Porous pavements for flow and pollutant discharge control. 5th International Conference on Urban Storm Drainage, Osaka, Japan, 1990.

Pratt, C. J., J. D. G. Mantle, P. A. Schofield. "Uk research into the performance of permeable pavement, reservoir structures in controlling stormwater discharge quantity and quality." Water Science and Technology **32**(1): 63-69, 1995.

Pratt, C. J., A. P. Newman, P. C. Bond. "Mineral oil bio-degradation within a permeable pavement: Long term observations." Water Science and Technology **39**(2): 103-109, 1999.

Prince George's County. "Low-impact development: An integrated design approach." Department of Environmental Resource Programs and Planning Division. 2000.

Puehmeier, T., D. D. Dreu, J. A. W. Morgan, A. Shuttleworth, A. P. Newman. Enhancement of oil retention and biodegradation in pervious pavements and infiltration systems. 10th International Conference on Urban Drainage, Copenhagen, Denmark, 2005.

Rankin, K., J. E. Ball. A review of the performance of permeable pavers. Cities as Catchments WSUD 2004. 2004 International Conference on Water Sensitive Urban Design, Adelaide, Australia, 2004.

Rodriguez, J., D. Castro, M. A. Calzada, J. W. Davies. Pervious pavement research in spain: Structural and hydraulic issues. 10th International Conference on Urban Drainage, Copenhagen, Denmark, 2005.

Roger, S., M. Montrejaud-Vignoles, M. C. Andral, L. Herremans, J. P. Fortune. "Mineral, physical and chemical analysis of the solid matter carrie by motorway runoff water." Water Research **32**(4): 1119-1125, 1998.

Rushton, B. T. "Low impact parking lot design reduces runoff and pollutant loads." Journal of Water Resources Planning and Management **127**(3): 172-179, 2001.

Sansalone, J. J., S. G. Buchberger. "An infiltration device as a best management practice for immobilizing heavy metals in urban highway runoff." <u>Water Science and Technology</u> **32**(1): 119-125, 1995.

Sartor, J., G. B. Boyd, F. J. Agardy. "Water pollution aspects of street surface contaminants." <u>Journal of the Water Pollution Control Federation</u> **46**(3): 458-465, 1974.

Schluter, W., A. Spitzer, C. Jefferies. <u>Performance of three sustainable urban drainage systems in east scotland</u>. 9th International Conference on Urban Drainage, Portland, Oregon, 2002.

Shackel, B., J. Ball, M. Mearing. <u>Using permeable eco-paving to achieve improved water quality for urban pavements</u>. 7th International Conference on Concrete Block Paving (PAVE AFRICA 2003), Sun City, South Africa, 2003.

Shackel, B., A. Pearson. <u>Permeable concrete eco-paving as best management practice in australian urban road engineering</u>. 21st Australia Road Research Board (ARRB) Conference, Cairns, Qld, Australia, 2003.

Simons, D. B., F. Senturk. <u>Sediment transport technology - water and sediment dynamics</u>, Water Resources Publications. 1992

Spicer, G. E., D. E. Lynch, A. P. Newman, S. J. Coupe. <u>The development of geotextiles incorporating slow release phosphate beads for the maintenance of oil degrading bacteria in permeable pavements</u>. 10th International Conference on Urban Drainage, Copenhagen, Denmark, 2005.

St. John, M. S., R. Horner. "Porous asphalt road shoulders: Effect of road sanding operations and their projected life span in: Washington water resource, volume 8, number 4." Renton: King County Department of Transportation. 1997.

Stenmark, C. "An alternative road construction for stormwater management in cold climates." <u>Water Science and Technology</u> **32**(1): 79-84, 1995.

Stotz, G., K. Krauth. "The pollution from pervious pavements of an experimental highway section: First results." <u>Science of the Total Environment</u> **146/147**: 465-470, 1994.

Sutherland, R. C., T. Martin. <u>Street cleaner pick-up performance testing</u>. StormCon 2006, Denver, Colorado, 2006.

Taebi, A., R. L. Droste. "Pollution loads in urban runoff and sanitary wastewater." <u>Science of the Total Environment</u> **327**: 175-184, 2004.

Teng, Z., J. Sansalone. "In situ partial exfiltration of rainfall runoff. Ii: Particle separation." Journal of Environmental Engineering, ASCE **130**(9): 1-13, 2004.

The City of Calgary Wastewater & Drainage. "Stormwater management & design manual." 2000.

United States Environmental Protection Agency. "Storm water technology fact sheet: Porous pavement." Office of Water. EPA 832-F-99-023, 1999.

United States Environmental Protection Agency. "Low impact development (lid): A literature review." Low-Impact Development Center. 2001.

United States Environmental Protection Agency. "Light-duty automotive technology and fuel economy trends: 1975 through 2006." EPA420-S-06-003, 2006.

Urban Water Resources Centre. "Permeable pavement – port adelaide enfield council car park." Study into permeable pavments for water quality improvement at Port Adelaide-Enfield Council car park, supported by Natural Heritage Trust. Project No. 07 67355, 2002a.

Urban Water Resources Centre. "Research into "Effective life" Of permeable pavement source control installations." Urban Water Resources Centre Division of IT, Engineering and the Environment. Final Report Project 07 67680, 2002b.

Walker, D. J., S. Hurl. "The reduction of heavy metals in a stormwater wetland." Ecological Engineering **18**: 407-414, 2002.

Washington State Department of Ecology. "Guidance for evaluating emerging stormwater treatment technologies, technology assessment protocol - ecology (tape)." Washington State Department of Ecology Water Quality Program. Publication Number 02-10-037, 2004.

Westerlund, C., M. Viklander, M. Backstrom. "Seasonal variations in road runoff quality in lulea, sweden." Water Science and Technology **48**(9): 93-101, 2003.

# APPENDIX A: SPECIFICATIONS FOR MONITORING EQUIPMENT AT CURRIE BARRACKS

The monitoring equipment for the field installations at Currie Barracks consisted of the following equipment, all of which were located in the monitoring manhole: Sigma 900 autosampler, Sigma 950 flow meter, Sigma 75 Khz ultra sonic flow sensor, and a v-notch weir.

Brad Dardis, of Westhoff Engineering Resources, was responsible for the initial design calculations for the v-notch weir. The following calculation was used for the maximum and minimum flows, and to generate a head vs. flow table (Based on modified equation for triangular (v-notch) weir (Kindsvater and Carter, 1957)):

$$Q = \frac{8}{15} C \sqrt{2g} \bullet \tan\left(\frac{\theta}{2}\right) \bullet \left(h_1 + k_h\right)^{5/2} \qquad \textbf{( A.1 )}$$

where:

$Q$ = flow rate (m$^3$/s)
$C$ = discharge coefficient
$g$ = gravitational acceleration (m/s$^2$)
$\theta$ = angle of v-notch
$k_h$ = constant representing the combined effects of fluid properties
$h_1$ = head above weir's crest (m)


$k_h$ = 0.0008 m
$C$ = 0.58
$\theta$ = 100°


The corresponding head vs. flow table is shown in Table A-1.

**Table A-1: Head vs. Flow Table for Weir at Currie Baracks**

|      | (m)  | Q (m³/s) | Q (L/s) |
|------|------|----------|---------|
| H1   | 0.05 | 0.00095  | 0.95    |
| H2   | 0.06 | 0.001488 | 1.49    |
| H3   | 0.07 | 0.002178 | 2.18    |
| H4   | 0.08 | 0.00303  | 3.03    |
| H5   | 0.09 | 0.004057 | 4.06    |
| H6   | 0.1  | 0.005268 | 5.27    |
| H7   | 0.11 | 0.006673 | 6.67    |
| H8   | 0.12 | 0.008282 | 8.28    |
| H9   | 0.13 | 0.010104 | 10.10   |
| H10  | 0.14 | 0.012147 | 12.15   |
| H11  | 0.15 | 0.01442  | 14.42   |
| H12  | 0.16 | 0.016931 | 16.93   |
| H13  | 0.17 | 0.019687 | 19.69   |
| H14  | 0.18 | 0.022696 | 22.70   |
| H15  | 0.19 | 0.025966 | 25.97   |
| H16  | 0.2  | 0.029503 | 29.50   |



**Figure A-1: Monitoring Manhole at Currie Barracks**

**Figure A-2: Weir in Manhole**

# APPENDIX B: PARTICLE SIZE DISTRIBUTION ANALYSIS USING LASER DIFFRACTION

The principle behind this analysis is as follows (from Malvern, 2006):

"During the laser diffraction measurement, particles are passed through a focused laser beam. These particles scatter light at an angle that is inversely proportional to their size. The angular intensity of the scattered light is then measured by a series of photosensitive detectors. The number and positioning of these detectors in the Mastersizer 2000 has been optimized to achieve maximum resolution across a broad range of sizes The map of scattering intensity versus angle is the primary source of information used to calculate the particle size. The scattering of particles is accurately predicted by the Mie scattering model. This model is rigorously applied within the Mastersizer 2000 software, allowing accurate sizing across the widest possible dynamic range."

The analyzer is capable of detecting particles in the range of 0.02μm to 2000μm. The accuracy, as stated by the manufacturer is $\pm$ 1%.

There currently exist a multitude of techniques to determine particle size distributions. However, in assessing the particle size distribution (PSD) of solids in a stormwater sample, the number of suitable techniques is considerably reduced due to the limited quantity of solids in a typical stormwater sample.

There are some obvious issues that arise when comparing the results from this method, which measures particle size by volume, with other methods that measure particle size by mass. The underlying assumption is that the density is constant for all

particles in the sample. This assumption is considered less valid the greater the organic content of the soil, or the larger proportion of high-density minerals such as magnetite, garnet, epidote, zircon, etc. (Brady and Weil, 2002). However, the TVS, which can be used as an approximate estimate of carbon-based organic material, was found to be approximately 4% in the sub-250 μm street sweepings, which is quite low. For mineral soils with less than 5% organic matter, a constant particle density of about 2650 kg/m$^3$ can be safely assumed (Brady and Weil, 2002).

# APPENDIX C: ESTIMATIONS FOR THE THRESHOLD OF INITIATION OF MOTION FOR PARTICLES IN RUNOFF

The following is a derivation of approximations for the maximum size of particle that could theoretically be transported during a storm event on a pavement surface. There are several different methods to establish this relation, and there is on-going debate over the reliability and accuracy of each of the methods. Two of the more common methods will be applied here.

It should be understood that these methods were originally designed for flow in smooth channels, assuming spherical particles. This is certainly not the case for the movement of sediment across permeable pavement. As such, it would be expected that these methods for determining the initiation of motion of a particle would return maximum particle sizes that are higher than those that would be seen in reality. These equations are to be used as approximations only.

**Method #1 – Shield's Diagram using Explicit Formulation**

One of the more traditionally used methods is the Shields diagram (Figure C-1). This is an empirical relationship derived by measuring bed-load transport for various values of shear stress and particle diameter. For Figure C-1 Ashley *et al* (2004) define the variables as follows:

$\theta_{cr}$ = critical Shield's parameter (dimensionless)
$u^*$ = shear velocity (m/s)
$D$ = sediment particle diameter (m)
$v$ = kinematic viscosity of fluid (m$^2$/s)

It should also be noted that $(u^*D)/\upsilon$ is equivalent to the particle Reynold's number, and in some texts is often labelled as such.

The critical Shield's parameter is defined as follows:

$$\theta_{cr} = \frac{\tau_c}{(\rho_s - \rho_f)gD}$$

where:

$\tau_c$ = critical shear stress (kg/m-s$^2$)
$\rho_s$ = density of sediment (kg/m$^3$)
$\rho_w$ = density of water (kg/m$^3$)
$g$ = gravitational acceleration (m/s$^2$)
$D$ = sediment particle diameter (m)
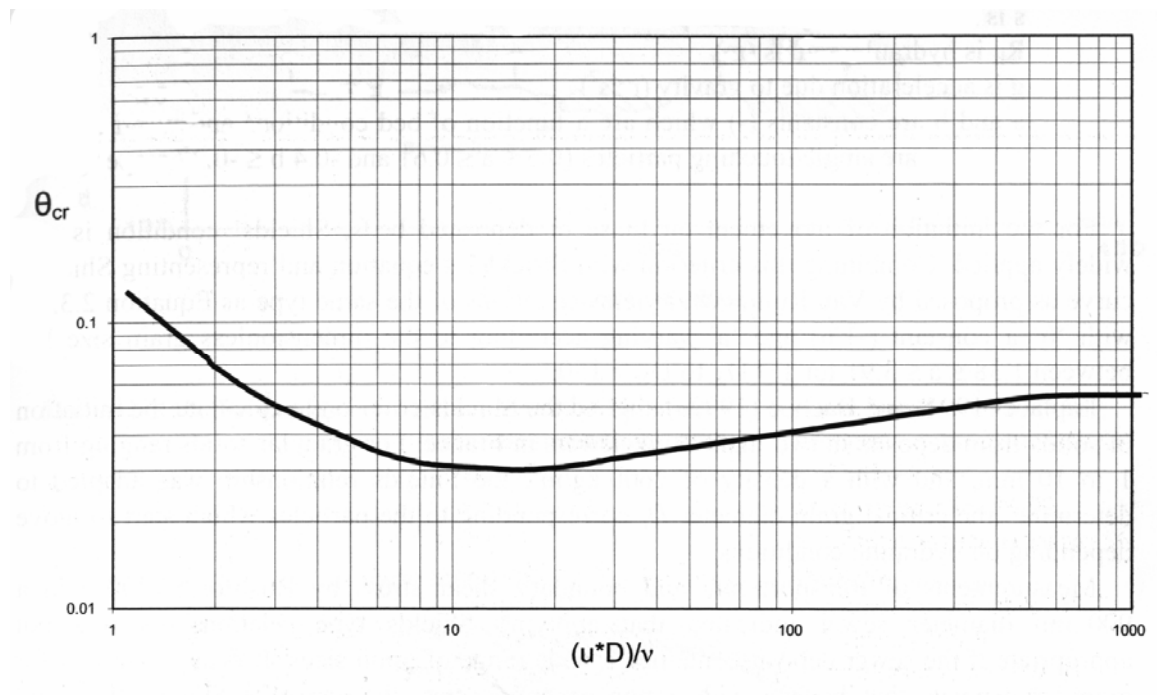


**Figure C-1: Shield's Diagram (from (Ashley *et al*, 2004))**

The problem with the Shields diagram is that it is cumbersome to apply in reality because the dependent variables (critical shear stress or grain size) appear in both ordinate and abscissa parameters (Simons and Senturk, 1992). Its implicit nature makes applications rather inconvenient (Cao *et al*, 2006). However, recently, Cao *et al* (2006) derived an explicit formulation of the Shields Diagram for incipient motion of sediment. The authors accomplished this using Guo's logarithmic matching method, and the result was the enabling of the critical Shield's parameter to be determined directly from fluid and sediment characteristics without having to use any trial and error procedure or iteration. The details of the mathematical derivations are not provided in this thesis, but their resulting formulas and general procedure of calculations for obtaining Shield's parameter and ultimately finding values for initiation of motion is as follows:

First of all, Reynold's number can be expressed as follows (Cao *et al*, 2006):

$$R = \frac{D\sqrt{sgD}}{\nu} \qquad \textbf{( C.2 )}$$

where:

      $R$ = particle Reynold's number (dimensionless)
      $D$ = sediment particle diameter (m)
      $s$ = specific gravity of sediment (dimensionless)
      $g$ = gravitational acceleration (m/s$^2$)
      $\upsilon$ = kinematic viscosity of fluid (m$^2$/s)

The shear stress on a particle in a bed can be expressed as:

$$\tau = \rho_w gh \sin \alpha \qquad \textbf{( C.3 )}$$

where:

$\tau$ = shear stress
$\rho_w$ = density of water (kg/m$^3$)
$g$ = gravitational acceleration (m/s$^2$)
$h$ = depth of fluid (m)
$\alpha$ = angle of slope of road (3% for the case of the roads at Currie Barracks)

The explicit expressions for the critical Shield's parameter derived from Cao *et al* (2006) are as follows:

If
6.61<R<282.84

$$\theta_{cr} = \frac{\left[1 + (0.0223R)^{2.8358}\right]^{0.3542}}{3.0946R^{0.6769}}$$

( C.4 )

If
R<6.61

$$\theta_{cr} = 0.1414R^{-0.2306}$$

( C.5 )

If
R>282.84

$$\theta_{cr} = 0.045$$

( C.6 )

where:

$\theta_{cr}$ = critical Shield's parameter (dimensionless)
$R$ = particle Reynold's number (dimensionless)

The variable that must be determined before the above equations can be utilized is h, the depth of water flowing down the channel (street). To determine this, a Flow/Velocity/Depth spreadsheet based on a Modified Manning's Equation was used with the following input parameters:

**Table C-1: Parameters used for QVD (Modified Manning's Equation) Spreadsheet**

|  | Manning's n | Width | Cross-slope | Elev_left | Elev_right |
|---|---|---|---|---|---|
|  | (-) | (m) | (-) | (m) | (m) |
| Left Private Property | 0.030 | N/A | 0.050 | N/A | 0.220 |
| Left Sidewalk (low) | 0.013 | 1.00 | 0.020 | 0.220 | 0.200 |
| Pavement | 0.013 | 6.06 | 0.020 | 0.000 | 0.121 |
| Right Sidewalk (high) | 0.013 | 1.00 | 0.020 | 0.321 | 0.341 |
| Right Private Property | 0.030 | N/A | 0.050 | 0.341 | N/A |

| Height left curb | 0.200 | m - artificial curb | |
|---|---|---|---|
| Height right curb | 0.200 | m - artificial curb | |
| Longitudinal Slope | 0.030 | (-) | 3 | % |

Using the area of the pavements at Currie Barracks with an I/P ratio of 4 (total area of 242.4 m², and a rainfall intensity of 100 mm/hr (1-in-100 year storm of 15 minute duration, according to City of Calgary (2000)), the depth of water from the QVD spreadsheet comes to approximately 0.006 m, or 0.6 cm. If a rainfall intensity of 15 mm/hr is used (1-in-2 year storm of 60 minute duration (The City of Calgary Wastewater & Drainage, 2000)), the depth of water from the QVD spreadsheet comes to approximately 0.001 m, or 0.1 cm. These two design storms are being used in this demonstration because they represent values at the "extreme" ends of the spectrum of rainfall intensities that are experienced in Calgary.

Using Equations C.2 – C.6, we come up with the following table of values:

**Table C-2: Initiation of Motion Values Using Explicit Shield's Formulation**

| Particle Diameter (m) | R | $\theta_{cr}$ | h for mobilization (m) |
|---|---|---|---|
| 0.0001 | 4.023244959 | 0.10257324 | 0.000564153 |
| 0.00025 | 15.90327207 | 0.050586659 | 0.000695567 |
| 0.0005 | 44.98124609 | 0.031459796 | 0.000865144 |
| 0.0006 | 59.12938356 | 0.030799457 | 0.001016382 |
| 0.001 | 127.2261766 | 0.035277107 | 0.001940241 |
| 0.002 | 359.8499687 | 0.045 | 0.00495 |
| 0.0025 | 502.9056199 | 0.045 | 0.0061875 |
| 0.003 | 661.0866055 | 0.045 | 0.007425 |
| 0.005 | 1422.431896 | 0.045 | 0.012375 |
| 0.01 | 4023.244959 | 0.045 | 0.02475 |

As can be seen, for the depth of 0.006 m, the maximum particle diameter that can be mobilized according to the Shield's relation appears to be approximately 2.5 mm, while for a depth of 0.001 m, the maximum particle diameter that can be mobilized is 0.6 mm.

**Method #2 – Lane Empirical Diagram**

Another method that can be used to determine initiation of motion for sediment particles is the critical tractive force vs. grain diameter diagram from Lane (1953) (Reprinted in Simons and Senturk (1992)). This diagram is a compilation of extensive field data to establish the critical tractive force diagram. It should be noted that the critical tractive force, expressed in $g/m^2$, is the same as critical shear stress, with the absence of the gravitational acceleration parameter.
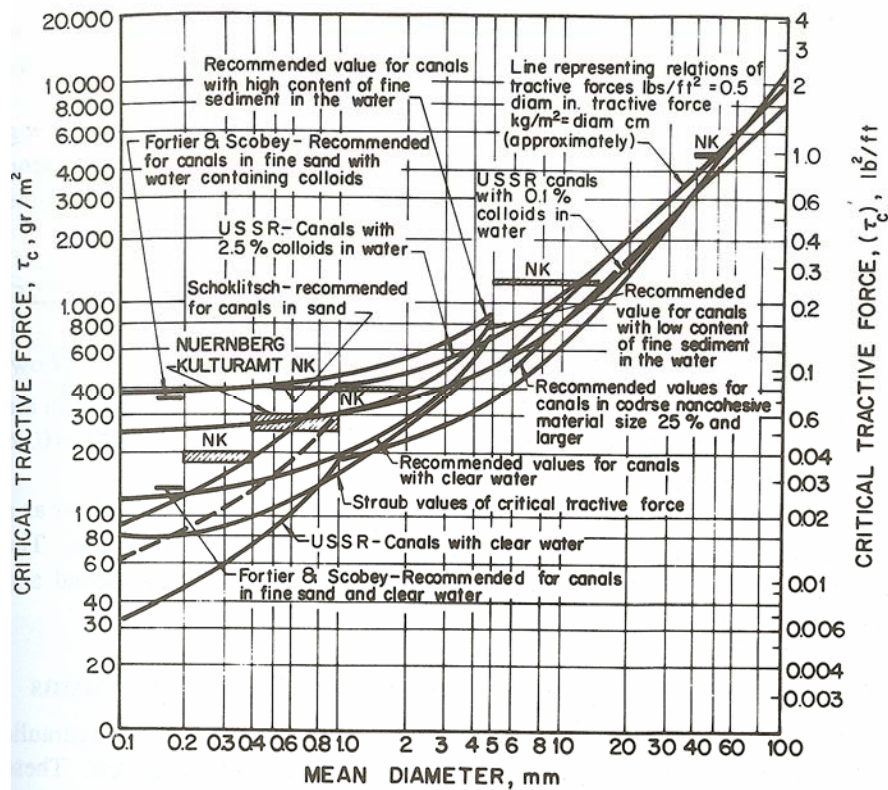
**Figure C-2: Critical shear stress as a function of grain diameter (reprinted from Simons and Senturk (1992), originally from Lane (1953))**

Using this method, if a depth of 0.006 m is assumed, Equation C.3 gives a shear stress of 1.766 kg/m-s$^2$, or a tractive force of 120 g/m$^2$. Similarly for a depth of 0.001 m, the tractive force is 20 g/m$^2$. From the Lane diagram, the resulting mean diameters vary considerably depending on the specific relationship that is chosen, anywhere from 0 to 0.8 mm. If the Straub relationship is used, for example, then the maximum sized particle that would be mobilized would be approximately 0.6 mm for a tractive force of 120 g/m$^2$. For a tractive force of 20 g/m$^2$, the lower limits of the graph are exceeded, but the value would be less than 0.1 mm. This method produces substantially smaller values for particle diameter than the Shields Method.

From the application of both of these methods, it can be postulated that the maximum particle sizes that could be mobilized from a 1-in-100 year storm of 15 minute duration in Calgary are either 0.6 mm or 2.5 mm, depending on the method used. For a 1-in-2 year storm of 60 minute duration, the maximum particle sizes that could be mobilized are either <0.1 mm or 0.6 mm, depending on the method used. These values provide verification that the sub-250 μm street sweeping sediment that was used to simulate stormwater runoff for both laboratory and field experiments was an appropriate representation. Particles larger than 250 μm are, based on the exercise in this Appendix, probably rarely mobilized during typical Calgary storm events.

**APPENDIX D: DETERMINATION OF CHARACTERISTICS FOR WINTER**

**SANDING MATERIAL IN LABORATORY EXPERIMENTS**

**Winter Sanding Quantity**

From the years 2001-2005, the average total winter sanding material that was applied to City of Calgary roads was 42,814 tonnes, or 42,814,000 kg. In 2005, the total length of all roads maintained by The City of Calgary was 4,416 km. If an average road width of 10 meters is assumed, the following mass of material is applied per square meter per single year:

$$\rho_A = \frac{m}{A}$$ ( D.1 )
$$= \frac{42814000kg}{4416000m \times 10m}$$
$$= 0.97kg / m^2$$

where:

$\rho_A$ = area density of winter sanding material for one year (kg/m$^2$)
$m$ = mass of material (kg)
$A$ = area of covered road surface (m$^2$)

Given the area of the winter sanding laboratory structure was 0.11 m$^2$ and using Equation D.1, the total mass of winter sanding material for one year's simulation in the laboratory is 0.11 kg.

**Winter Sanding Crushing Characteristics**

It appeared at the Currie Barracks field installation that a portion of the winter sanding material was being broken down into finer particles by vehicular traffic. This was evidenced by the presence of particles that upon visual inspection appeared to be sized from approximately 500 μm to 5 mm. These particles likely would not be carried by runoff, as indicated by the initiation of motion calculations made in Appendix C, and would be quite heavy to have been transported by tire tracking. Therefore, their presence was likely due to the breakdown of winter sanding material that had been applied through the winter months. Additionally, qualitative inspection seemed to show that the mineral type of the 500 μm to 5 mm material was similar to that of the winter sanding material. To verify whether these observations were plausible, a very quick and rudimentary laboratory analysis of the "crushing load" for various winter sanding particles was performed. It should be noted that this test was performed to provide rough indications only. Ideally, a more thorough and accurate test, such as the Los Angeles test (American Society for Testing Materials, 1989) would be performed to determine the resistance of aggregate to fragmentation. However, this test is detailed and time-consuming, and it was beyond the scope of this thesis to perform such an in-depth analysis.

For this basic analysis, 100 particles of the winter sanding material, selected as best as possible to represent a broad cross-section of sizes, shapes, and mineral types, were subjected to a gradually and continuously increasing point load until the "breakage force" had been reached. For the purposes of this experiment, "breakage force" was defined as the measured force at the moment at which the particle had fractured and split into 2 or more visible sub-particles. In almost every instance, this fracturing and splitting

was accompanied by an audible cracking noise, which further assisted in the indication of precisely when a breakage had occurred. Not surprisingly, given the high variability in shape, size and mineral type of the winter sanding material, there was an equal variability in the point force required to initiate breakage in the material. Although no quantitative analysis of particle type, size, and shape was correlated with the corresponding breakage forces, a general observation was that the most significant factor in determining the ease with which a particle was fractured was its mineral type. The results for the 100 particles are shown in Figure D-2.

The average breakage force was 320.4 N, with a standard deviation of 249.8 N. Some particles broke at forces as low as 20-40 N, while the maximum observed breakage force was 1306.5 N. If an average sanding particle diameter (based on the median of the gradation presented in Figure D-1) of 0.5 cm is assumed, that means that the average "breakage pressure" that initiated breaking in the experiments was approximately 1633 $N/cm^2$, while the minimum was 102 $N/cm^2$ and the maximum was 6657 $N/cm^2$. The problem with this assumption is that the size of the particle itself may well have an influence on the breakage pressure, but for the purposes of this rough investigation, the assumption of a 0.5 cm diameter will suffice.

To compare whether these ranges of forces and pressures are achievable with regular vehicular traffic, a brief analysis of tire loadings is necessary. The average mass of light-duty vehicle models in 2006 was 1883 kg (United States Environmental Protection Agency, 2006). Assuming 4-wheel vehicles, the force exerted per tire is:

$$F_t = \frac{1883\,\text{kg} \times 9.81\,\text{m/s}^2}{4\text{ tires}}$$

$$= 4618\,\text{N/tire}$$

<div align="right">( D.2 )</div>

where:

$V$ = equivalent volume of yearly precipitation (L)
$d$ = yearly depth of precipitation in Calgary (m)
$A$ = permeable pavement area (m$^2$)
$I/P$ = impervious to pervious area ratio (dimensionless)

If the entire load of the tire was supported by a single 0.5 cm particle, the exerted pressure would be approximately 23531 N/cm$^2$, which is about 3.5 times the maximum observed breakage pressure in the laboratory, and therefore all particles would be crushed under this assumption. However, most vehicles would not exert a "point load" on a winter sanding particle. More likely, the load of a single tire would be partially dispersed along the road's surface, and partially dispersed on the particle itself. The degree to which the tire's load would be spread on the road surface and the particle itself is dependent on several factors, including the height of the particle and the compressibility of the tire, which is dependent on tire pressure and the material of the tire itself. It is in fact very difficult and far beyond the scope of this thesis to determine precisely what percentage of a single tire loading would be exerted on a given sanding particle. However, the exerted pressure of a tire on flat ground can be determined, and some deductions can be made. The most common "footprint" for light-duty vehicular tires is approximately 12.7 cm X 10.16 cm, or 129 cm$^2$ (Dunlop Tires, 2006). Ignoring the effect of tread-pattern voids on area and using the results from Equation D.2, the pressure exerted by an average tire on completely flat ground would be 36 N/cm$^2$.

This value is approximately 2.25 times lower than the minimum observed breakage pressure in the lab. However, this is assuming a completely smooth tire on a completely flat surface, and assuming that 100% of the load is directed to the ground. This condition would not occur in reality. Tires are not smooth due to the presence of tread patterns, and a percentage (probably a significant percentage, especially in the case of larger particles) of the exerted pressure would be distributed on the particle itself. In addition, no road surfaces, and especially permeable pavement surfaces, are completely flat. Furthermore, heavier duty vehicles, which are not at all uncommon at the Currie Barracks field location, would increase the exerted pressure. Another factor to consider is the gradual weakening of sanding particles over time due to the repeated impact of vehicular momentum. It can be said with confidence from the results of this rudimentary experiment that a portion of the winter sanding particles dispersed on road surfaces can be broken into smaller particles by ordinary vehicular traffic.

Based on the observations in this experiment that indeed some winter sanding particles would be crushed by regular vehicular traffic, along with qualitative observations of the proportion of particle sizes on the surface of the road at Currie Barracks, it was decided that 20% of the winter sanding material applied in the laboratory would be "crushed". The crushing procedure involved randomly selecting 20% by mass of the applied particles, and applying a point load on the particle until fracture. It is understood that this is not an extremely precise method to simulate vehicular crushing of winter maintenance aggregate, but given the resources and time available for this project, it was felt that it was more important to approximate, as best as possible, a crushing technique, rather than ignore the component altogether.
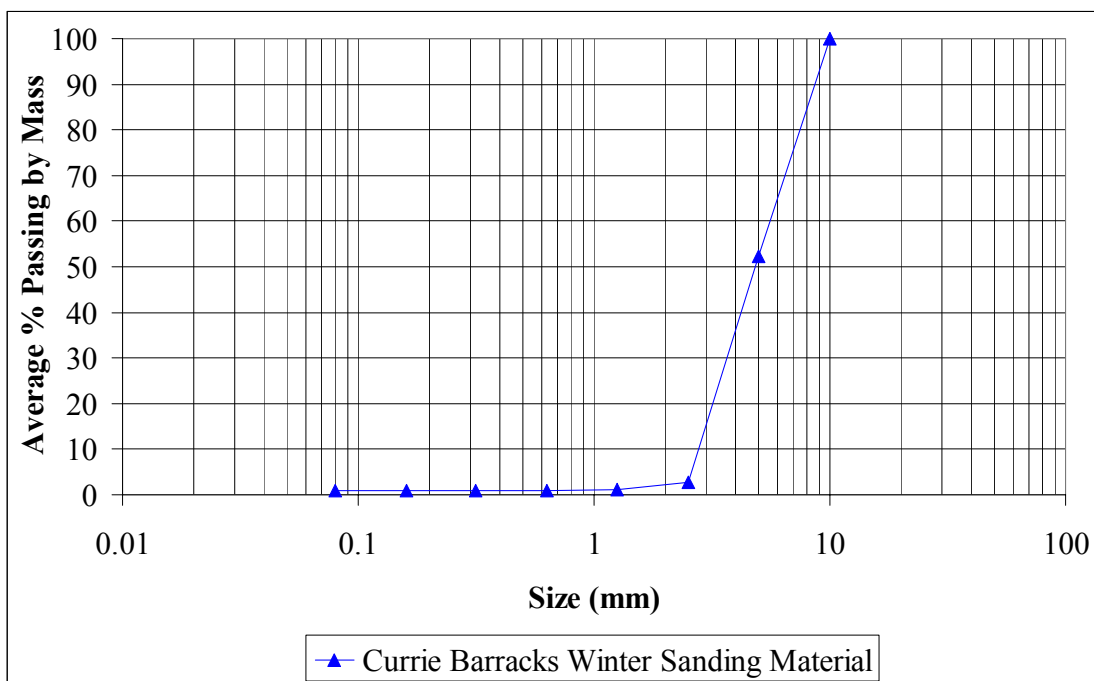
**Figure D-1: Particle Size Distribution of Winter Sanding Material Used at Currie Barracks**
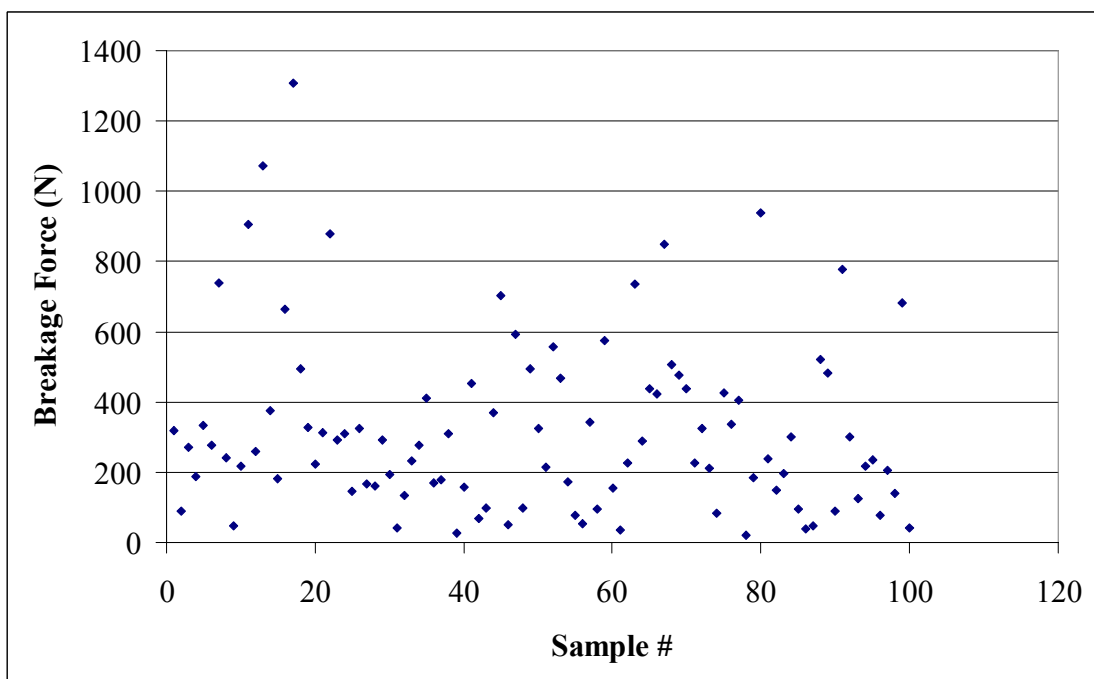


**Figure D-2: Breakage Forces for 100 Winter Sanding Particles**

**APPENDIX E: TSS AND PSD OF VARIOUS ROAD LOCATIONS**

**Table E-1: TSS in Runoff for Various Storm Events and Catchbasins in Calgary**

| Location | Date | TSS in Runoff (mg/L) (2 L grab samples, taken at various stages of storm event) |
|---|---|---|
| Catchbasin, Sierra Morena Blvd SW | 01/07/2006 | 306 |
| Catchbasin, 37 St NW | 06/07/2006 | 552 |
| Catchbasin, Sierra Morena Rd SW | 09/07/2006 | 22 |
| Catchbasin, Sierra Morena Blvd SW | 09/08/2006 | 112 |
| Catchbasin, Sierra Morena Rd SW | 11/08/2006 | 267 |
| Catchbasin, 37 St NW | 11/08/2006 | 48 |
| Catchbasin, 37 St NW | 13/09/2006 | 498 |
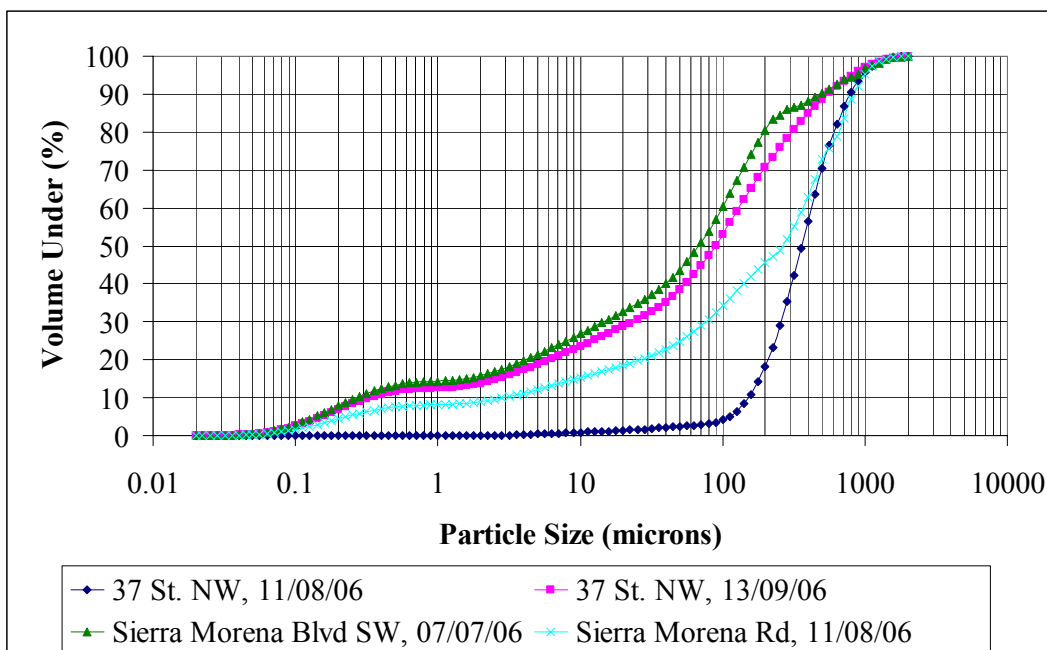
**Figure E-1: Particle Size Distribution from Runoff Collected at Various Catchbasins across Calgary**
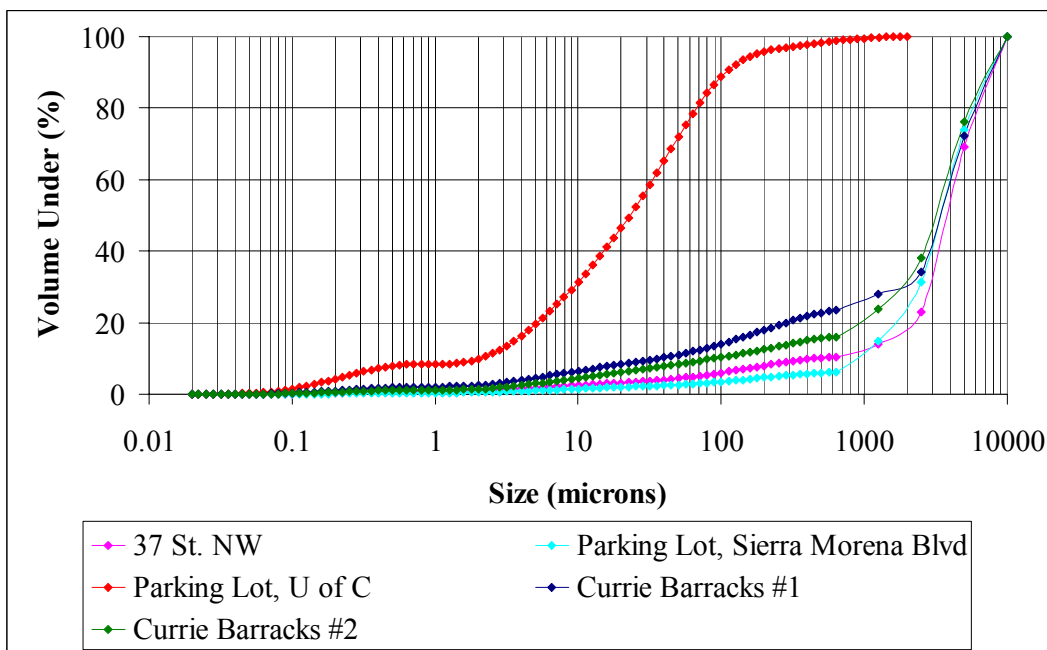


**Figure E-2: Particle Size Distribution from Melted Snow Runoff at Various Locations across Calgary**

**Figure E-3: Snowbank, Hochwald Avenue (Currie Barracks)**



**Figure E-4: Snowbank, 37 St. NW, nearby 32 Ave (just in front of catchbasin)**

**Figure E-5: Snow Bank, Parking Lot 13, University of Calgary Engineering Building**



**Figure E-6: Snowbank, Parking Lot, Sierra Morena Blvd. SW**

**Figure E-7: Catchbasin, Sierra Morena Blvd. SW**



**Figure E-8: Catchbasin, Sierra Morena Rd. SW**

## APPENDIX F: SCHWARZE A8000 VACUUM SWEEPER DETAILS

The vacuum sweeper used for the maintenance experiments at the Currie Barracks test site was a Schwarze A8000 Regenerative Air Sweeper. The A8000 is a chassis-mounted sweeper with a 5.8 cubic yard capacity hopper. According to Schwarze,

"This highly efficient system ensures that even hard-to-reach particles hidden within pavement cracks and irregularities are removed, including the "PM-10 fines" known to contain a high percentage of heavy metals and other pollutants. Double-belted curtains on the front and rear of the sweeping head contain the circulating air flow to assure debris transfer with minimal escape of fugitive dust."

"The A8000's Schwarze-exclusive Whisper Wheel blower system generates a high velocity air column that is propelled into the top of the sweeping head through a 14-inch blast tube. The air is first pressurized in the upper chamber of the sweeping head, and then expelled into the head's lower chamber through what is called a "blast orifice." This is a slot in the sweeping head that forces the air against the pavement at an angle, creating a "peeling" or "knifing" effect. This high volume air blast loosens the debris from the pavement surface, then transports it across the width of the sweeping head and lifts it into the containment hopper via a 14-inch suction tube. The A8000's vertical, steel-digger gutter brooms measure 44 inches in diameter and are driven hydraulically. Their free-floating design allows them to follow the contour of the pavement and gutter, while a spring impact protection system enables an inward swing of the broom(s) when an immovable object is encountered. These features help to eliminate excessive wear, and prevent the possibility of gutter broom breakage due to striking an obstacle. The use of

two gutter brooms extends the total sweeping width of the Schwarze A8000 to 138 inches. This features in-cab controls, with 11 water nozzles located as follows: 5 on the sweeping head, 2 at each gutter broom, and 2 inside the hopper."